

University of Alberta

Studies on Electron Transfer in the DmsA subunit of
Dimethyl Sulfoxide Reductase of *Escherichia coli*

by

Catharine Ann Trieber



A thesis submitted to the Faculty of Graduate Studies and Research in partial fulfillment
of the requirements for the degree of Doctor of Philosophy

Department of Biochemistry

Edmonton, Alberta

Fall 1996



National Library
of Canada

Acquisitions and
Bibliographic Services Branch

395 Wellington Street
Ottawa, Ontario
K1A 0N4

Bibliothèque nationale
du Canada

Direction des acquisitions et
des services bibliographiques

395, rue Wellington
Ottawa (Ontario)
K1A 0N4

Your file Votre référence

Our file Notre référence

The author has granted an irrevocable non-exclusive licence allowing the National Library of Canada to reproduce, loan, distribute or sell copies of his/her thesis by any means and in any form or format, making this thesis available to interested persons.

L'auteur a accordé une licence irrévocable et non exclusive permettant à la Bibliothèque nationale du Canada de reproduire, prêter, distribuer ou vendre des copies de sa thèse de quelque manière et sous quelque forme que ce soit pour mettre des exemplaires de cette thèse à la disposition des personnes intéressées.

The author retains ownership of the copyright in his/her thesis. Neither the thesis nor substantial extracts from it may be printed or otherwise reproduced without his/her permission.

L'auteur conserve la propriété du droit d'auteur qui protège sa thèse. Ni la thèse ni des extraits substantiels de celle-ci ne doivent être imprimés ou autrement reproduits sans son autorisation.

ISBN 0-612-18118-9

Canada

University of Alberta
Library Release Form

Name of Author: Catharine Ann Trieber

Title of Thesis: Studies on Electron Transfer in the DmsA subunit of
Dimethyl Sulfoxide Reductase of *Escherichia coli*

Degree: Doctor of Philosophy

Year this Degree Granted: 1996

Permission is hereby granted to the University of Alberta Library to reproduce single copies of this thesis and to lend or sell such copies for private, scholarly, or scientific research purposes only.

The author reserves all other publication and other rights in association with the copyright in the thesis, and except as hereinbefore provided, neither the thesis nor any substantial portion thereof may be printed or otherwise reproduced in any material form whatever without the author's prior written permission.

Catharine Trieber


23 Woodvale Village
Edmonton, Alberta
T6L 1W4

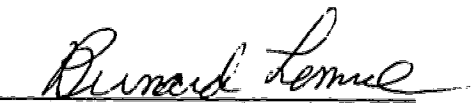
Date May 2, 1996


University of Alberta

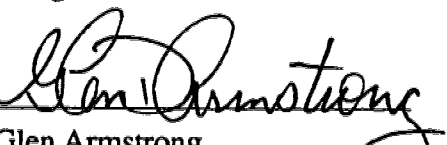
Faculty of Graduate Studies and Research


The undersigned certify that they have read, and recommend to the Faculty of Graduate Studies and Research for acceptance, a thesis entitled Studies on Electron Transfer in the DmsA subunit of Dimethyl Sulfoxide Reductase of *Escherichia coli* submitted by Catharine Ann Trieber in partial fulfillment of the requirements for the degree of Doctor of Philosophy.


Joel H. Weiner


Bernard D. Lemire


Douglas G. Scraba


Glen Armstrong


Robert Gennis

Dated April 30, 1996



University of Alberta
Edmonton

Department of Biochemistry

Canada T6G 2H7

474 Medical Sciences Building, Telephone (403)

Fax (403) 492-0886

May 1, 1996

Permission is granted to Catharine A. Trieber to include the following publications in her doctoral thesis.

Catharine A. Trieber, Richard A. Rothery, and Joel H. Weiner. "Engineering a Novel Iron-Sulfur Cluster into the Catalytic Subunit of *Escherichia coli* Dimethyl Sulfoxide Reductase" *J. Biol. Chem.* 271:4620-4626. (1996).

Catharine A. Trieber, Richard A. Rothery, and Joel H. Weiner. "Multiple Pathways of Electron Transfer in Dimethyl Sulfoxide Reductase of *Escherichia coli*." *J. Biol. Chem.* 269:7103-7109. (1994).

Joel H. Weiner

Richard A. Rothery



University of Alberta
Edmonton

Department of Biochemistry

Canada T6G 2H7

474 Medical Sciences Building, Telephone (403)

Fax (403) 492-0886

1836

March 5, 1996

Editorial Office,
American Society for Biochemistry
and Molecular Biology, Inc.
9650 Rockville Pike
Bethesda, MD
20814

Dear Editorial Staff,

I am writing to request permission to include material published in the Journal of Biological Chemistry, authored by myself, my supervisor (the corresponding author) and another group member, in my doctoral thesis. The publications I wish to use are cited below and they would each comprise one chapter of my thesis.

Catharine A. Trieber, Richard A. Rothery, and Joel H. Weiner (1994) "Multiple pathways of electron transfer in dimethyl sulfoxide reductase of *Escherichia coli*" *J. Biol. Chem.* **269**, 7103-7109.

Catharine A. Trieber, Richard A. Rothery, and Joel H. Weiner (1996) "Engineering a novel iron-sulfur cluster into the catalytic subunit of *Escherichia coli* dimethyl sulfoxide reductase. *J. Biol. Chem.* **271**, 4620-4626.

Yours sincerely,

Catharine A. Trieber

PERMISSION GRANTED
contingent upon obtaining that of the author

Barbara A. Gordon / J.H.W.

MAR 1996

For Dennis Michael

We all miss you.

Abstract

Dimethyl sulfoxide reductase (DmsABC) of *Escherichia coli* is a complex [Fe-S] molybdoenzyme. The DmsA subunit, shares seven regions of sequence identity with a family of molybdoenzymes. Cys-38, Cys-42 and Cys-75, Lys-28 and Arg-77 of Region 1 were examined by site-directed mutagenesis. Cys-38, Cys-42 and Arg-77 were essential for growth on dimethyl sulfoxide (DMSO). Benzyl viologen:DMSO oxidoreductase activity was severely reduced in C42S. Activity with dimethylnaphthoquinol was reduced in C38S, C42S and C75S and almost totally eliminated in R77S. C38S, C42S and R77S were unable to support quinol oxidation although electron transfer from the quinone pool to the [Fe-S] centers in DmsB was normal. Region 1 is involved in functional electron transfer from the quinone pool to DMSO. Electrons from benzyl viologen, dimethylnaphthoquinol and menaquinol may follow different pathways within DmsA.

DmsABC contains four [4Fe-4S] clusters and five potential [4Fe-4S] cluster ligating Cys Groups. Mutagenesis of DmsA Cys-38 to either Ser or Ala promotes assembly of a fifth [Fe-S] cluster. The C38S and C38A enzymes ligate [3Fe-4S] clusters that are unstable in redox titrations and have midpoint potentials of 178 mV and 140 mV. Mutagenesis of the DmsA Cys group to resemble a [4Fe-4S] cluster binding sequence did not change the cluster type. All four [4Fe-4S] clusters in the wild-type enzyme are ligated by DmsB. Wild-type DmsA does not ligate an [Fe-S] cluster that is visible by EPR spectroscopy.

Ser-176 in DmsA is a putative molybdenum ligand. Mutagenesis of Ser-176 to Ala, Cys or His abolished growth on DMSO and activity with benzyl viologen. The EPR line shape and midpoint potentials of the Mo were drastically altered in the mutant enzymes. The S176A enzyme could be oxidized to Mo(V) but not to Mo(VI) with ferricyanide. Titration of the S176C mutant produced several Mo(V) signals. Mo(V)

was not visible in S176H membranes. The S176C mutation altered the EPR line shape of the reduced enzyme, suggesting a conformational link between this residue and at least one of the [Fe-S] clusters.

Acknowledgments

I would like thank my supervisor, Joel Weiner, for his guidance and encouragement throughout my graduate studies. I am grateful to Raymond Turner, Joanne Simala Grant and Damaraju Sambasivarao for their helpful advice and useful discussions during my time in the laboratory.

Special acknowledgment is due to my husband, Richard Rothery, who provided not only moral support, but has also been a collaborator in this work. I would like to thank my family, especially my parents, for their love and encouragement throughout my studies.

Financial support from the Alberta Heritage Foundation for Medical Research and the Department of Biochemistry is gratefully acknowledged.

Table of Contents

| | | |
|-----------|--|----|
| Chapter 1 | General Introduction | 1 |
| I. | Introduction..... | 2 |
| II. | The Respiratory Chains of <i>E. coli</i> | 2 |
| A. | Energy transduction | 4 |
| B. | Aerobic Respiration | 4 |
| C. | Anaerobic Respiration..... | 6 |
| 1. | Glycerol 3-Phosphate Dehydrogenase..... | 6 |
| 2. | Formate Dehydrogenases..... | 8 |
| 3. | Nitrate Reductase | 8 |
| 4. | Fumarate reductase | 10 |
| III. | DMSO Reductase of <i>E. coli</i> | 11 |
| A. | Ecology | 11 |
| B. | Bacterial Reduction of S-and N-oxides | 12 |
| C. | Bioenergetics of Growth via DmsABC | 12 |
| 1. | Growth on S- and N-oxides | 12 |
| 2. | The Electron Transport Chain Terminating in DmsABC..... | 13 |
| 3. | H ⁺ /2e ⁻ Stoichiometry..... | 13 |
| D. | The <i>dms</i> Operon | 14 |
| 1. | Structure of the Operon | 14 |
| 2. | Organization of the <i>dms</i> Operon | 14 |
| E. | Regulatory mechanisms | 16 |
| 1. | FNR..... | 17 |
| 2. | Nitrate | 17 |
| 3. | TorR | 18 |

| | | |
|-----------|--|----|
| 4. | Molybdenum..... | 18 |
| 5. | ArcAB..... | 19 |
| F. | Enzymology of DmsABC | 19 |
| G. | Topological Organization of DMSO reductase | 20 |
| H. | DmsA | 21 |
| 1. | DmsABC is a Molybdoenzyme | 21 |
| 2. | Comparison with Other Molybdoenzymes | 23 |
| 3. | The Molybdenum Cofactor..... | 23 |
| 4. | The Molybdenum Environment..... | 26 |
| 5. | Sequence Analysis of DmsA | 27 |
| I. | DmsB | 30 |
| 1. | DmsB is an [Fe-S] Protein | 30 |
| 2. | Electron Flow in DmsABC..... | 31 |
| 3. | Comparison with other [Fe-S] Proteins | 32 |
| 4. | Mutagenesis of the Cys Groups | 36 |
| J. | DmsC | 37 |
| 1. | Anchor Function | 37 |
| 2. | Quinone Binding..... | 37 |
| IV. | Thesis Objectives | 39 |
| V. | Bibliography | 40 |
| Chapter 2 | Multiple Pathways of Electron Transfer in Dimethyl Sulfoxide Reductase of <i>Escherichia coli</i> | 48 |
| I. | Introduction..... | 49 |
| II. | Materials and Methods | 52 |
| A. | Bacterial Strains and Plasmids | 52 |
| B. | Materials..... | 52 |
| C. | Oligonucleotide-Directed Mutagenesis..... | 54 |

| | | |
|-----------|---|----|
| D. | Growth of Bacteria | 54 |
| E. | Preparation of Membrane Fractions..... | 54 |
| F. | Enzyme Assays | 56 |
| G. | Protein Determination and Polyacrylamide Gel Electrophoresis | 56 |
| H. | EPR Spectroscopy | 56 |
| III. | Results..... | 57 |
| A. | Preparation of Mutants | 57 |
| B. | Expression and Localization of Mutant Enzymes..... | 57 |
| C. | Growth Characteristics of the Mutant Enzymes | 59 |
| D. | Electron Transfer from the Artificial Electron Donor Benzyl Viologen | 61 |
| E. | Electron Transfer from the Quinol Analog Dimethylnaphthoquinol | 61 |
| F. | Ability of Wild-type and Mutant Enzymes to Oxidize the Menaquinone pool..... | 63 |
| IV. | Discussion..... | 67 |
| V. | Bibliography | 69 |
| Chapter 3 | Engineering a Novel Iron-Sulfur Cluster into the Catalytic Subunit of <i>Escherichia coli</i> Dimethyl Sulfoxide Reductase | 73 |
| I. | Introduction | 74 |
| II. | Materials and Methods | 76 |
| A. | Bacterial Strains and Plasmids | 76 |
| B. | Materials..... | 77 |
| C. | Site-Directed Mutagenesis | 77 |
| D. | Growth of Bacteria | 77 |
| E. | Harvesting of Cells and Preparation of Membrane Fractions..... | 78 |
| F. | Protein Determination and Polyacrylamide Gel Electrophoresis | 78 |

| | | |
|-----------|---|-----|
| | G. Enzyme Assays | 78 |
| | H. EPR Spectroscopy | 79 |
| III. | Results..... | 80 |
| | A. Growth Properties and Enzyme Activities of the Cys-38 Mutants..... | 80 |
| | B. EPR Characteristics of Dithionite Reduced F36 Membranes Containing Overexpressed Wild-Type and Mutant DmsABC | 80 |
| | C. EPR Characteristics of Oxidized F36 Membranes Containing Amplified Wild-Type and Mutant DmsABC..... | 83 |
| | D. Redox Titrations of the C38A and C38S Mutant Enzymes | 85 |
| | E. Mutagenesis of the DmsA Cys Group to a Consensus Ferredoxin Cys Group..... | 90 |
| IV. | Discussion..... | 92 |
| V. | Bibliography | 95 |
| Chapter 4 | Identification of a Molybdenum Ligand in <i>Escherichia coli</i> Dimethyl Sulfoxide Reductase | 98 |
| I. | Introduction..... | 99 |
| II. | Materials and Methods | 100 |
| | A. Bacterial Strains and Plasmids..... | 100 |
| | B. Materials..... | 100 |
| | C. Site-Directed Mutagenesis | 102 |
| | D. Growth of Bacteria | 102 |
| | E. Harvesting of Cells and Preparation of Membrane Fractions..... | 102 |
| | F. Protein Determination | 103 |
| | G. Enzyme Assays | 103 |
| | H. EPR Spectroscopy..... | 103 |
| III. | Results..... | 104 |

| | | |
|-----------|---|-----|
| A. | Growth Characteristics and Enzyme Activities of the Ser-176 Mutants | 104 |
| B. | Mo(V) EPR Spectra in the Wild-Type and Mutant Enzymes | 104 |
| C. | Redox Titration of the Wild-type DmsABC Mo(V) Signal | 108 |
| D. | Redox Titrations of the Mo(V) Signals in the Ser-176 Mutants | 108 |
| E. | EPR Spectra of Dithionite-Reduced Membranes | 110 |
| IV. | Discussion | 113 |
| V. | Bibliography | 117 |
| Chapter 5 | Discussion and Conclusions | 121 |
| I. | Discussion and Conclusions | 122 |
| A. | Electron Transfer Properties of Region 1 | 122 |
| B. | The Role of Region 1 in [Fe-S] Cluster Ligation | 124 |
| C. | The Function of Region 1 | 126 |
| D. | The Ligation of the Molybdenum | 127 |
| E. | Structure of the Mo Cofactor in DmsABC | 130 |
| F. | The Reaction Mechanism of DmsABC | 132 |
| G. | Model for Electron Transfer | 134 |
| II. | Future Studies | 136 |
| A. | The Mo-MGD Cofactor | 136 |
| B. | The [4Fe-4S] Clusters | 137 |
| C. | Quinone Binding | 137 |
| D. | Subunit Interactions | 138 |
| E. | Kinetic Studies | 138 |
| III. | Bibliography | 139 |

List of Tables

| | | |
|-----------|---|-----|
| Table 1-1 | Redox Potentials and Free Energy Changes of Alternative Respiratory Electron Acceptors | 5 |
| Table 1-2 | Prokaryotic Molybdoenzymes | 9 |
| Table 2-1 | Bacterial Strains and Plasmids..... | 53 |
| Table 2-2 | DNA Sequence Analyses of Mutants in DmsA..... | 55 |
| Table 2-3 | Expression of DmsA in <i>E. coli</i> Cells Harboring Wild-Type and Mutant Plasmids | 58 |
| Table 2-4 | Growth Characteristics of Cells Harboring Mutant and Wild-Type DmsABC Plasmids | 60 |
| Table 2-5 | Specific Activities of Membrane Preparations Containing Amplified Levels of Mutant and Wild-Type DmsABC | 62 |
| Table 3-1 | Characteristics of the DmsA Mutant Enzymes..... | 81 |
| Table 3-2 | Midpoint Potentials of Wild-Type and Mutant DmsABC..... | 88 |
| Table 4-1 | Enzyme Activities of Membranes Containing Amplified Levels of Wild-Type and Mutant DmsABC..... | 105 |
| Table 4-2 | Spin Quantitation and Midpoint Potentials of the EPR Signals from HB101 Expressing Wild-Type or Mutant DmsABC | 106 |

List of Figures

| | | |
|------------|--|-----|
| Figure 1-1 | The <i>E. coli</i> Respiratory Systems..... | 3 |
| Figure 1-2 | The Anaerobic Respiratory Chain Comprised of GlpACB and DmsABC..... | 7 |
| Figure 1-3 | Organization of the <i>dms</i> Operon..... | 15 |
| Figure 1-4 | Topology and Mechanism in DmsABC | 22 |
| Figure 1-5 | Molybdopterin Cofactors..... | 24 |
| Figure 1-6 | Molybdoenzyme Signature Sequences in DmsA | 28 |
| Figure 1-7 | The Cys Groups of DmsB and Other Related Iron-Sulfur Proteins | 33 |
| Figure 1-8 | Interactions of the Cys Groups in DmsB | 35 |
| Figure 2-1 | Sequence Alignment of Region 1 | 50 |
| Figure 2-2 | Q-Pool Coupling | 51 |
| Figure 2-3 | Oxidation of the Q-Pool by DmsABC..... | 64 |
| Figure 2-4 | Ability of the Mutant Enzymes to Oxidize the Q-Pool | 66 |
| Figure 2-5 | Model for Electron Transfer Through DmsABC..... | 70 |
| Figure 3-1 | Sequence Alignment of the Cysteine Residues in Region 1..... | 75 |
| Figure 3-2 | EPR Spectra of Reduced F36 Membranes..... | 82 |
| Figure 3-3 | EPR Spectra of Oxidized Membranes | 84 |
| Figure 3-4 | Microwave Power Dependences of the [3Fe-4S] Clusters | 86 |
| Figure 3-5 | Temperature Dependences of the [3Fe-4S] Cluster..... | 87 |
| Figure 3-6 | Redox Titration Curves of the New [3Fe-4S] Cluster | 89 |
| Figure 3-7 | EPR Spectra of Oxidized Membranes of DmsA Mutants | 91 |
| Figure 4-1 | Sequence Alignment of the Putative Mo Binding Domain | 101 |
| Figure 4-2 | Mo(V) EPR Spectra of HB101 Membranes | 107 |
| Figure 4-3 | Redox Titration Curves of the Mo(V) Signals in HB101 Membranes | 109 |

| | | |
|------------|--|-----|
| Figure 4-4 | EPR Spectra of HB101/pS176C Membranes During Reductive Titration | 111 |
| Figure 4-5 | EPR Spectra of the Reduced Membranes at 12 K | 112 |
| Figure 5-1 | The Proposed Structure of the Mo Cofactor in <i>E. coli</i> DmsABC | 131 |
| Figure 5-2 | Proposed Mechanism of Oxygen Transfer in DmsABC | 133 |
| Figure 5-3 | Summary of Electron Transfer Through DmsABC..... | 135 |

List of Abbreviations

| | |
|------------------------------------|--|
| ATP | adenosine triphosphate |
| AOR | aldehyde ferredoxin oxidoreductase from <i>Pyrococcus furiosus</i> |
| BV ²⁺ /BV ^{•+} | oxidized and reduced benzyl viologen |
| CHES | 2-[N-cyclohexylamino]-ethanesulfonic acid |
| $\Delta G_0'$ | Gibbs free energy change calculated from apparent equilibrium constants |
| DHAP | dihydroxyacetone phosphate |
| DMF | dimethylformamide |
| DMN/DMNH ₂ | oxidized and reduced forms of 2,3-dimethyl-1,4-naphthoquinone |
| DMS | dimethyl sulfide |
| DMSO | dimethyl sulfoxide |
| E _h | actual redox potential |
| E _{m,7} | midpoint potential at pH 7 |
| EDTA | ethylenediamine tetraacetic acid |
| EPR | electron paramagnetic resonance |
| EXAFS | extended X-ray absorption fine structure |
| FAD | flavin adenine dinucleotide |
| FDH | formate dehydrogenase, FDH-H, formate hydrogenlyase (FdhF), FDH-N, nitrate linked formate dehydrogenase (FdnGHI), FDH-O aerobic formate dehydrogenase (FdoGHI) |
| [Fe-S] | iron-sulfur cluster |
| FMN | flavin mononucleotide |
| G3P | glycerol-3-phosphate |
| HOQNO | 2-n-heptyl-4-hydroxyquinoline-N-oxide |
| MCD | molybdopterin cytidine dinucleotide |
| MGD | molybdopterin guanine dinucleotide |

| | |
|---------------------|---|
| MOP | aldehyde oxidoreductase from <i>Desulfovibrio gigas</i> |
| MOPS | 3-[N-morpholino]propanesulfonic acid |
| MQ/MQH ₂ | oxidized and reduced menaquinone-8 |
| NADH | nicotinamide adenine dinucleotide |
| P _{1/2} | microwave power required for half saturation of a paramagnetic center |
| Q-pool | reduced and oxidized quinones present in the membrane |
| SDS | sodium dodecyl sulfate |
| TMAO | trimethylamine-N-oxide |
| UQ/UQH ₂ | oxidized and reduced ubiquinone-8 |
| $\Delta\mu_{H^+}$ | proton electrochemical potential. |

Chapter I

General Introduction

I. Introduction

The facultative anaerobe *Escherichia coli* has developed several systems for energy generation and selects the most efficient system for a particular environment (1,2). The most wasteful form of energy metabolism is fermentation, in which energy is derived only from substrate level phosphorylation reactions. When an exogenous electron acceptor such as O₂, nitrate, dimethyl sulfoxide (DMSO) or fumarate is available, *E. coli* switches to respiration. Specialized electron transfer chains consisting of a primary dehydrogenase, a membrane soluble quinone, and a terminal reductase generate a transmembrane proton gradient (proton motive force, $\Delta\mu_{H^+}$) (3-6). The $\Delta\mu_{H^+}$ is comprised of a chemical (ΔpH) and an electrical ($\Delta\Psi$) gradient, and is the driving force for ATP synthesis via the F₁/F₀ ATPase, active transport of molecules across the cytoplasmic membrane, motility and other energy requiring processes.

The ability to generate a $\Delta\mu_{H^+}$ through the reduction of S- and N-oxides is widespread among prokaryotes and eukaryotes (6-8). DMSO reductase (DmsABC) of *E. coli* is a complex, membrane bound, [Fe-S] and molybdenum containing enzyme with a broad substrate specificity (6,9). The enzyme has been over-expressed in membranes and purified. DmsABC has been well characterized at the biochemical, biophysical and genetic level and is proving to be an excellent model system for investigating the structure and mechanism of electron transfer chain complexes and molybdoenzymes. The aim of this introduction is to describe some of the major enzymes involved in *E. coli* respiration, review the current state of knowledge of DmsABC and provide a model for electron transfer through this enzyme.

II. The Respiratory Chains of *E. coli*

E. coli has a diverse repertoire of respiratory enzymes that utilize a number of different electron donors and terminal electron acceptors (Figure 1-1) (3,10). Succinate,

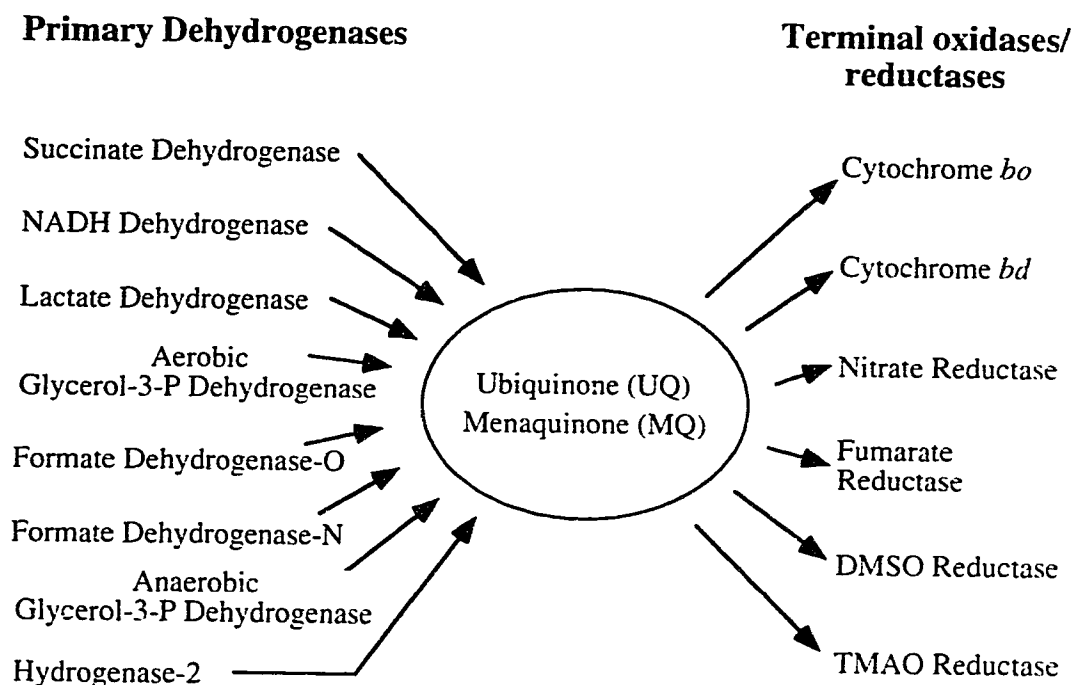


Figure 1-1 The *E. coli* Respiratory Systems

The design of the *E. coli* respiratory systems is modular. The primary dehydrogenases and the terminal oxidases and reductases are linked through the quinone pool. Energy from the oxidation of substrates by the primary dehydrogenases is used to reduce quinone (UQ, MQ) to quinol (UQH₂, MQH₂) which is oxidized by the terminal oxidases/reductases, generating a proton gradient in the process.

lactate, glycerol, formate, NADH and H_2 serve as electron donors aerobically, while all of the substrates but succinate can be used anaerobically. Ubiquinone (UQ) and menaquinone (MQ), function as electron collectors which shuttle between the dehydrogenases and the terminal oxidases/reductases. *E. coli* produces two quinol oxidases which reduce O_2 , and at least five terminal reductases which reduce nitrate, fumarate, DMSO, trimethylamine N-oxide (TMAO) and a host of other S- and N-oxides in anaerobic environments. The choice of the terminal electron acceptor is hierarchical, governed by accessibility and the free energy available from the reduction of the electron acceptor (2,3,10). In a given growth medium, the compound with the largest free energy change ($\Delta G_0'$) upon reduction (highest redox potential, $E_{m,7}$) is preferred (Table 1-1). The simplicity of the respiratory chains together with the ease of genetic manipulations in *E. coli* have contributed significantly to the understanding of the mechanisms of energy transduction.

A. Energy transduction

Formation of a proton gradient by a respiratory system can occur as a result of proton translocation across a membrane (vectorial protons), utilization of protons in the reactions catalyzed by the electron transfer enzymes (scalar protons), or a combination of these two mechanisms. The formation of a gradient using scalar reactions couples the movement of electrons from the positive (periplasmic) to the negative (cytoplasmic) side of the membrane to the consumption of protons from the cytoplasm and release of protons into the periplasm. This corresponds to the electron-carrying limb of the redox loop mechanism proposed by Mitchell (12).

B. Aerobic Respiration

The *E. coli* cell is most efficient at energy generation when oxygen is used as the terminal electron acceptor. A variety of primary dehydrogenases (Figure 1-1) may be produced, depending on the growth conditions, which couple oxidation of substrate to

TABLE 1-1
Redox Potentials and Free Energy Changes of
Alternative Respiratory Electron Acceptors

| Acceptor | $E_{m,7}$ (mV) | $\Delta G_o'$ (NADH as donor) (kJ mol ⁻¹) |
|----------|-------------------|--|
| Oxygen | +820 | -220 |
| Nitrate | +420 | -143 |
| DMSO | +160 | -92 |
| TMAO | +130 | -87 |
| Fumarate | +30 | -67 |

$\Delta G_o'$ values are calculated from the $E_{m,7}$ obtained from (3,10,11).

reduction of UQ to ubiquinol (UQH₂). UQ is the primary quinone species produced under aerobic conditions and acts as an electron carrier between the dehydrogenases and the terminal oxidases. The two enzymes involved in O₂ reduction are cytochrome *bo* and cytochrome *bd*. Cytochrome *bd* has a higher affinity for O₂ than cytochrome *bo* and is expressed under conditions of low O₂ tension (13). The quinol oxidases employ different mechanisms of energy transduction (14). Cytochrome *bd* relies on two spatially-separated active sites; cytoplasmic protons are consumed in the reduction of O₂ to water while the quinol oxidation and release of protons occurs on the periplasmic side of the membrane. Cytochrome *bo* uses the same chemical reactions to translocate protons but also pumps additional cytoplasmic protons into the periplasm.

C. Anaerobic Respiration

In the absence of oxygen, the enzyme composition of the membrane changes. A number of new primary dehydrogenases and terminal reductases are synthesized and MQ becomes the major quinone species present (3,10). The cell respire using a wide variety of electron donors such as glycerol, formate, and H₂. Nitrate, fumarate, DMSO and TMAO are used as terminal electron acceptors by the reductases. Several enzymes involved in anaerobic electron transport are described below.

1. Glycerol 3-Phosphate Dehydrogenase

Growth on glycerol in an anaerobic environment is due primarily to the anaerobic glycerol 3-phosphate (G3P) dehydrogenase which catalyzes the oxidation of G3P to dihydroxyacetone phosphate (DHAP) and the reduction of MQ to menaquinol (MQH₂) (Figure 1-2). This enzyme consists of three subunits (GlpACB) which are organized into a catalytic dimer (GlpAC) held loosely to the inner surface of the cytoplasmic membrane by a membrane anchor (GlpB) (15). The enzyme is a flavoprotein and potential binding sites for FAD and FMN were identified in GlpA and GlpC, respectively. At least one [Fe-S] cluster is present in GlpB and appears to be linked to the quinone pool (16). In the

Cytoplasm

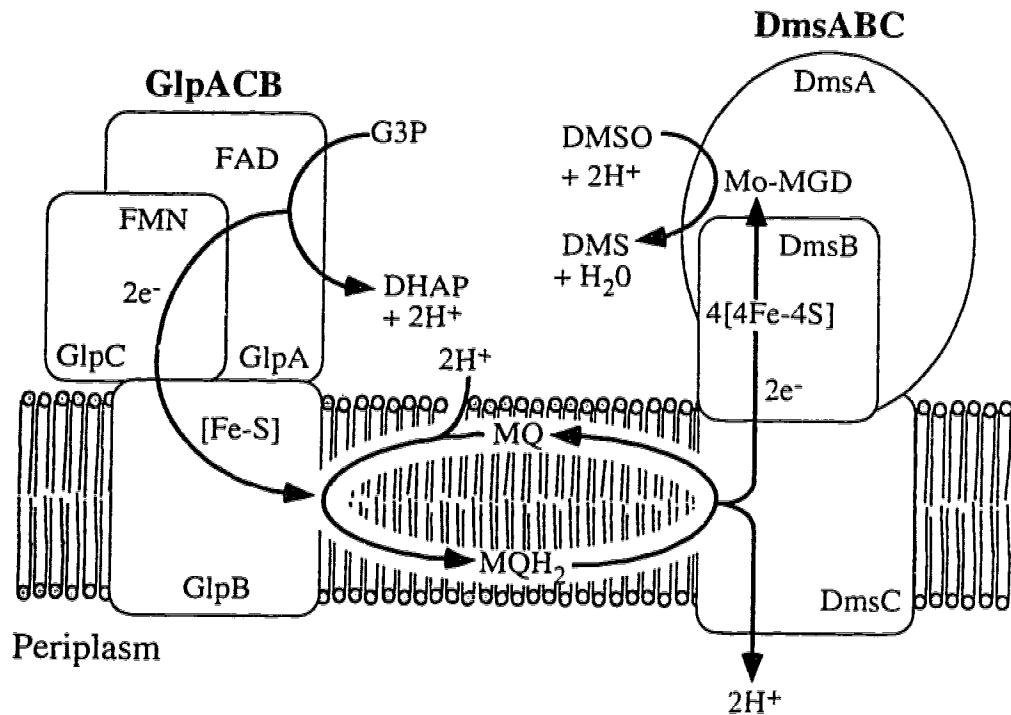


Figure 1-2 The Anaerobic Respiratory Chain Comprised of GlpACB and DmsABC

E. coli grown anaerobically on glycerol and DMSO, produces a simple electron transport chain comprised of a primary dehydrogenase (GlpACB), the menaquinone pool, and a terminal reductase (DmsABC). GlpABC oxidizes G3P to DHAP and reduces MQ. GlpABC contains FAD and may also contain FMN and at least one [Fe-S] cluster. DmsABC oxidizes MQH₂, releasing two protons into the periplasm and transferring two electrons through the [4Fe-4S] clusters in DmsB to the molybdenum cofactor (Mo-MGD) in DmsA. DMSO is reduced to DMS at the Mo-MGD cofactor, consuming cytoplasmic protons.

proposed mechanism of electron transfer in GlpABC; an equal amount of protons are produced by oxidation of G3P and consumed by quinone reduction.

2. Formate Dehydrogenases

E. coli has three formate dehydrogenases, FDH-H, FDH-N, and FDH-O, which are all molybdenum and selenium containing enzymes (Table 1-2). All three enzymes are involved in anaerobic electron transfer but FDH-O is also expressed and active in aerobic cells (60). The FDH-H (FdhF) is part of the formate hydrogenlyase complex with hydrogenase-3 which couples the oxidation of formate to the production of H₂. This sequence of reactions consumes a proton from the cytoplasm to form H₂ which can be used by hydrogenase-2 for quinone reduction. FdhF contains a Mo cofactor and a selenocysteine (Se-Cys) involved in formate oxidation and may contain an [Fe-S] cluster involved in electron transfer to hydrogenase-3. FDH-N (FdnGHI) and FDH-O (FdoGHI) are very similar in sequence and are both comprised of a catalytic subunit containing a Mo cofactor and a Se-Cys residue, an electron transfer subunit with the capacity to ligate multiple [Fe-S] clusters, and a membrane intrinsic subunit containing two *b*-type hemes (34,36,60). The mechanism of energy generation by FDH-N (and FDH-O) is based on the proposed organization of the enzyme in the membrane. Formate oxidation to CO₂, which produces protons, occurs on the periplasmic side of the membrane, electrons are transferred through the redox centers of the enzyme to the cytoplasmic side of the membrane which is the site of quinone reduction (uptake of protons) (26). However, the orientation of FDH-N has not been experimentally determined.

3. Nitrate Reductase

E. coli contains two membrane-bound nitrate reductases involved in electron transfer. The enzymes are highly homologous (approximately 80% amino acid sequence identity) but NarGHI is the major anaerobic enzyme while NarZYV is produced aerobically (21,23). The nitrate reductases have subunit compositions similar to FDH-N.

TABLE 1-2
Prokaryotic MolybdoEnzymes

| Enzyme | Subunits | Organism | Location | Prosthetic Groups | References |
|---------------------------------|---------------------|--|----------------|--|--------------|
| DMSO reductase | DmsABC | <i>E. coli</i> , <i>Haemophilus influenza</i> | membrane-bound | Mo-MGD, 4[4Fe-4S] | (17-20) |
| nitrate reductases | NarGHI & NarZYV | <i>E. coli</i> , <i>Bacillus subtilis</i> , <i>Thiosphaera pantotropha</i> | membrane-bound | Mo-MGD, 3[4Fe-4S], [3Fe-4S], cyt <i>b</i> | (21-26) |
| polysulfide reductase | PsrABC | <i>Wolinella succinogenes</i> | membrane-bound | Mo-MGD, 4-5[4Fe-4S]* | (27-29) |
| thiosulfate reductase | PhsABC | <i>Salmonella typhimurium</i> | membrane-bound | Mo cofactor*, 4-5[4Fe-4S]* | (30) |
| formate hydrogenlyase | FdhF + Hyc proteins | <i>E. coli</i> | membrane-bound | Mo cofactor, Se-Cys, [4Fe-4S]* | (31-33) |
| formate dehydrogenases | FdnGHI & FdoGHI | <i>E. coli</i> | membrane-bound | Mo-MGD, Se-Cys, 4-5[4Fe-4S]*, cyt <i>b</i> | (5,24,34-36) |
| | FdhABC | <i>Methanobacterium formicicum</i> | membrane-bound | Mo-MGD, FAD, 2-3[4Fe-4S] | (37-40) |
| | FdhABC | <i>W. succinogenes</i> | membrane-bound | Mo-MGD, 4-5[4Fe-4S]*, cyt <i>b</i> | (28,41) |
| nitrate reductase | NapAB | <i>T. pantatrophia</i> , <i>E. coli</i> , <i>Alcaligenes eutrophus</i> | periplasmic | Mo cofactor, [4Fe-4S], cyt <i>c</i> | (42-46) |
| assimilatory nitrate reductases | NasAC | <i>Klebsiella pneumoniae</i> | cytoplasmic | Mo cofactor*, [4Fe-4S]*, FAD*, NADH* | (47,48) |
| | NarB | <i>Synechococcus</i> ssp. 7, <i>Oscillatoria chalybea</i> | cytoplasmic | Mo cofactor*, [4Fe-4S]* | (49,50) |
| | NasCB | <i>B. subtilis</i> | cytoplasmic | Mo cofactor*, FAD*, NADH* | (51) |
| DMSO reductase | Dmsr | <i>Rhodobacter capsulatus</i> , <i>R. sphaeroides</i> | periplasmic | Mo-MGD | (52,53) |
| TMAO reductase | TorA | <i>E. coli</i> | periplasmic | Mo cofactor | (54,55) |
| biotin sulfoxide reductases | BisC & BisZ | <i>E. coli</i> , <i>R. sphaeroides</i> , <i>H. influenza</i> | cytoplasmic | Mo cofactor | (20,56-59) |

* existence of prosthetic group is based on sequence homology

The catalytic subunits (NarG and NarZ) contain a Mo cofactor, the electron transfer subunits (NarH and NarY) ligate one [3Fe-4S] cluster and three [4Fe-4S] clusters, and the membrane anchor subunits contain two *b*-type hemes (Table 1-2). The NarG and NarH (NarZY) subunits form a catalytic dimer in the cytoplasm. The model of electron transfer proposed for NarGHI is similar to that of the redox loop in which quinol oxidation occurs at the periplasmic surface with release of protons and transfer of electrons through the hemes and the [Fe-S] clusters to the Mo cofactor, at which nitrate reduction and consumption of protons occurs (26). Most anaerobic electron transfer enzymes use MQ exclusively but nitrate reductase is able to oxidize both UQH₂ and MQH₂ (5).

4. Fumarate reductase

Fumarate reductase (FrdABCD) is an anaerobic terminal reductase that catalyzes the reduction of fumarate to succinate (61). It is very similar to succinate dehydrogenase which catalyzes the reverse reaction under aerobic conditions, and FrdABCD can also catalyze succinate oxidation. FrdABCD comprises a catalytic subunit containing a covalently bound FAD (FrdA), an electron transfer subunit containing multiple [Fe-S] clusters (FrdB) and two membrane anchor subunits which function in MQH₂ oxidation (FrdCD) (61-63). FrdB ligates three iron-sulfur clusters; Center FR1 is a [2Fe-2S] cluster, $E_{m,7} = -20$ mV, Center FR2 is a [4Fe-4S] cluster, $E_{m,7} = -330$ mV and Center FR3 is a [3Fe-4S] cluster, $E_{m,7} = -70$ mV (61). The proposed mechanism of electron transfer through fumarate reductase involves two quinone binding sites similar to the sites in the photoreaction center (63-65). A loosely bound quinone cycles through the reduced, semiquinone and oxidized states at the Q_B site. Electrons from the quinol oxidation are transferred to the tightly bound quinone at the Q_A site which cycles between the semiquinone and oxidized states; however, no semiquinone radical has been reported for FrdABCD. The [3Fe-4S] cluster in FrdB is believed to be close to a quinone binding site

and would accept electrons from the Q_A semiquinone (66). Electrons are transferred through the $[2Fe-2S]$ cluster to the FAD for the reduction of fumarate. The $E_{m,7}$ of FR2 is much lower than those of the MQ/MQH_2 ($E_{m,7} = -74$ mV) or fumarate/succinate ($E_{m,7} = 30$ mV) couples but there is evidence that this cluster may also be involved in electron transfer (67,68).

III. DMSO Reductase of *E. coli*

A. Ecology

DMSO and TMAO reduction has been studied extensively, because of the natural abundance and importance of these compounds. DMSO arises naturally from phytoplankton degradation in marine environments and from photo-oxidation of dimethyl sulfide (DMS) in the atmosphere (13). DMS is the major source of reduced sulfur in the global sulfur cycle, accounting for 50% of the total biogenic input of sulfur to the environment. It is emitted by oceans and plays a role in global climate control (69-71). DMS is both consumed by microorganisms in sea water and produced by the reduction of DMSO by microorganisms. DMSO is of low volatility and highly hygroscopic. It is therefore scavenged from the atmosphere by rain and returned to earth (71). A number of man made processes contribute to the buildup of DMSO in the environment. It is present as a waste product of paper mills, used as a solvent and as a vehicle for the administration of drugs. Production of DMS occurs during the course of degradation of sulfur containing pesticides. Delineation of the mechanism of DMSO reduction may contribute to our understanding of the overall global sulfur cycle (7,69-72).

TMAO is a major osmolyte and is found in relatively high concentrations in marine invertebrates and fish (8,73,74). TMAO has been shown to protect proteins from the effects of denaturants such as urea and from high concentrations of ions which would normally perturb enzyme function (73,74). After death of a TMAO containing organism, the TMAO is reduced to trimethylamine by bacteria; this produces the distinctive odor of

rotting fish (8). TMAO reduction by bacteria is a major cause of spoilage of fish and therefore of great concern to the fishing industry.

B. Bacterial Reduction of S-and N-oxides

DMSO and TMAO reductase activity is widespread in microorganisms and is coupled to generation of a proton gradient (6). Most DMSO reductases have a broad substrate specificity, reduce both DMSO and TMAO (in addition to other S- and N-oxides) and contain molybdenum at their active sites (9,54,75,76). TMAO reductase is also a molybdoenzyme and reduces many of the same N-oxide substrates as the DMSO reductases, but it does not have the ability to reduce S-oxides (77,78). The TMAO reductases and the majority of DMSO reductases, with the exception of DmsABC, are periplasmic, monomeric enzymes containing only one prosthetic group, the Mo cofactor (Table 1-2). These periplasmic enzymes are thought to interact with *b*- and *c*-type cytochromes to accept reducing equivalents but the mechanism of energy transduction is not understood (11,79). DmsABC is a heterotrimer, located on the cytoplasmic surface of the plasma membrane, and contains multiple [Fe-S] clusters in addition to the Mo cofactor (19,80).

C. Bioenergetics of Growth via DmsABC

1. Growth on S- and N-oxides

Bilous and Weiner demonstrated that *E. coli* is able to grow using DMSO as the sole terminal electron acceptor and that growth on DMSO leads to the formation of a $\Delta\mu_{H^+}$ (81,82). DmsABC was shown to be solely responsible for growth on DMSO in *E. coli* (83). This enzyme is also able to sustain bacterial growth on TMAO, methionine sulfoxide, pyridine N-oxide, 3-picoline N-oxide, and 4-picoline N-oxide (78,81).

2. The Electron Transport Chain Terminating in DmsABC

The non-fermentable substrate glycerol is most frequently used as both an energy and carbon source for growth with DMSO as terminal oxidant. Glycerol is phosphorylated to G3P prior to oxidation by the anaerobic G3P dehydrogenase, GlpACB (3). Glycerol can be replaced by H₂, formate and substrates which generate NADH, but apparently not by D- or L-lactate (81,82). Reducing equivalents from the oxidation of G3P are used to reduce MQ. Most anaerobic terminal reductases, including DmsABC, accept reducing equivalents solely from MQH₂ (6). A redox loop model for $\Delta\mu_{\text{H}^+}$ generation by electron flow from G3P to DMSO is presented in Figure 1-2. This mechanism relies on the scalar distribution of redox reactions across the cytoplasmic membrane to generate the observed $\Delta\mu_{\text{H}^+}$. The site of MQ reduction by GlpACB is formally on the cytoplasmic side of the membrane, whereas the site of MQH₂ oxidation by DmsABC is formally on the periplasmic side. A total of two protons disappear from the cytoplasm and are released into the periplasm per pair of electrons.

3. H⁺/2e⁻ Stoichiometry

Measurements of the H⁺/2e⁻ ratio in whole cells, using glycerol as the electron donor, gave a value of 2.9 H⁺/2e⁻ for DMSO respiration and 3.3 H⁺/2e⁻ for nitrate respiration (82). The model of the electron transfer chain (Figure 1-2) allows for 2 H⁺ to be translocated per pair of electrons via the oxidation of MQH₂ at DmsC. The additional H⁺ measured suggests there may be two sites of proton translocation during electron flow from GlpABC to DMSO or nitrate. Proton translocation coupled to DMSO reduction was not inhibited by azide or cyanide but was inhibited by the MQ analog 2-n-heptyl-4-hydroxyquinoline N-oxide (HOQNO).

D. The *dms* Operon

1. Structure of the Operon

The *dmsABC* operon is located at 20' minutes on the *E. coli* chromosome and contains three open reading frames encoding polypeptides of 87 350, 23 070 and 30 789 Da (Figure 1-3) (17,84). Preceding the predicted ATG start of *dmsA* is a GGCGG Shine-Dalgarno sequence (85). The ribosome binding site of *dmsB* overlaps the *dmsA* stop codon and that of *dmsC* overlaps *dmsB*. A transcription start site has been determined by Eiglmeier *et al.* (86), 218 nucleotides upstream from the initiating ATG. This is an unusually long 5' untranslated region and the reason for this is not known. The transcriptional start is preceded by a typical -10 region but a consensus -35 region is not present. This is typical of genes that are under positive regulation by a DNA-binding protein (87). An FNR binding site is predicted to be about 40 base pairs upstream of the transcriptional start. Three potential half-sites for NarL binding have been identified at positions -39, -19 and +3 relative to the transcriptional start site, the first two of which are shown in Figure 1-3 (86,88). Seven base pairs following *dmsC* is a classical p-independent transcriptional terminator comprising a symmetrical G-C rich region preceding a stretch of T residues (17). A second *dmsABC* operon has been sequenced from *Haemophilus influenzae* (20).

2. Organization of the *dms* Operon

The organization of the polypeptides encoded by the *dms* operon closely parallels that seen for the operons encoding fumarate reductase, nitrate reductase, polysulfide reductase, thiosulfate reductase and formate dehydrogenase (6). These enzymes are all membrane-bound components of electron transfer chains and, with the exception of fumarate reductase, are molyboenzymes (Table 1-2). In all cases, the 5' proximal gene (*dmsA*, *frdA*, *narG*, *narZ*, *psrA*, *phsA*, *fdnG*, *fdoG*, *W. succinogenes FdhA*) encodes a large catalytic subunit which contains an electron collecting cofactor, Mo cofactor or FAD,

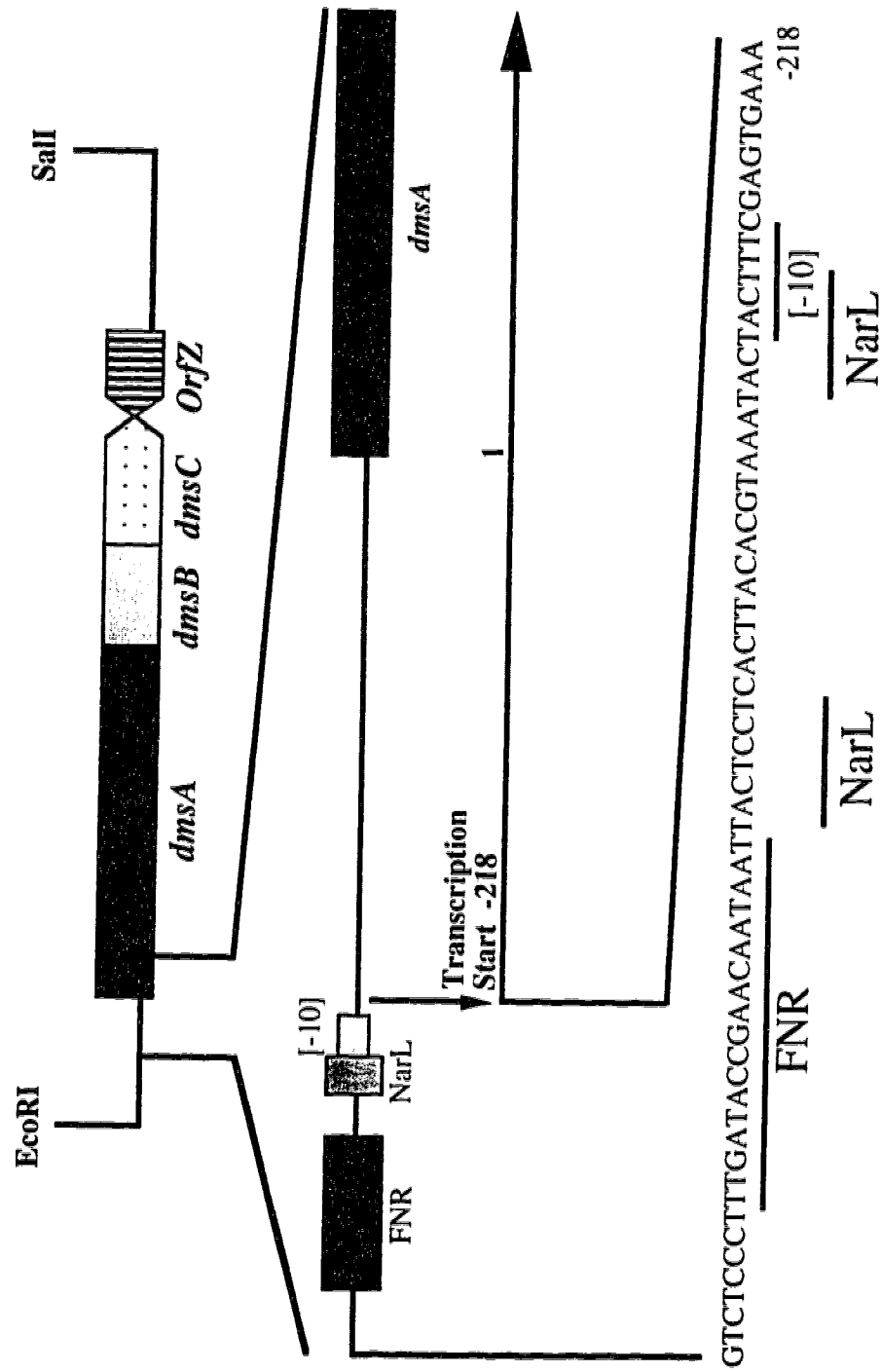


Figure 1-3 Organization of the *dms* Operon

The DNA fragment containing the *dmsABC* operon is depicted. The promoter region and the putative FNR and NarL binding sequences are described in the text.

able to undergo one or two electron oxidation-reduction. The next gene (*dmsB*, *frdB*, *narH*, *narY*, *psrB*, *phsB*, *fdnH*, *fdoH*, *W. succinogenes FdhB*) encodes an electron-transfer subunit containing multiple groups of Cys residues which ligate [Fe-S] clusters. The distal gene(s) (*dmsC*, *frdCD*, *narI*, *narV*, *psrC*, *phsC*, *fdnI*, *fdoH*, *W. succinogenes FdhC*) encode the membrane anchor function. These subunits are membrane intrinsic and anchor the soluble catalytic subunits to the membrane, in addition to binding quinone and stabilizing the catalytic subunits.

The subunits and their organization in this group of enzymes are not completely homologous. In fumarate reductase the anchor function is contained in two small, closely associated subunits. The membrane intrinsic subunits of the nitrate reductases and formate dehydrogenases contain *b*-type hemes which are not found in the other enzymes. The *nar* operons encode a fourth subunit (*narJ*, *narY*) which is necessary for the formation of the active enzyme (89,90). The formate dehydrogenase from *Methanobacterium formicicum* (*fdhCAB*) and the succinate dehydrogenase (*sdhCDAB*) from *E. coli* share this type of subunit composition but the genes are organized so that the membrane anchor(s) is followed by the catalytic and electron transfer subunits (37,39,61).

E. Regulatory mechanisms

E. coli selects the most efficient energy generating system for a particular environment (1,2). Thus O₂ will be used in preference to nitrate, DMSO or fumarate, and nitrate will be used in preference to fumarate or DMSO. There does not seem to be any selection between DMSO, TMAO and fumarate, although the synthesis of TMAO reductase is induced by TMAO in the medium (81,91). DMSO reductase is expressed under anaerobic conditions in the absence of nitrate (9,82,84).

1. FNR

DmsABC is induced about 65-fold by anaerobiosis via a positive gene activator protein (FNR) and Eiglmeier *et al.* have shown that this is due to an increase in *dmsABC* mRNA transcription (86). FNR is a global regulator which induces the expression of several anaerobic enzymes including nitrate reductase, fumarate reductase, and cytochrome *bd* (87,92) but not TMAO reductase (93). It also represses the expression of selected aerobic enzymes such as cytochrome *bo* (94,95). FNR is composed of two domains. The carboxy proximal domain is very similar to the CRP protein (which mediates cAMP dependent catabolite repression) and contains a helix-turn-helix motif predicted to bind to DNA, as has been shown for the analogous region of CRP (96). The half-site sequence of the consensus FNR binding site (AAATTGAT) is very similar to that of CRP and purified FNR has been shown to bind as a dimer to inverted repeats of this sequence (86,97-99). The amino proximal domain of FNR is responsible for sensing the redox state of the cell and contains four Cys residues, three of which, together with one Cys outside of this region, are essential for function (100). FNR contains Fe and sulfide and is likely to ligate one [4Fe-4S] cluster per monomer (101,102). The presence of the [Fe-S] cluster under anaerobic conditions increased dimerization and the DNA binding affinity. The [Fe-S] cluster is extremely sensitive to oxygen and loss of the cluster inactivates FNR, suggesting that oxygen regulates FNR through the lability of the [Fe-S] cluster.

2. Nitrate

The presence of nitrate in the growth medium represses the synthesis of the less energetically favorable respiratory pathways terminating in DMSO, TMAO or fumarate reduction (2,103). This level of regulation is mediated by two interacting, two-component regulatory systems, NarXL and NarPQ, which control the transcription from nitrate and nitrite regulated promoters. NarX and NarQ are the “sensors” and detect the availability or

change in the nitrate and nitrite concentrations. In the presence of nitrate both NarX and NarQ autophosphorylate at a His residue and transfer this phosphate group to the response regulator proteins, NarL or NarP (104,105). Upon phosphorylation, NarL and NarP activate or repress the transcription of sensitive genes by binding to a specific DNA sequence. A consensus half-site for NarL binding, TAC(C/T)N(A/C)T has been proposed on the basis of sequence comparisons and limited mutational analyses (88). NarP and NarL appear to regulate different promoters (103,106). Both NarX and NarQ will phosphorylate NarL but NarX can also rapidly dephosphorylate NarL (104,105). Nitrate regulation is complex but a model of the interaction of the regulatory components has been proposed by Rabin and Stewart (106). In the presence of nitrate both sensor proteins would phosphorylate both NarL and NarP. In the presence of nitrite NarQ phosphorylates NarP and NarL but the NarL phosphorylation is either blocked by NarX or NarX dephosphorylates NarL.

3. TorR

Yamamoto *et al.* (107) have described a locus in *E. coli*, *torR*, that appears to be necessary for *dmsABC* expression as well as for expression of the TMAO reductase, nitrate reductase and two formate dehydrogenases (H and N). Membranes from the *torR* mutant strain show decreased levels of activity of these enzymes. The level of molybdenum cofactor is normal in this strain. The *torR* locus maps to 80' on the *E. coli* chromosome, making it distinct from the FNR and nitrate regulation systems. The response regulator gene for induction of TMAO reductase by TMAO (108,109) has also been designated *torR* and must be distinguished from the locus described by Yamamoto *et al.* (107).

4. Molybdenum

Uptake of molybdate into *E. coli* is largely dependent on the proteins encoded by the *modABCD* operon (formerly *chlD*) although some transport at higher molybdate

concentrations occurs with the sulfate transport system and an as yet undefined transporter (110). ModABC form a periplasmic binding protein-dependent transport system for molybdate while ModD is suggested to be an outer membrane protein that helps molybdate enter into the periplasm (110,111). Expression of the molybdate transporter is repressed by Mo (110,112). This repression relies on the presence of a regulatory motif in the *mod* promoter region, implicating the participation of a molybdenum-responsive regulatory protein (112). Molybdate also has an effect on the expression of operons encoding Mo cofactor containing enzymes. Expression of a *dmsABC-lacZ* fusion was repressed in a *mod* mutant indicating that molybdenum is required for maximal expression (113). The *fdhF* and *hyc* operons which encode formate hydrogenlyase also require molybdate for expression (110). The effects of molybdate on gene expression are independent of the *moa*, *moe*, *mob* and *mog* gene products required for synthesis of the molybdopterin guanine dinucleotide (see Section H-1) (110,113) and also appears to be distinct from the nitrate regulatory system (114).

5. ArcAB

ArcA and ArcB are members of a two component regulatory system which represses the expression of genes for proteins involved in aerobic metabolism under anaerobic conditions (1,87). There is no evidence that this global regulator modulates DMSO reductase expression.

F. Enzymology of *DmsABC*

Purified enzyme is a heterotrimer of the *DmsABC* subunits and catalyzes DMSO-dependent oxidation of reduced benzyl viologen (BV^{•+}). It has a very broad substrate specificity and is able to reduce many S- and N-oxide compounds as well as chlorate. Maximal activity is observed with TMAO, but the enzyme has the lowest K_m for DMSO: 180 μ M vs. 700 μ M (9). The catalytic dimer, *DmsAB*, is able to reduce DMSO using

BV^{•+} as the electron donor but DMSO dependent oxidation of the MQ analog, 2,3-dimethyl-1,4-naphthoquinol (DMNH₂) requires the presence of the holoenzyme (83). BV^{•+}, reduced methyl viologen and DMNH₂ are efficient electron donors and exhibit a stoichiometry of 2 BV^{•+}/DMSO, 2 methyl viologen/DMSO and 1 DMNH₂/DMSO. Exogenous ammonium molybdate has no effect on activity. Optimal activity is obtained at pH 6.8 with MOPS (3-[N-morpholino]propanesulfonic acid) buffer, whereas potassium phosphate buffer inhibits activity (6,8,27). Fe²⁺ was reported to increase enzyme activity but this occurs only in phosphate buffer, indicating that the decrease in activity in phosphate buffer may be due to loss of Fe from the enzyme.

Comparison of DmsABC with the periplasmic DMSO reductases indicates a similar substrate specificity. DMSO reductase from *Rhodobacter sphaeroides* and *Rhodospirillum rubrum* can reduce DMSO, TMAO, methionine sulfoxide and chlorate (115,116). The periplasmic enzymes displayed maximal activities with TMAO but the K_m values for DMSO (15 μM and 670 μM) are much lower than those for TMAO (1000 μM and 2400 μM). The substrate specificity of the TMAO reductases from *E. coli* and *Roseobacter denitrificans* is restricted primarily to N-oxides. Both enzymes reduce TMAO, picolinic N-oxide, hydroxylamine and either chlorate or bromate but do not reduce S-oxides (117,118). The periplasmic DMSO and TMAO reductases are more stable than DmsABC. The DMSO reductase activity of the periplasmic enzyme can be detected on polyacrylamide gels run under both denaturing and non-denaturing conditions (76) while the DmsABC activity is very susceptible to SDS and all activity is lost at 0.001% SDS. The TMAO reductase activity is stable at 70°C for at least one hour (119) while less than 10% of DmsABC activity remains after 5 minutes incubation at 65°C (6).

G. Topological organization of DMSO reductase

Everted vesicles isolated from bacteria overexpressing DMSO reductase are studded by dumb-bell type structures randomly arranged over the membrane as judged by

negative stain electron microscopy (80). The structures were not seen in the wild-type or in strains deleted for the DmsC polypeptide, and were shown to be the DmsAB subunits by immunogold electron microscopy with anti-DmsA or anti-DmsB antibodies. These studies suggest that DmsA and B form a side-by-side dimer on the cytoplasmic surface which is held to the membrane by the integral DmsC subunit (Figure 1-4). The cytoplasmic surface location has been confirmed by a combination of thin section immunogold electron microscopy, antibody labelling, proteolytic digestion, substrate accessibility, and lactoperoxidase catalyzed iodination (80). Electron paramagnetic resonance (EPR) spectroscopy studies using the paramagnetic broadening reagent, dysprosium(III), have confirmed the cytoplasmic location of one of the [Fe-S] clusters (120).

H. DmsA

1. DmsABC is a Molybdoenzyme

DmsABC was shown to contain a Mo cofactor by a variety of methods. In all molybdoenzymes except nitrogenase, the Mo cofactor comprises a Mo atom associated with a substituted pterin molecule (molybdopterin). There are several genetic loci (*moa*, *mob*, *mod*, *moe*, and *mog*, formerly named *chlA*, *chlB*, *chlD*, *chlE*, and *chlG*) involved in the synthesis of the Mo cofactor (121). The *moa* and *moe* operons are involved in the synthesis of the molybdopterin from guanosine. The *mob* gene products are involved in further modification of the molybdopterin by addition of a guanine nucleotide. *mod*, as previously mentioned, is a Mo transporter. The function of *mog* is unclear but it may play a role in Mo association with the molybdopterin. The *moa*, *mod*, *moe*, and *mog* loci are necessary for growth on DMSO and this growth is inhibited by tungstate (81).

Extracts from purified DmsABC were able to complement the *Neurospora crassa* aponitrate reductase which is missing Mo cofactor. Oxidized derivatives of the cofactor

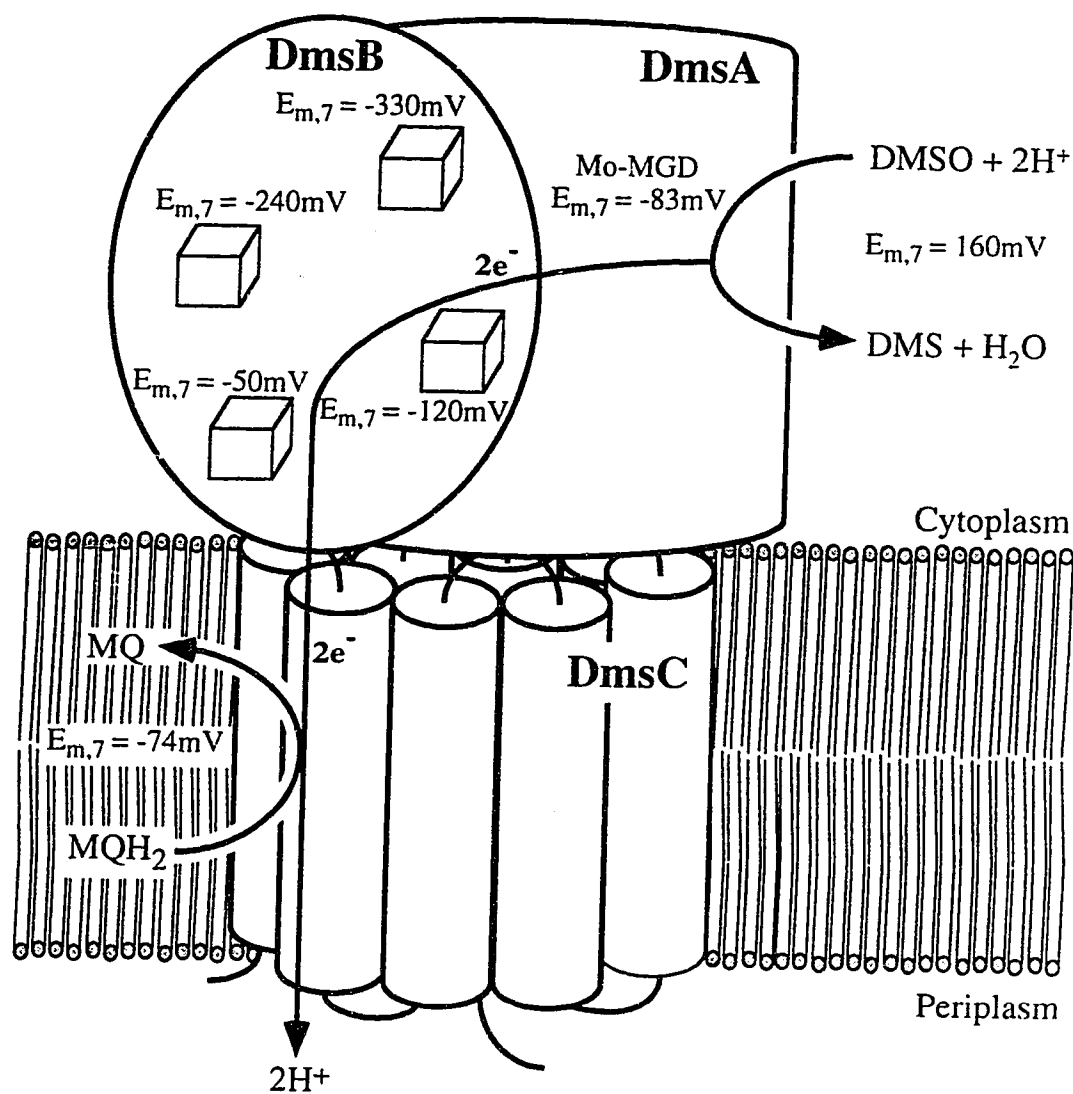


Figure 1-4 Topology and Mechanism in DmsABC

DmsA and DmsB are located on the inner surface of the cytoplasmic membrane. The membrane intrinsic subunit, DmsC, has eight transmembrane helices and the amino and carboxyl termini are located in the periplasm. DmsC contains the active site for quinol oxidation and transfers two electrons through the [Fe-S] clusters in DmsB to the Mo-MGD cofactor in DmsA, where the S- or N-oxide substrate is reduced. The midpoint potentials of the redox components are as shown.

were detected by optical and fluorescence spectroscopy after treatment of DmsABC with I_2 and KI at acidic pH (9). The presence of Mo in purified DmsABC was demonstrated by EPR spectroscopy (19). Sequence homologies with other prokaryotic molybdoenzymes indicate that DmsA binds the Mo cofactor.

2. Comparison with Other Molybdoenzymes

A large number of enzymes sharing homology with DmsA and containing Mo cofactors have the characteristics shown in Table 1-2. The existence of many of the prosthetic groups is proposed on the basis of sequence homologies and has not been proven experimentally. There are three distinct subgroups within this family. The membrane-bound enzymes are one such group that share a similar genetic organization and subunit makeup. FDH-H (FdhF) interacts with the gene products of the *E. coli hyc* operon to form formate hydrogenlyase (33), making its organization more complex than the rest of the enzymes in this group. The second group is composed of the assimilatory nitrate reductases and the periplasmic respiratory nitrate reductases which are soluble but contain a second subunit that fulfills an electron transfer capacity. The third group are soluble, monomeric enzymes such as the periplasmic TMAO and DMSO reductases and the biotin sulfoxide reductases. *b* and *c*-type cytochromes are involved in the reduction of TMAO and DMSO by the periplasmic reductases (11,79) and the electron donor for *E. coli* BisC is a small, heat-stable protein (protein-SH), similar to thioredoxin (122).

3. The Molybdenum Cofactor

Because the Mo cofactor is extremely labile, its structure was initially determined indirectly by analysis of oxidation products (reviewed in (121)). The structure of the molybdopterin cofactor, as proposed by Ragajopalan and colleagues, is shown in Figure 1-5. The 6-alkyl pterin has a four carbon sidechain containing a dithiolene, a hydroxyl group and either a terminal phosphate or a nucleotide. In DmsA and other *E. coli* molybdoenzymes the cofactor contains molybdopterin guanine dinucleotide (MGD)

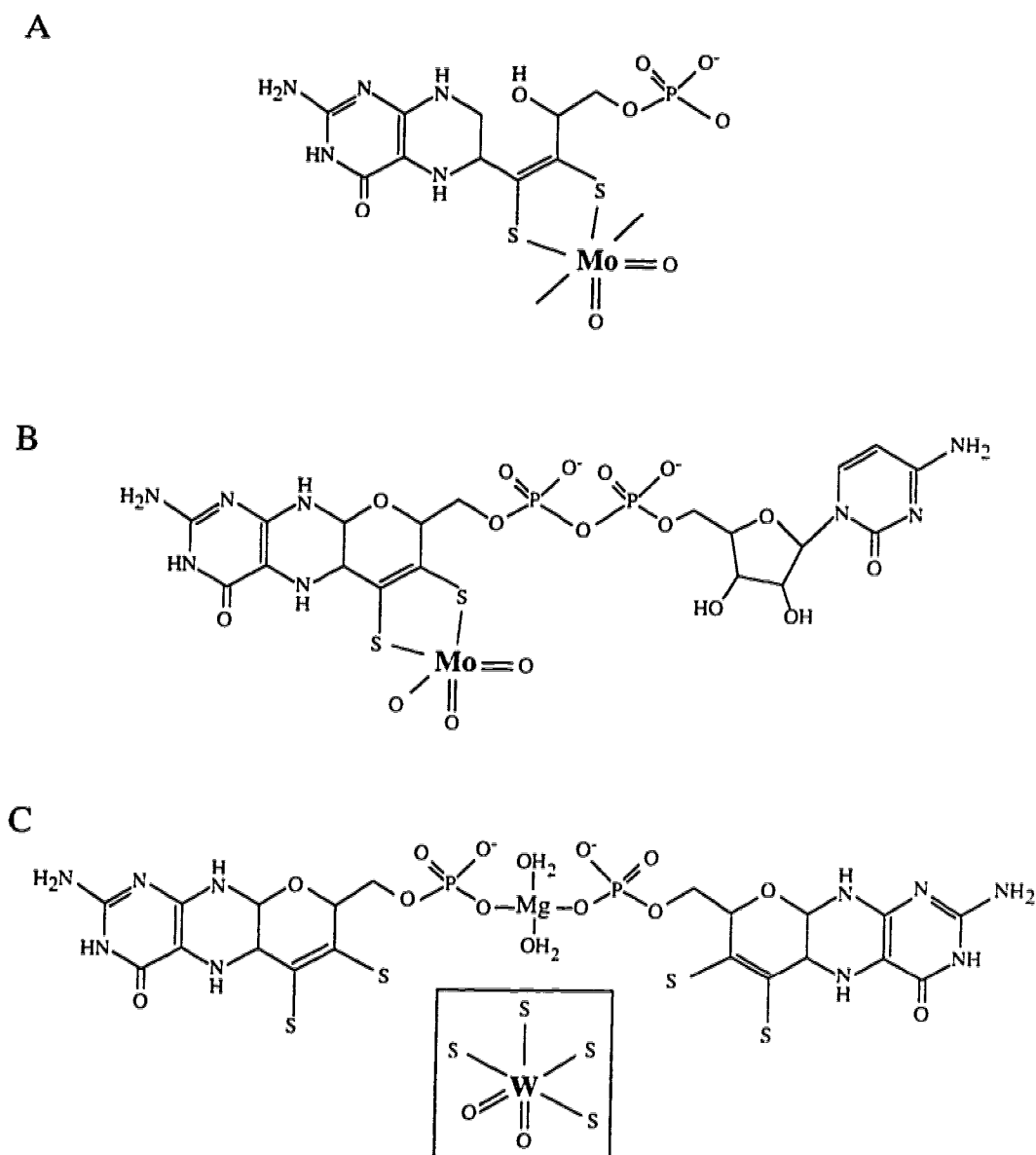


Figure 1-5 Molybdopterin Cofactors

A) The structure of the Mo-molybdopterin cofactor determined from chemical studies. B) The structure of Mo-molybdopterin cytidine dinucleotide from aldehyde oxidoreductase of *Desulfovibrio gigas*. C) The W-molybdopterin cofactor from *Pyrococcus furiosus* aldehyde ferredoxin oxidoreductase. The two molybdopterins are linked through their phosphate groups which coordinate a Mg ion. The inset shows the coordination of the W atom.

(18,121). In enzymes from other species the base can be guanine, cytidine, adenine or hypoxanthine, but Mo-MGD appears to be the most common cofactor (121). The dinucleotide forms of the cofactor appear to be exclusive to bacterial enzymes while the simple molybdopterin cofactor can be used by both prokaryotes and eukaryotes.

The crystal structures of two molybdopterin containing enzymes have recently been determined and the cofactors are shown in Figure 1-5. *Pyrococcus furiosus* aldehyde ferredoxin oxidoreductase (AOR) contains a novel tungsten dimolybdopterin cofactor (123) and the cofactor in *Desulfovibrio gigas* aldehyde oxidoreductase (MOP) is a Mo molybdopterin cytidine dinucleotide cofactor (Mo-MCD) (124). The molybdopterin in both structures was essentially identical to the previously determined structure with one small exception. An intramolecular cyclization of the sidechain by the hydroxyl group occurred to form a tricyclic compound. The tricyclic structure may only exist in the protein bound cofactor where it can be stabilized by the protein (123,124). In both structures the molybdopterin was hydrogen bonded to a Cys residue which ligated an [Fe-S] cluster, suggesting that the pterin ring may be involved in the electron transfer between the [Fe-S] clusters and the Mo (or W). In both enzymes the molybdopterin cofactor is located in the center of the enzyme with only a long, narrow tunnel for substrate access. Insertion of the cofactor would require either a significant structural rearrangement or sequential cofactor association and folding.

Recently, the Mo cofactor from *R. sphaeroides* DMSO reductase was demonstrated to contain two MGD molecules and one Mo atom for each mole of protein (125). Direct comparisons of the cofactors from *R. sphaeroides* DMSO reductase and DmsABC have indicated that the cofactor is the same. A partially purified prep of DmsABC was found to contain approximately 30% of the amount of MGD contained in the *R. sphaeroides* enzyme (18). Analysis of previously purified DmsABC indicated that only 0.3 moles of Mo were present per mole of enzyme (9). These studies suggest that the stoichiometry of the Mo to MGD to enzyme is the same in both enzymes and that the

cofactor in DmsABC is likely to be a dimolybdopterin. The proposed structure of the *R. sphaeroides* DMSO reductase Mo cofactor is similar to that of the tungsten cofactor structure in which the Mo is coordinated by the two dithiolene sulfurs from each molybdopterin.

4. The Molybdenum Environment

Molybdoenzymes catalyze a wide variety of two electron reactions involving the transfer of oxygen between substrate and water (126,127). Like flavins and quinones, Mo cofactors are able to accept/donate electrons singly or in pairs. The Mo cycles between the Mo(IV), Mo(V), and Mo(VI) oxidation states, and the oxygen transfer reactions of the molybdoenzymes occur at the Mo containing active site (126,127). The coordination of the Mo is of great interest in determining the reaction mechanism and the ligation of the Mo by both the protein and the molybdopterin. Most information on the Mo environment has come from EPR and extended X-ray absorption fine structure (EXAFS) spectroscopy. Most molybdoenzymes contain two oxo ligands (or one oxo and one sulfido ligand) to the Mo(VI) which become one oxo and one hydroxyl (or sulfhydryl) to Mo(V) and Mo(VI) (126,127). This redox chemistry is proposed to be important for the reaction mechanism although a complete mechanism has not been worked out for any molybdoenzyme (127). The sulfido group can be converted to an oxo group by an irreversible reaction with cyanide to give the inactive desulfo form of the enzyme. The enzymes which have a sulfido ligand (the molybdenum hydroxylases and formate dehydrogenase) have Mo centers with very low redox potentials (40,128). In addition to the oxo ligands, two to three sulfur linkages and a possible oxygen or nitrogen linkage are usually detected. Two of the sulfur ligands are the dithiolene groups of the molybdopterin and the third may come from a Cys residue in the protein as might the putative oxygen/nitrogen ligand. In the AOR structure, the W has four dithiolene ligands from the two molybdopterin and two additional ligands that may be oxo groups or glycerol from

the buffer or both (123). The Mo in MOP is five coordinate with two ligands from the dithiolene group of the molybdopterin and three oxygen ligands (124). Two of the oxygens are most likely the oxo groups as the enzyme crystallized was the inactive desulfo form while the third may represent a ligand from the protein.

The ability of DmsABC to generate a proton gradient across membrane vesicles is not inhibited by cyanide, indicating that the enzyme does not contain a sulfido ligand to the Mo. The EPR signal of Mo(V) in DmsABC membranes is similar to the high-pH form of the cofactor from *E. coli* nitrate reductase, indicating a similar ligand coordination and geometry (19). In *E. coli* nitrate reductase only one oxo ligand was detected in the EXAFS studies of the oxidized (Mo(VI)) enzyme (129). The Mo in DmsABC may also contain only one oxo ligand. The midpoint potentials of the Mo center in DmsABC are pH dependent but no coupled proton has been detected as in nitrate reductase. Recent experiments with *E. coli* formate dehydrogenase H (FdhF), which belongs to the DmsA family, indicate that the Se-Cys residue in this enzyme is a Mo ligand (130). In sequence alignments, the residue in DmsA corresponding to the Se-Cys is a Ser which could provide an oxygen ligand to the Mo (Section H-5). A total of four additional ligands to the Mo will come from the molybdopterin, providing the cofactor has two molybdopterin molecules.

5. Sequence Analysis of DmsA

DmsABC was one of the first bacterial molybdoenzymes sequenced and it was noted at that time that DmsA shared sequence identity with two molybdoenzymes from *E. coli*, FdhF and BisC (17). As more enzymes became sequenced, it was possible to define regions of homology (6,131,132). Figure 1-6 shows the sequence of DmsA with the seven regions of sequence identity underlined. Regions 2-7 are conserved in all of the enzymes.

| | | |
|-----|---|-----|
| 1 | MASSALTLPFSSRIAHAVDSAIPKTSDEKVIWSACTVNCGRCP [•] LRMHVVD [•] | 50 |
| 51 | <u>GEIKYVETDNTGDDNYDGLHOVRACLRGRSMRRRVYNPDRLKYPMKRVGA</u> Region 1 | 100 |
| 101 | <u>RGEGKFERISWEEAYDIIATNMORLIKEYGNESIYLN</u> [*] <u>NYGTGTLGGTMTRS</u> Region 2 | 150 |
| 151 | WPPGNTLVARLMNCCGGYLNHYGDYSSAOIAEGLNYTYGGWADGN [◆] SPSDI | 200 |
| 201 | <u>ENSKLVVLFGNPGETRMSGGGVTTYLEOAROKSNARMIIDPRYTD</u> Region 3 | 250 |
| 251 | <u>GREDEWIPIRPGTDAALVNGLAYVMITENLVDOAF</u> [*] <u>LDKYCVGYDEKTLPA</u> Region 4 | 300 |
| 301 | SAPKNGHYKAYILGEGPDGVAKTPEWASOITGVPADKIIKLAREIGSTKP | 350 |
| 351 | <u>AFISOGWGPORHANGEIATRAISMLAILTGNVGINGGNSGAREGS</u> Region 5 | 400 |
| 401 | VRMPTLENPIQTSISMFMWTD [*] AIERGPEMTALRDGVRGDKLDVPIKMIW | 450 |
| 451 | NYAGNCLINQHSEINR ^{**} THEILQDDKKCE [*] LIVVIDCHMTSSAKYADILLPD | 500 |
| 501 | <u>CTASEOMDFALDASCGNMSYVIFNDOVIKPRFECKTIYEMTSELAKRLGV</u> Region 6 | 550 |
| 551 | <u>EOOFTEGRTOEEWMRHL</u> YAQSREAIPELPTFEEFRKQGIFKKRDPQGHV | 600 |
| 601 | AYKAFREDPQANPLTTPSGKIEIYSQALADIAATWELPEGDVIDPLPIYT | 650 |
| 651 | PGFESYQDPLNKQYPLQLTG [*] FHYKSRVHSTYGNVDVLKAACRQEMWINPL | 700 |
| 701 | <u>DAOKRGIHNGDKVRIFNDRGEVHIEAKVTPRMMPGVVALGEGAWYDPDAK</u> Region 7 | 750 |
| 751 | RVDKGGCINVLTTQRPSP [*] LAKGNPSHTNLVQVEKV | 785 |

Figure 1-6 Molybdoenzyme Signature Sequences in DmsA

The sequence of DmsA is shown with the regions of sequence homology underlined. These regions were identified using the Blast network service at the National Center for Biotechnology Information (USA). Conserved residues are marked with a *. The Cys residues implicated in [Fe-S] binding (•) and the DmsA residue which corresponds to the FdhF Se-Cys (◆) are also marked.

Region 1 is conserved in all but the monomeric enzymes, *i.e.* the biotin sulfoxide reductases and the periplasmic DMSO reductases and TMAO reductase. The multi-subunit enzymes contain the consensus sequence, CysX₂₋₃CysX₃CysX_nCysX(Lys/Arg)Gly, where X is any amino acid and n is 27-39 residues. The arrangement of the four Cys residues is similar to that of sequences known to bind [4Fe-4S] clusters (Section I-3). The periplasmic nitrate reductase from *T. pantotropha*, NapAB, contains an EPR visible [4Fe-4S] cluster which is believed to be ligated by this sequence, raising the possibility that other enzymes in this family may ligate an [Fe-S] cluster in Region 1 (42). In the *E. coli* nitrate reductases, the first Cys residue is replaced by a His but His may also ligate a [4Fe-4S] cluster (133). This region may be involved in electron transfer between the catalytic subunits and the electron transfer subunits.

Region 2 contains a conserved Arg residue, at position 90 in DmsA, and a conserved proline. The Arg-90 sidechain may form ion pairs with the phosphate groups of the cofactor (6,132) but it should be noted that in the MOP structure the phosphate groups are not in contact with positively charged amino acids (123,124). Also in this region is a conserved Trp residue which is part of an SerTrpGluGluAla motif found in all of the proteins. In the MOP structure, π - π interactions were suggested to occur between the molybdopterin and a coplanar Phe residue located 3.4Å away (124). The conserved Trp in this region may interact with the pterin ring.

The Se-Cys residue of the *E. coli* formate dehydrogenases is located in Region 3. Replacement of the Se-Cys in FdhF with Cys by site-directed mutagenesis has shown the Se-Cys to be important for both catalytic activity and substrate binding (134). The Se-Cys has recently been demonstrated to be a ligand to the Mo, confirming its proximity to the active site (130). This residue in the other enzymes is a Cys in the remainder of the formate dehydrogenases and the nitrate reductases and a Ser in the S- and N-oxide reductases. All three residues would be capable of coordinating the molybdenum. The

reason for the difference of residue at this position is unclear but it is possible that the coordination at this position plays a role in modulating the midpoint potential of the Mo.

Regions 6 and 7 contain the sequences designated molybdopterin-binding oxidoreductase signatures 2 and 3 in the Prosite Dictionary. Not enough is known about these enzymes to propose specific roles for most of the homologous regions. The enzymes of this family probably all bind a Mo-MGD and the great degree of similarity indicates that the structures of these proteins will be similar. In AOR and MOP the cofactor is buried in the center of the enzyme, accessible only through a narrow channel (123,124). The narrowness of the substrate access tunnel makes it likely that the protein will fold around the cofactor (124). Residues from several different regions may contact the cofactor. Region 1 may form a separate domain as is seen in the AOR and MOP structures which have [Fe-S] and Mo domains.

I. DmsB

1. DmsB is an [Fe-S] Protein

The amino acid sequence of DmsB contains sixteen Cys residues arranged into four groups resembling sequences known to bind [4Fe-4S] clusters (17). The EPR spectrum of both purified and membrane bound DmsABC is a composite spectra of overlapping [4Fe-4S] clusters (19). With the magnetic interactions it is not possible to assign the features to individual clusters but the spectrum has been interpreted as two pairs of interacting clusters, based on comparisons with the eight iron ferredoxins (19). Potentiometric analyses of the enzyme indicated that four clusters are present with midpoint potentials, $E_{m,7} = -50, -120, -240, \text{ and } -330 \text{ mV}$. The Mo and the $E_{m,7} = -120 \text{ mV}$ cluster have been shown to interact when both are paramagnetic (19). The redox behavior of the two highest potential clusters has been shown to be similar to that of the two [4Fe-4S] cluster ferredoxins, indicating that the $E_{m,7} = -50 \text{ and } -120 \text{ mV}$ clusters are

ligated by one pair of Cys Groups in DmsB and that the two lowest potential clusters are ligated by the second pair (135).

2. Electron Flow in DmsABC

DmsABC catalyzes the two-electron reduction of S- and N-oxides. Data from *R. sphaeroides* DMSO reductase as well as studies on the mechanism of molybdoenzymes, such as xanthine oxidase, indicate that the reduction/oxidation of substrate occurs in a two electron reaction (127,136). Electron transfer between the Mo and the other redox groups present in the enzyme (or exogenous electron donors in the case of *R. sphaeroides* DMSO reductase) probably occurs as single electron transfers. Electron transfer catalyzed by DmsABC is between MQH₂ (MQH₂/MQ, $E_{m,7} = -74$ mV (10)) and DMSO (DMSO/DMS, $E_{m,7} = 160$ mV (3)). At least two of the redox centers of DmsABC do not appear to be thermodynamically capable of being reduced by MQH₂ (the $E_{m,7} = -240$ and -330 mV [4Fe-4S] clusters). Many other complex electron transfer enzymes also share this feature of apparently non-reducible/oxidizable redox centers (fumarate reductase (68), nitrate reductase (26), the *Desulfovibrio gigas* hydrogenase, (133)). These clusters may be structurally important and not involved in electron transfer. Certainly, mutagenesis studies of DmsABC, NarGHI and fumarate reductase have indicated that disrupting [Fe-S] clusters often leads to defects in enzyme assembly (68,115,137). While the [Fe-S] clusters may indeed have a role in bringing together and stabilizing parts of the protein, they may still be involved in electron transfer. The low potential of the clusters means that they will not work as electron storage units, but if they are located between the electron donor and acceptor may enhance the rate of electron transfer (132). In the crystal structure of *D. gigas* hydrogenase, a high potential [3Fe-4S] cluster lies between two [4Fe-4S] clusters with physiological midpoint potentials, suggesting that it is involved in electron transfer (133). In fumarate reductase, the $E_{m,7}$ of center FR2 (-330 mV) is much lower than the midpoint potentials of the MQ/MQH₂ and fumarate/succinate couples suggesting

that only the two clusters with highest midpoint potentials should be able to mediate electron transfer. However, lowering the midpoint potential of FR2 by mutagenesis did affect electron transfer, lowering growth rates and *in vitro* activity, indicating that FR2 is involved in electron transfer (68).

3. Comparison with other [Fe-S] Proteins

DmsB is homologous to the [Fe-S] containing subunits of several membrane bound molybdoenzymes as well as other electron transfer complexes and hydrogenases. These subunits all contain multiple Cys residues organized in Groups reminiscent of the [4Fe-4S] binding Cys Groups of the seven and eight Fe bacterial ferredoxins (138,139). The sequence of a common Cys Group is CysXXCysXXCysXXXCysPro where the X can be any amino acid. The Cys Groups are paired so that a [4Fe-4S] cluster is ligated by the first three Cys residues of one Group and the last Cys of a second Group. The seven Fe ferredoxins are missing the second Cys of one Cys Group and ligate one [4Fe-4S] and one [3Fe-4S] cluster. An alignment of the Cys Groups in DmsB and related proteins is shown in Figure 1-7. Of these proteins, only DmsB and NarH, have been shown to ligate four [Fe-S] clusters by EPR spectroscopy.

Groups I and III belong to the Cys Group type described above. The membrane-bound nitrate reductases (NarH and NarY) are missing the second Cys of Group III and have been shown to ligate a [3Fe-4S] cluster (22,115). Group II has two extra amino acids between the second and third Cys residues which can also be found in *Azotobacter vinlandii* ferredoxin I (146,147). Group IV is atypical in the unusually large spacing between the second and third Cys residues. In addition to the Cys residues a number of amino acids are conserved around the Groups. Two models for the ligation of the [Fe-S] clusters and the folding of DmsB are shown in Figure 1-8. Comparison of DmsB with the eight Fe ferredoxins indicates that the positioning of Groups II and III most resembles the structure of the ferredoxins, suggesting that the model of folding shown in Figure 1-8A is

GROUP III

| | | | | | | |
|---------|-----|--------|---|---|---|---|
| | | | • | • | • | • |
| Ec DmsB | 92 | VVDEDV | C | I | G | C |
| Hi DmsB | 92 | IVNEEI | C | I | G | C |
| Ws PsrB | 87 | SVNVDL | C | V | G | C |
| St PhsB | 96 | QVDKSR | C | I | G | C |
| Ec NarH | 211 | LIDQDK | C | R | G | W |
| Ec NarY | 210 | LIDQDK | C | R | G | W |
| Ec FdnH | 127 | DFQSEN | C | I | G | C |
| Ec FdoH | 127 | DFQSEQ | C | I | G | C |
| Ws FdhB | 85 | LHDKEK | C | I | G | C |
| Ec HycB | 76 | QLNESL | C | V | S | C |
| Ec HydN | 83 | HVMQER | C | I | G | C |
| Rr CooF | 90 | QIVEQH | C | I | G | C |
| Dv Hmc2 | 136 | TYDGSL | C | V | G | C |
| Ec NrfC | 119 | DVNPDL | C | V | G | C |
| Ec HybA | 139 | HYDKDV | C | T | G | C |

GROUP IV

| | | | | | | | | |
|---------|-----|-------|---|---|---|---|---|---|
| | | | • | • | | | • | • |
| Ec DmsB | 121 | GHMTK | C | D | G | C | Y | D |
| Hi DmsB | 120 | GHMTK | C | D | G | C | Y | S |
| Ws PsrB | 116 | KAPDK | C | N | F | C | K | D |
| St PhsB | 125 | GVADK | C | N | F | C | A | D |
| Ec NarH | 239 | GKSEK | C | I | F | C | Y | P |
| Ec NarY | 238 | GKSEK | C | I | F | C | Y | P |
| Ec FdnH | 155 | NRVYK | C | T | L | C | V | D |
| Ec FdoH | 155 | NRVYK | C | T | L | C | V | D |
| Ws FdhB | 118 | GPMDK | C | T | F | C | A | G |
| Ec HycB | 138 | AIAVK | C | D | L | C | S | F |
| Ec HydN | 126 | AEANK | C | D | L | C | N | H |
| Rr CooF | 128 | GVAKK | C | D | L | C | V | D |
| Dv Hmc2 | 167 | PLIQK | C | T | M | C | H | P |
| Ec NrfC | 148 | KTADK | C | D | F | C | R | K |
| Ec HybA | 170 | GALHK | C | E | L | C | N | Q |

Figure 1-7 The Cys Groups of DmsB and Other Related Iron-Sulfur Proteins

The sequence alignments were generated using the programs Fasta and Pileup (Genetics Computer Group, University of Wisconsin, USA). The sequences shown are from *E. coli* DmsB (17), *H. influenza* DmsB (20), *W. succinogenes* PsrB (27), *S. typhimurium* PhsB (30), *E. coli* NarH (23), *E. coli* NarY (21), *E. coli* FdnH (34), *E. coli* FdoH (36), *W. succinogenes* FdhB (41), *E. coli* formate hydrogenlyase subunit, HycB (140), *E. coli* HydN, of unknown function, (141), *Desulfovibrio vulgaris* Hmc2 protein, involved in transfer of electrons from periplasmic hydrogenases to the cytoplasmic sulfate reductases (142), *E. coli* Hydrogenase-2 subunit, HybA (143), *Rhodospirillum rubrum* carbon monoxide dehydrogenase subunit, CooF (144), *E. coli* cytochrome *c* nitrite reductase subunit, NrfC (145).

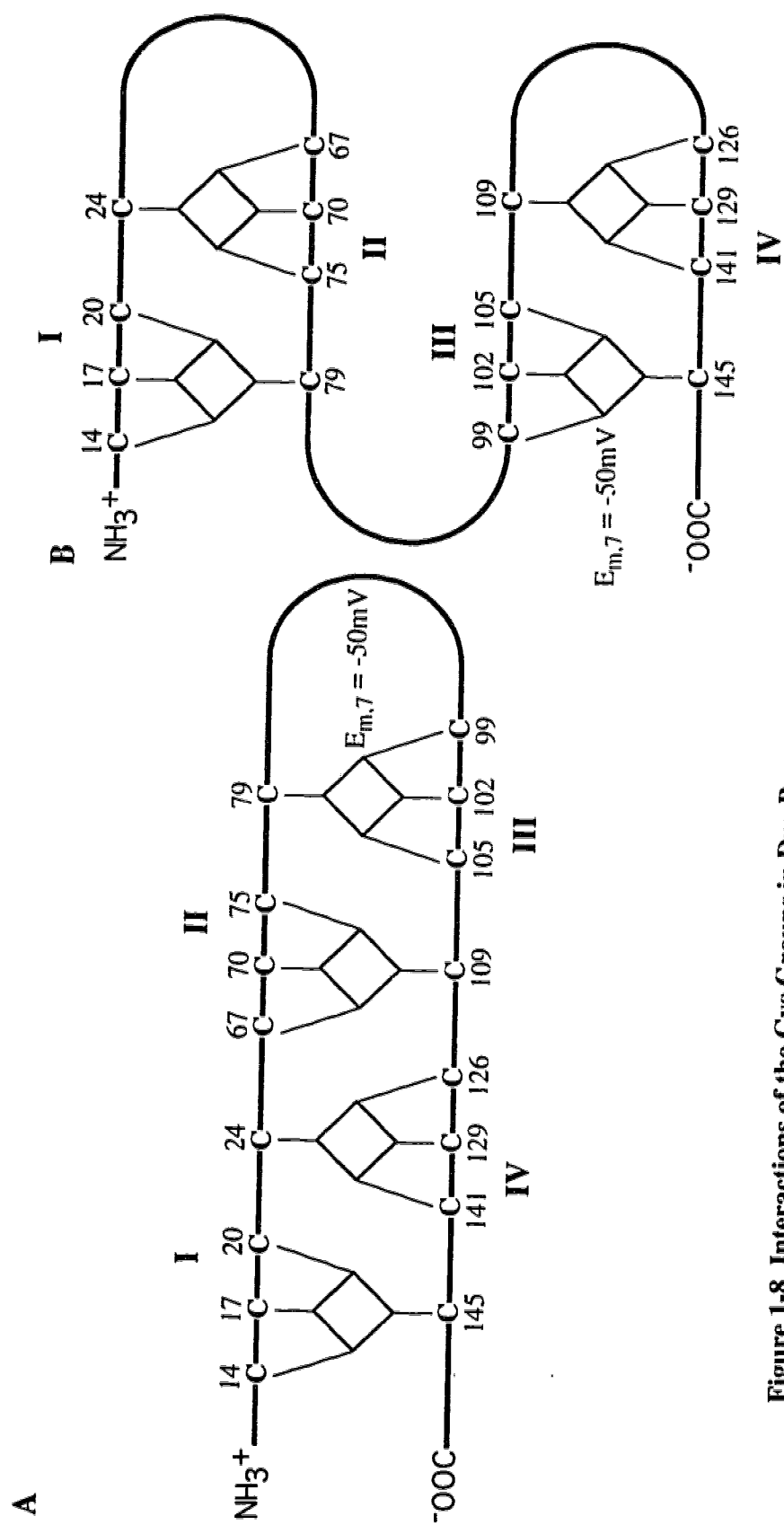


Figure 1-8 Interactions of the Cys Groups in DmsB

Two models have been proposed for arrangement of the [4Fe-4S] clusters in DmsB. Sequence comparisons of DmsB with the eight-Fe ferredoxins indicate that the model (A) is the most likely folding pattern. Group III has been demonstrated to ligate the $E_{m,7} = -50 \text{ mV}$ [4Fe-4S] cluster.

the correct (135) model. In this model Groups II and III form one pair and Groups I and IV form the second pair. An alternate model pairing Groups I and II and Groups III and IV is also shown (6).

4. Mutagenesis of the Cys Groups

Site-directed mutagenesis of the DmsB Cys Groups has been carried out to characterize the ligation of the [4Fe-4S] clusters. Mutagenesis of the second Cys of Group III, Cys-102, changed the $E_{m,7} = -50$ mV [4Fe-4S] cluster to a [3Fe-4S] cluster with an $E_{m,7} = 220$ mV for C102W and $E_{m,7} = 260$ mV for C102S (135,148). These mutants are not able to support growth on DMSO and are blocked in electron transfer from MQH₂ to DmsA but not in electron transfer from DmsB to MQ. In the oxidized mutant enzyme, this cluster is magnetically isolated (it is paramagnetic when the other clusters in the enzyme are diamagnetic) and its position has been determined to be on the inner surface of the cytoplasmic membrane, 21Å from the surface of the DmsAB dimer (120). Recent experiments with this mutant and HOQNO have indicated that this cluster is functionally and conformationally linked to the HOQNO (and presumably the MQH₂) binding site in DmsC (135). The $E_{m,7} = -50$ mV center is the most thermodynamically competent to accept electrons from MQH₂ and is located at the membrane interface, supporting its proposed role in transferring electrons from the oxidation of quinol to the [Fe-S] cluster that it interacts with, the -120 mV center. Unfortunately, mutants generated so far in Groups II and IV do not assemble into the membrane bound holoenzyme. Group I mutants are expressed and assemble but at a lower level than the wild-type enzyme which makes characterization difficult (Rothery and Weiner, unpublished results).

J. DmsC

1. Anchor Function

DmsC is a hydrophobic, membrane-intrinsic polypeptide of 287 amino acids which acts as the membrane anchor for the soluble subunits. Analyses of gene fusions of DmsC to β -lactamase and alkaline phosphatase have demonstrated that DmsC contains eight transmembrane helices (149). Both termini are located in the periplasmic space. The fusions containing a truncated DmsC resulted in DmsAB accumulating in the cytoplasm as had previously been seen when the *dmsC* gene was deleted from the chromosome (83). The entire DmsC protein is needed to perform the anchor function. DmsC is also important in stabilizing the enzyme activity to thermal inactivation at 30°C (83).

2. Quinone Binding

Only the presence of the catalytic dimer, DmsAB, is required for the reduction of DMSO with an artificial electron donor such as BV^{•+}. DmsC is needed for both growth on DMSO and *in vitro* reduction of DMSO with the quinol analog DMNH₂ (83). This indicates that the site of MQH₂ interaction is in DmsC.

Important information about quinone binding in DmsC has come from the study of the engineered [3Fe-4S] cluster in DmsB. The line-shape of the C102S mutant was affected by the menaquinone analog, HOQNO, but almost no HOQNO effect was seen with the C102W mutant. In fumarate reductase, a residue involved in quinol oxidation, His-82, has been identified (62,63). A similar residue, His-65, was identified at the periplasmic end of helix 2 in DmsC (135). Mutation of His-65 to Arg inhibited growth and quinol oxidation. A double mutant of C102S and H65R exhibited an EPR spectrum identical to that of the C102S mutant. However, upon addition of HOQNO, the change in line shape of the [3Fe-4S] cluster was almost totally eliminated, suggesting that the DmsC H65R substitution interferes with HOQNO binding or disrupts a conformation link between the quinone binding site and the [3Fe-4S] cluster. In a double mutant of C102W

and H65R, the His-65 substitution broadened and decreased the intensity of the [3Fe-4S] cluster signal. Again, HOQNO had little effect on the spectrum. The effect of H65R on the C102W mutant suggests that these residues may be in close proximity in the holoenzyme.

The one-way electron transfer seen in the Cys-102 mutant enzymes also has important implications for the quinone binding (135). The backwards flow of electrons may be explained by a change in the affinity for quinone such that MQH₂ binding affinity is decreased while the MQ affinity is unaltered, inhibiting the oxidation of MQH₂. Alternatively, this one-way electron flow may indicate the presence of two quinone binding sites in the enzyme. Electron flow from the MQH₂ site would be disrupted by the Cys-102 mutation while reduction of MQ would take place at a separate site in which the electron transfer is undisturbed. Two quinone binding sites have been demonstrated for a number of proteins. The mitochondrial *bc₁* complex has two quinol binding sites which is central to the mechanism of the proton motive Q-cycle (150). The photoreaction center has a Q_A site which contains a tightly bound quinone that mediates electron transfer to a disassociable quinone at the Q_B site (65). *E. coli* cytochrome *bo* has been demonstrated to have two quinone binding sites, a high affinity site and an exchangeable low affinity site, proposed to operate analogous to the photoreaction center (151). In succinate dehydrogenase, two interacting semiquinone radicals have been observed during reduction of ubiquinone (152). Fumarate reductase, which related to succinate dehydrogenase, has also been proposed to have Q_A and Q_B sites in the membrane anchor subunits (63,64). His-82 in FrdC is proposed to be part of the Q_B site. The proposed topology of the membrane FrdC and FrdD anchor subunits means that the His-82 (Q_B site) is on the opposite side of the membrane from DmsB His-65. However, the topologies of FrdC and FrdD have never been determined experimentally and may not be correct, or perhaps helix2 in DmsC may be shifted in the membrane to bring His-65 closer to the cytoplasmic side of the membrane.

IV. Thesis Objectives

DmsABC is a member of an emerging family of molybdoenzymes which have similar properties and share a large amount of sequence similarity. At the time these studies were initiated very little information was available on these enzymes regarding their electron transfer properties, cofactors, and cofactor binding. The sequences of six molybdoenzymes were known and multiple amino acid sequence alignments identified several regions of similarity among the Mo cofactor binding subunits. We chose to investigate the functions of the enzymes through site-directed mutagenesis of the conserved sequences in DmsA.

Chapter 2 describes the mutagenesis of the conserved residues of Region 1. The electron transfer capabilities of the mutant enzymes were ascertained using several different assays. The mutants were tested for growth, *in vitro* reductase activity, and the ability to interact with the quinol pool.

Chapter 3 describes the further characterization of the Cys-38 mutants from Chapter 2. Region 1 had been determined to ligate a [4Fe-4S] cluster in a DmsA related enzyme, suggesting that DmsA Region I may also ligate a cluster. The [Fe-S] content and EPR characteristics of the wild-type DmsABC enzyme and the Cys-38 mutant enzymes from Chapter 2 were examined to determine if DmsA ligates an [Fe-S] cluster. A double mutant of DmsA was constructed to further pursue this question.

The Mo cofactor binding was addressed in Chapter 4. Studies with FdhF had determined that the Se-Cys was a ligand of the Mo. This residue falls in Region 3 of the conserved sequences. In DmsA and the other S- and N-oxide reductases this residue is a Ser, which may also coordinate the Mo. Ser-176 of DmsA was mutated to Cys, Ala, and His. Mutant enzymes were analyzed for their ability to support growth and reduce substrate *in vitro*. The characteristics of the Mo were examined using EPR spectroscopy.

V. Bibliography

1. Iuchi, S., and Lin, E. C. C. (1991) *Cell* **66**, 5-7
2. Gunsalus, R. P. (1992) *J. Bacteriol.* **174**, 7069-7074
3. Lin, E. C. C., and Kuritzkes, D. R. (1987) in *Escherichia coli and Salmonella typhimurium* (Neidhardt, F. C., ed) Vol. I, pp. 201-221, Am. Soc. Microbiol., Washington, D. C.
4. Cole, S. T., Grundström, T., Jaurin, B., Robinson, J. J., and Weiner, J. H. (1982) *Eur. J. Biochem.* **126**, 211-216
5. Stewart, V. (1988) *Microbiol. Rev.* **52**, 190-232
6. Weiner, J. H., Rothery, R. A., Sambasivarao, D., and Trieber, C. A. (1992) *Biochim. Biophys. Acta* **1102**, 1-18
7. Zinder, S. H., and Brock, T. D. (1978) *J. Gen. Microbiol.* **105**, 335-342
8. Barrett, H. S., and Kwan, H. S. (1985) *Ann. Rev. Microbiol.* **39**, 131-149
9. Weiner, J. H., MacIsaac, D. P., Bishop, R. E., and Bilous, P. T. (1988) *J. Bacteriol.* **170**, 1505-1510
10. Ingledew, W. J., and Poole, R. K. (1984) *Microbiol. Rev.* **48**, 222-271
11. McEwan, A. G., Richardson, D. J., Hudig, H., Ferguson, S. J., and Jackson, J. B. (1989) *Biochim. Biophys. Acta* **973**, 308-214
12. Nicholls, D. G. (1982) *Bioenergetics: an introduction to chemiosmotic theory*, Academic Press, New York
13. Anraku, Y., and Gennis, R. B. (1987) *Trends. Biochem. Sci.* **12**, 262-266
14. Trumpower, B. L., and Gennis, R. B. (1994) *Annu. Rev. Biochem.* **63**, 675-715
15. Cole, S. T., Eiglmeier, K., Ahmed, S., Honoré, N., Elmes, L., Anderson, W. F., and Weiner, J. H. (1988) *J. Bacteriol.* **170**, 2448-2456
16. Varga, M. E. R., and Weiner, J. H. (1995) *Biochem. Cell. Biol.* **73**, 147-153
17. Bilous, P. T., Cole, S. T., Anderson, W. F., and Weiner, J. H. (1988) *Mol. Microbiol.* **2**, 785-795
18. Rothery, R. A., Simala Grant, J. L., Johnson, J. L., Rajagopalan, K. V., and Weiner, J. H. (1995) *J. Bacteriol.* **177**, 2057-2063
19. Cammack, R., and Weiner, J. H. (1990) *Biochemistry* **29**, 8410-8416

20. Fleischmann, R. D., Adams, M. D., White, O., Clayton, R. A., F., K. E., Kerlavage, A. R., Bult, C. J., Tomb, J.-F., Dougherty, B. A., Merrick, J. M., McKenney, K., Sutton, G., Fitzhugh, W., Fields, C. A., Gocayne, J. D., Scott, J. D., Shirley, R., Liu, L.-I., Glodek, A., Kelley, J. M., Weidman, J. F., Phillips, S. C. A., Spriggs, T., Hedblom, E., Cotton, M. D., Utterback, T. R., Hanna, M. C., Nguyen, D. T., Saudek, D. M., Brandon, R. C., Fine, L. D., Fritchman, J. L., Fuhrmann, J. L., Geoghagen, N. S. M., Gnehm, C. L., McDonald, L. A., Small, K. V., Fraser, C. M., Smith, H. O., and Venter, J. C. (1995) *Science* **269**, 496-512
21. Blasco, F., Iobbi, C., Ratouchniak, J., Bonnefoy, V., and Chippaux, M. (1990) *Mol. Gen. Genet.* **222**, 104-111
22. Guigliarelli, B., Asso, M., More, C., Augier, V., Blasco, F., Pommier, J., Giordano, G., and Bertrand, P. (1992) *Eur. J. Biochem.* **207**, 61-68
23. Blasco, F., Iobbi, C., Giordano, G., Chippaux, M., and Bonnefoy, V. (1989) *Mol. Gen. Genet.* **218**, 249-256
24. Johnson, J., Indermaur, L., and Rajagopalan, K. (1991) *J. Biol. Chem.* **266**, 12140-12145
25. Ballard, A. L., and Ferguson, S. J. (1988) *Eur. J. Biochem.* **174**, 207-212
26. Berks, B. C., Page, M. D., Richardson, D. J., Reilly, A., Cavill, A., Outen, D., and Ferguson, S. J. (1995) *Mol. Microbiol.* **15**, 319-331
27. Krafft, T., Bokranz, M., Klimmek, O., Schröder, I., Fahrenholz, R., Kojro, E., and Kröger, A. (1992) *Eur. J. Biochem.* **206**, 503-510
28. Jankielewicz, A., Schmitz, R. A., Klimmek, O., and Kröger, A. (1994) *Arch. Microbiol.* **162**, 238-242
29. Schröder, I., Kröger, A., and Macy, J. M. (1988) *Arch. Microbiol.* **149**, 572-579
30. Heinzinger, N. K., Fujimoto, S. Y., Clark, M. A., Moreno, M. S., and Barrett, E. L. (1995) *J. Bacteriol.* **177**, 2813-2820
31. Zinoni, F., Birkmann, A., Stadtman, T. C., and A., B. (1986) *Proc. Natl. Acad. Sci. U.S.A.* **83**, 4650-4654
32. Axley, M. J., Grahame, D. A., and Stadtman, T. C. (1990) *J. Biol. Chem.* **265**, 18213-18218
33. Sauter, M., Böhm, R., and Böck, A. (1992) *Mol. Microbiol.* **6**, 1523-1532
34. Berg, B. L., Li, J., Heider, J., and & Stewart, V. (1991) *J. Biol. Chem.* **266**, 22380-22385
35. Pommier, J., Mandrand, M. A., Holt, S. E., Boxer, D. H., and Giordano, G. (1992) *Biochim. Biophys. Acta* **1107**, 305-313

36. Plunkett, G. I., Burland, B.D., Daniels, D. L., Blattner, F.R. (1993) *Nucleic Acids Res.* **21**, 3391-3398
37. Shuber, A. P., Orr, E. C., Recny, M. A., Schendel, P. F., May, H. D., Schauer, N. L., and Ferry, J. G. (1986) *J. Biol. Chem* **261**, 12942-12947
38. Johnson, J., Bastian, N., Schauer, N., Ferry, J., and Rajagopalan, K. (1991) *FEMS Microbiol. Lett.* **77**, 213-216
39. White, W. B., and Ferry, J. G. (1992) *J. Bacteriol.* **174**, 4997-5004
40. Barber, M. J., Siegel, L. M., Schauer, M. L., May, H. D., and Ferry, J. G. (1983) *J. Biol. Chem.* **258**, 10839-10845
41. Bokranz, M., Guttman, M., Körtner, C., Kojro, F., Fahrenholz, F., Lauterbach, F., and & Kröger, A. (1991) *Arch. Microbiol.* **156**, 119-128
42. Breton, J., Berks, B. C., Reilly, A., Thomson, A. J., Ferguson, S. J., and Richardson, D. J. (1994) *FEBS Letters* **345**, 76-80
43. Berks, B. C., Richardson, D. J., Robinson, C., Reilly, A., Apline, R. T., and Ferguson, S. J. (1994) *Eur. J. Biochem.* **220**, 117-124
44. Siddiqui, R. A., Warnecke-eberz, U., Hengsberger, A., Schneider, B., Kostka, S., and Friedrich, B. (1993) *J. Bacteriol.* **175**, 5867-5876
45. Berks, B. C., Richardson, D. J., Reilly, A., Willis, A. C., and Ferguson, S. J. (1995) *Biochem. J.* **309**, 983-992
46. Richterich, P., Lakey, N., Gryan, D., Jaehn, L., Mintz, L., Robison, K., and Church, G. M. (1993) *EMBL database*, Accession number U00008
47. Lin, J. T., Goldman, B.S., Stewart, V. (1993) *J. Bacteriol.* **175**, 2370-2378
48. Lin, J. T., Goldman, B. S., and Stewart, V. (1994) *J. Bacteriol* **176**, 2551-2559
49. Andriesse, X., and Bakker, H. (1993) *EMBL database*, Accession number X74597
50. Unthan, M., Klipp, W., and Schmid, G. H. (1995) *EMBL database*, Accession number X89445
51. Ogawa, K.-I., Akagawa, E., Yamane, K., W., S. Z., Lacelle, M., Zuber, P., and Nakano, M. M. (1995) *J. Bacteriol.* **177**, 1409-1413
52. Johnson, J. L., Bastian, N. R., and Rajagopalan, K. V. (1990) *Proc. Natl. Acad. Sci. USA* **87**, 3190-3194
53. Barber, M. J., Valkenburgh, H. V., Trimboli, A. J., Pollock, V. V., Neame, P. J., and Bastian, N. R. (1995) *Arch. Biochem. Biophys.* **320**, 266-275
54. Satoh, T., and Kurihara, F. N. (1987) *J. Biochem.* **102**, 191-197

55. Méjean, V., Iobbi-Nivol, C., Lepelletier, M., Giordano, G., Chippaux, M., and Pascal, M.-C. (1994) *Mol. Microbiol.* **11**, 1169-1179
56. Pierson, D. E., and Campbell, A. (1990) *J. Bacteriol.* **172**, 2194-2198
57. del Campillo Campbell, A., and Campbell, A. (1982) *J. Bacteriol.* **149**, 469-478
58. Pollock, V. V., and Barber, M. J. (1995) *Arch. Biochem. Biophys.* **318**, 322-332
59. del Campillo-Campbell, A., and Campbell, A. M. (1995) *EMBL database*, Accession number U38839
60. Sawers, G. (1994) *Antonie van Leeuwenhoek* **66**, 57-88
61. Cole, S. T., Condon, C., Lemire, B. D., and Weiner, J. H. (1985) *Biochim. Biophys. Acta* **811**, 381-403
62. Weiner, J. H., Cammack, R., Cole, S. T., Condon, C., Honoré, N., Lemire, B. B., and Shaw, G. (1986) *Proc. Natl. Acad. Sci. USA* **83**, 2056-2060
63. Westenberg, D. J., Gunsalus, R. P., Ackrell, B. A. C., and Cecchini, G. (1990) *J. Biol. Chem.* **265**, 19560-19567
64. Westenberg, D. J., Gunsalus, R. P., Ackrell, B. A. C., Sices, H., and Cecchini, G. (1993) *J. Biol. Chem.* **268**, 815-822
65. Okamura, M. Y., and Feher, G. (1992) *Ann. Rev. Biochem.* **61**, 861-896
66. Cecchini, G., Sices, H., Schröder, I., and Gunsalus, R. P. (1995) *J. Bacteriol.* **177**, 4587-4592
67. Sucheta, A., Cammack, R., Weiner, J., and Armstrong, F. A. (1993) *Biochemistry* **32**, 5455-5465
68. Kowal, A. T., Werth, M. T., Manodori, A., Cecchini, G., Schröder, I., Gunsalus, R. P., and Johnson, M. J. (1995) *Biochemistry* **34**, 12284-12293
69. Kiene, R. P., and Bates, T. S. (1990) *Nature* **345**, 702-704
70. Lovelock, J. E., Maggs, R. J., and Ramussen, R. A. (1972) *Nature* **237**, 452-453
71. Kellogg, N. W., Cadle, R. D., Allen, E. R., Lazrus, A. L., and Martell, E. A. (1972) *Science* **175**, 587-596
72. Zeyer, J., Eicher, P., Wakeham, S. G., and Schworzenbach, R. P. (1987) *Appl. Env. Microbiol.* **53**, 2026-2032
73. Bowlus, R. D., and Somero, G. N. (1979) *J. Exp. Zoo.* **208**, 137-151
74. Somero, G. N. (1983) *Comp. Biochem. Phys.* **76**, 621-633

75. Styrvold, O. B., and Strøm, A. R. (1984) *Arch. Microbiol.* **140**, 74-78
76. McEwan, A. G., Wetzstein, H. G., Meyer, O., Jackson, J. B., and Ferguson, S. J. (1987) *Arch. Microbiol.* **147**, 340-345
77. Silvestro, A., Pommier, J., Pascal, H. C., and Giordano, G. (1989) *Biochim. Biophys. Acta* **999**, 208-216
78. Sambasivarao, D., and Weiner, J. H. (1991) *Curr. Microbiol.* **23**, 105-110
79. Bragg, P. D., and Hackett, N. R. (1983) *Biochim. Biophys. Acta* **725**, 168-177
80. Sambasivarao, D., Scraba, D. G., Trieber, C., and Weiner, J. H. (1990) *J. Bacteriol.* **172**, 5938-5948
81. Bilous, P. T., and Weiner, J. H. (1985) *J. Bacteriol.* **162**, 1151-1155
82. Bilous, P. T., and Weiner, J. H. (1985) *J. Bacteriol.* **163**, 369-375
83. Sambasivarao, D., and Weiner, J. H. (1991) *J. Bacteriol.* **173**, 5935-5943
84. Bilous, P. T., and Weiner, J. H. (1988) *J. Bacteriol.* **170**, 1511-1518
85. Shine, J., and Dalgarno, L. (1974) *Proc. Natl. Acad. Sci. USA* **71**, 1342-1346
86. Eiglmeier, K., Honoré, N., Luchi, S., Lin, E. C. C., and Cole, S. T. (1989) *Mol. Microbiol.* **3**, 869-878
87. Spiro, S., and Guest, J. R. (1990) *FEMS Microbiol. Rev.* **75**, 399-428
88. Tyson, K. L., Bell, A. I., Cole, J. A., and Busby, S. J. W. (1993) *Mol. Microbiol.* **7**, 151-157
89. Blasco, F., Pommier, J., Augier, M., Chippaux, M., and Giordano, G. (1992) *Mol. Microbiol.* **6**, 221-230
90. Dubourdieu, M., and DeMoss, J. A. (1992) *J. Bacteriol.* **174**, 867-872
91. Yamamoto, I., Hinakura, M., Seki, S., Seki, Y., and Kondo, H. (1989) *J. Gen. Appl. Microbiol.* **35**, 253-259
92. Melville, S. B., and Gunsalus, R. P. (1990) *J. Biol. Chem.* **265**, 18733-18736
93. Pascal, M. C., Burini, J. F., and Chippaux, M. (1984) *Mol. Gen. Genet.* **195**, 351-355
94. Gennis, R. B. (1987) *FEMS Microbiol. Rev.* **46**, 381-389
95. Frey, B., Janel, G., Michelson, U., and Kerstein, H. (1989) *J. Bacteriol.* **171**, 1524-1530
96. Schultz, S. C., Shields, G. C., and Steitz, T. A. (1991) *Science* **352**, 1001-1007

97. Bell, A. I., Gaston, K. L., Cole, J. A., and Busby, S. J. W. (1989) *Nucleic Acids Res.* **17**, 3865-3874
98. Green, J., Trageser, M., Six, S., Unden, G., and Guest, J. R. (1991) *Proc. R. Acad. Lond.* **244**, 137-144
99. Lazazzera, B. A., Bates, D. M., and Kiley, P. J. (1993) *Genes Dev.* **7**, 1993-2005
100. Spiro, S., and Guest, J. R. (1988) *Mol. Microbiol.* **2**, 701-707
101. Lazazzera, B. A., Beinert, H., Khoroshilova, N., Kennedy, M. C., and Kiley, P. F. (1996) *J. Biol. Chem.* **271**, 2762-2768
102. Khoroshilova, N., Beinert, H., and Kiley, P. J. (1995) *Proc. Natl. Acad. Sci. USA* **92**, 2499-2503
103. Stewart, V. (1993) *Mol. Microbiol.* **9**, 425-434
104. Walker, M. S., and DeMoss, J. A. (1993) *J. Biol. Chem.* **268**, 8391-8393
105. Schröder, I., Wolin, C. D., Cavicchioli, R., and Gunsalus, R. P. (1994) *J. Bacteriol.* **176**, 4985-4992
106. Rabin, R. S., and Stewart, V. (1993) *J. Bacteriol.* **175**, 3259-3268
107. Yamamoto, I., Yamazaki, N., Hohmura, M., and Ishimoto, M. (1990) *J. Gen. Appl. Microbiol.* **36**, 357-363
108. Pascal, M. C., Lepelletier, M., Giordano, G., and Chippaux, M. (1991) *FEMS Microbiol. Lett.* **78**, 297-300
109. Simon, G., Méjean, V., Jourlin, C., Chippaux, M., and Pascal, M.-C. (1994) *J. Bacteriol.* **176**, 5601-5606
110. Rosentel, J. K., Healy, F., Maupin-Furlow, J. A., Lee, J. H., and Shanmugam, K., T. (1995) *J. Bacteriol.* **177**, 4857-4864
111. Maupin-Furlow, J. A., Rosentel, J. K., Lee, J. H., Deppenmeier, U., Gunsalus, R. P., and Shanmugam, K. T. (1995) *J. Bacteriol.* **177**, 4851-4856
112. Rech, S., Deppenmeier, U., and Gunsalus, R. P. (1995) *J. Bacteriol.* **177**, 1023-1029
113. Cotter, P. A., and Gunsalus, R. P. (1989) *J. Bacteriol.* **171**, 3817-3823
114. Collins, L. A., Egan, S. M., and Stewart, V. (1992) *J. Bacteriol.* **174**, 3667-3675
115. Augier, V., Guigliarelli, B., Asso, M., Bertarand, P., Frixon, C., Giordano, G., Chippaux, M., and Blasco, F. (1993) *Biochemistry* **32**, 2013-2023

116. Satitz, P., Klemme, J.-H., Koch, H.-G., and Molitor, M. (1993) *Z. Naturforsch.* **48c**, 812-814
117. Augier, V., Asso, M., Guigliarelli, B., More, C., Bertrand, P., Santini, C.-L., Blasco, F., Chippaux, M., and Giordano, G. (1993) *Biochemistry* **32**, 5099-5108
118. Arata, H., Shimizu, M., and Takamiya, K. (1992) *J. Biochem.* **112**, 470-475
119. Daruwala, R., and Meganathan, R. (1991) *FEMS Microbiol. Lett.* **83**, 255-260
120. Rothery, R. A., and Weiner, J. H. (1993) *Biochemistry* **32**, 5855-5861
121. Rajagopalan, K. V., and Johnson, J. L. (1992) *J. Biol. Chem.* **267**, 10199-10202
122. del Campillo-Campbell, A., Dykhuizen, D., and Cleary, P. P. (1979) *Methods Enzymol.* **62**, 379-385
123. Chan, M. K., Mukund, S., Kletzin, A., Adams, M. W. W., and Rees, D. C. (1995) *Science* **267**, 1463-1469
124. Romao, M. J., Archer, M., Moura, I., Moura, J. J. G., LeGall, J., Engh, R., Schneider, M., Hof, P., and Huber, R. (1995) *Science* **270**, 1170-1176
125. Hilton, J. C., and Rajagopalan, K. V. (1996) *Arch. Biochem. Biophys.* **325**, 139-143
126. Bray, R. C. (1988) *Q. Rev. Biophys.* **21**, 299-329
127. Hille, R. (1994) *Biochim. Biophys. Acta* **1184**, 143-169
128. Barber, M. J., Coughlan, M. P., Rajagopalan, K. V., and Siegel, L. M. (1982) *Biochemistry* **21**, 3561-3568
129. George, G. N., Turner, N. A., Bray, R. C., Morpeth, F. F., Boxer, D. H., and Cramer, S. P. (1989) *Biochem. J.* **259**, 693-700
130. Gladyshev, V. N., Khangulov, S. V., Axley, M. J., and Stadtman, T. C. (1994) *Proc. Natl. Acad. Sci. USA* **91**, 7708-7711
131. Wootton, J. C., Nicolson, R. E., Cock, J. M., Waters, D. E., Burke, J. F., Doyle, W. A., and Bray, R. C. (1991) *Biochim. Biophys. Acta* **1057**, 157-185
132. Berks, B. C., Ferguson, S. J., Moir, J. W. B., and Richardson, D. J. (1995) *Biochim. Biophys. Acta* **1232**, 97-123
133. Volbeda, A., Charon, M.-H., Piras, C., Hatchikian, E. C., Frey, M., and Fontecilla-Camps, J. C. (1995) *Nature* **373**, 580-587
134. Axley, M. J., Böck, A., and Stadtman, T. C. (1991) *Proc. Natl. Acad. Sci. USA* **88**, 8450-8454

135. Rothery, R. A., and Weiner, J. H. (1996) *Biochemistry* **35**, 3247-3257
136. Bastian, N., Kay, C., Barber, M., and Rajagopalan, K. (1991) *J. Biol. Chem.* **266**, 45-51
137. Manodori, A., Cecchini, G., Schröder, I., Gunsalus, R. P., Werth, M. T., and Johnson, M. K. (1992) *Biochemistry* **31**, 2703-2712
138. Bruschi, M., and Guerlesquin, F. (1988) *FEMS Microbiol. Rev.* **54**, 155-176
139. Matsubara, J., and Saeki, K. (1992) *Adv. Inorg. Chem.* **38**, 223-280
140. Böhm, R., Sauter, m., and Böck, A. (1990) *Mol. Microbiol.* **4**, 231-243
141. Ikebukuro, K., Nishio, M., Yano, K., Tomiyama, N., Tamiya, E., and Karube, I. (1993) *EMBL database*, Accession number D14422
142. Rossi, M., Pollock, W. B. R., Reij, M. W., Deon, R. G., Fu, R., and Voordouw, F. (1993) *J. Bacteriol* **175**, 4699-4711
143. Menon, N. K., Chatelus, C. Y., Dervartanian, M., Wendt, J. C., Shanmugam, K. T., Peck, H. D. J., and Przybyla, A. E. (1994) *J. Bacteriol.* **176**, 4416-4423
144. Kerby, R. L., Hong, S. S., Ensign, S. A., Coppoc, L. j., Ludden, P. W., and Roberts, G. P. (1992) *J. Bacteriol.* **174**, 5284-5294
145. Hussain, H., Grove, J., Griffiths, L., Busby, S., and Cole, J. (1994) *Mol. Microbiol.* **12**, 153-163
146. Stout, G. H., Turley, S., Sieker, L. C., and Jensen, L. H. (1988) *Proc. Natl. Acad. Sci. U. S. A.* **85**, 1020-1022
147. Morgan, T. V., Stephens, R. J., Burgess, B. K., and Stout, C. D. (1984) *FEBS Lett.* **167**, 137-141
148. Rothery, R. A., and Weiner, J. H. (1991) *Biochemistry* **30**, 8296-8305
149. Weiner, J. H., Shaw, G., Turner, R. J., and Trieber, C. A. (1993) *J. Biol. Chem.* **268**, 3238-3244
150. Trumpower, B. L. (1990) *Microbiol. Rev.* **54**, 101-129
151. Sato-Watanabe, M., Mogi, T., Ogura, T., Kitagawa, T., Miyoshi, H., Iwamura, H., and Anraku, Y. (1994) *J. Biol. Chem.* **269**, 28908-28912
152. Hederstedt, L., and Ohnishi, T. (1992) in *Molecular Mechanisms in Bioenergetics* (Ernster, L., ed), pp. 163-198, Elsevier Science Publishers, B. V., Amsterdam

Chapter 2

Multiple Pathways of Electron Transfer in Dimethyl Sulfoxide Reductase of *Escherichia coli**

* A version of this chapter has been published. Trieber, C. A., Rothery, R. A. and Weiner, J. H. (1994) J. Biol. Chem. 260, 7103-7109

I. Introduction

DmsABC is a member of a family of molybdenum-containing oxidoreductases with highly conserved organization and sequence (1-4). At the time this work was completed, nine members of the family had been identified. They are prokaryotic enzymes which reduce DMSO, nitrate (2,5), biotin sulfoxide (6) and polysulfide (7) or oxidize formate (8-13). Each contains a large catalytic subunit with a noncovalently bound molybdopterin cofactor. Eight of these enzymes are membrane-bound and contain a subunit with multiple [Fe-S] clusters and a membrane anchor subunit. An alignment of the catalytic subunits shows extensive regions of sequence identity throughout the length of the polypeptide. The amino terminal region is shown in Figure 2-1. Three cysteine residues and two basic amino acids, Cys-38, Cys-42, Cys-75, Lys-28 and Arg-77 of DmsA, are conserved in eight of the nine sequences. Only biotin sulfoxide reductase, BisC, lacks this region. As BisC is the only member of this group which does not accept electrons from an iron-sulfur subunit (6) this suggested to us that these Cys residues and basic amino acid residues might participate in electron transfer from the [Fe-S] containing subunit to the catalytic subunit.

The activity of DmsABC can be monitored by: 1) measuring DMSO-dependent anaerobic growth (14); 2) a spectrophotometric assay using an artificial electron donor, BV^{•+} (15), 3) a more physiological spectrophotometric assay using the quinol analog DMNH₂ as the electron donor (16), and 4) the quinone pool (Q-pool) coupling EPR assay (17). The Q-pool coupling assay takes advantage of the large amount of fumarate reductase, FrdABCD, present in *E. coli* DSS301 membrane preparations. FrdABCD and DmsABC are menaquinol oxidoreductases which are in equilibrium with the Q-pool in the membrane (Figure 2-2). DmsABC contains [4Fe-4S] clusters which are EPR visible in the reduced form (18). FrdABCD contains a [2Fe-2S] cluster, center FR1, visible when reduced, and a [3Fe-4S] cluster, center FR3, which is visible when oxidized (19). The

| | | |
|----------|--|-----|
| Ec DmsA: | MASSALTLPFSSRIAHAVDSAI | 21 |
| Ec NarG: | MSKFL-----DRFRYFKQKG-ETFADGHGQLLN-TNRDWEDGYRQ-- | 36 |
| Ec NarZ: | MSKLL-----DRFRYFKQKG-ETFADGHGQVMH-SNRDWEDSYRQ-- | 36 |
| Ec FdnG: | MDV-----SRRQFFKICA-GGMAGTTVAALGFAPKQALAQARNY- | 36 |
| Ws FdhA: | MSEALSGRGNDRRKFLKMSALAGVAGVSQAVGSDQSKVLRPATKQEL | 47 |
| Ec FdhF: | | |
| Mb FdhA: | | |
| Ws PsrA: | METTMTRRDFLKSAGAAGAAGLVWS--QTIPGTLGALEKQEI | 40 |
| Ec BisC: | | |
| | 28 34 38 42 | |
| Ec DmsA: | PTK-SDE <u>K</u> VIWSA C TVN C SGR C PLRMHVVDGEIKYV---ETDNTGD | 63 |
| Ec NarG: | --RWQHD K IVRST H GVN C TG S C S WKIYVKNGLVTWETQQTDYP--R | 80 |
| Ec NarZ: | --RWQFD K IVRST H GVN C TG S C S WKIYVKNGLVTWETQQTDYP--R | 80 |
| Ec FdnG: | --KLLRA K EIRNT C TY- C SVG C GLLMY-SLGDGAKNAR-EAIYHIE | 79 |
| Ws FdhA: | IEKYPV S K KVKT I C TY- C SVG C GIIAEVVDGV---WVRQEVAAAA | 83 |
| Ec FdhF: | ---M K KVVTV C PY- C ASG C KINL-VVDNGKIVRA--EAA---- | 32 |
| Mb FdhA: | MDI K YVPT I C PY- C GVG C GMNL-VVKD-----EKVVGVE | 32 |
| Ws PsrA: | KGS --A K FVPS I C EM- C TSS C TIEARV-EG-----DKGVFIR | 73 |
| Ec BisC: | | |
| | 75 77 90 | |
| Ec DmsA: | DNYD-GLHQVRA C L R G----RSMRRRVYNPD R LKY P MKRVGARG | 102 |
| Ec NarG: | TRPDLPNHEPRG C PRG----ASYSWYLYSAN R LKY P MMRKRLMW | 120 |
| Ec NarZ: | TRPDLPNHEPRG C PRG----ASYSWYLYSAN R LKY P LIRKRLIE | 120 |
| Ec FdnG: | GDPDHPVSRGAL C P K G----AGLLDYVNSE N RLRY P EYRAPGSD | 119 |
| Ws FdhA: | --QDHPISQGGH C C K G----ADMIDKARSET R LRY P IEKVGKGW | 121 |
| Ec FdhF: | QGKTN---QGT L C L K GYGWDFINDTQILT P R L K T P M I RRQRGG | 73 |
| Mb FdhA: | PWKRHPVNEGKL C P K G----NFCYEIIHRED R L T T P L I K ENGFE | 72 |
| Ws PsrA: | GNPKDKSRGGK V C ARG----GSGFNQLYDP Q R L V K P IMRVGERG | 113 |
| Ec BisC: | MENSL--Q-----SAVRDQVHSN T R V R F P M V R K GFLA | 30 |

Figure 2-1 Sequence Alignment of Region 1

The sequence alignment of *E. coli* DmsA (1), *E. coli* NarG (2), *E. coli* NarZ (5), *E. coli* FdnG (8), *W. succinogenes* FdhA (9), *E. coli* FdhF (11), *M. formicicum* FdhA (13), *W. succinogenes* PsrA (7), and *E. coli* BisC (6) was generated using the Pileup program (Genetics Computer Group, University of Wisconsin). Conserved residues are shown in bold and the DmsA residues examined in this study are underlined.

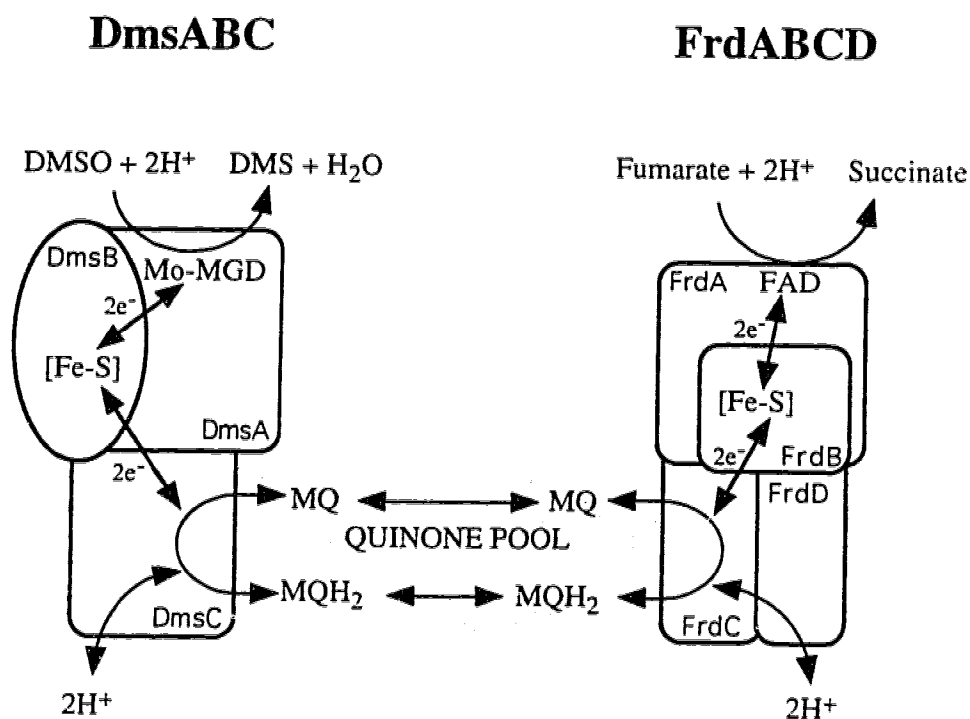


Figure 2-2 Q-Pool Coupling

DmsABC and FrdABCD are linked through the oxidation and reduction of the menaquinone pool.

[4Fe-4S] cluster of FrdABCD, center FR2, manifests as a broad resonance underlying the FR1 signal and is not readily observable in DSS301 membrane preparations. In the assay, the [Fe-S] clusters of both enzymes are reduced with dithionite. Addition of DMSO causes DmsABC to consume electrons and oxidize menaquinol. As the Q-pool becomes oxidized, electrons flow from FrdABCD to reduce menaquinone to menaquinol which is in turn oxidized by DmsABC. In this way, the [Fe-S] clusters of both enzymes become oxidized. Addition of fumarate causes FrdABCD to consume electrons and the [Fe-S] clusters of both enzymes to become oxidized. A block in electron flow causes the centers before the block to become oxidized upon addition of substrate, whereas the centers after the block remain reduced.

We have used site-directed mutagenesis to investigate the roles of DmsA residues Lys-28, Cys-38, Cys-42, Cys-75, and Arg-77. The growth, expression, localization, and electron transfer properties of the mutant enzymes were examined.

II. Materials and Methods

A. Bacterial Strains and Plasmids

The *E. coli* strains and plasmids used in this study are listed in Table 2-1.

B. Materials

Oligonucleotides were synthesized on an Applied Biosystems 392 DNA Synthesizer in the DNA Core Facility in the Dept. of Biochemistry, University of Alberta. DMN was a kind gift of Dr. A. Kröger, J.W. Goethe University, Frankfurt, Germany. Restriction endonucleases and modifying enzymes were from Life Technologies Inc. DNA sequencing was carried out in the DNA core facility using Sequenase and Sequenase reaction kits, Version 2.0, from United States Biochemical Corporation. The *in vitro* mutagenesis system was from Amersham. Protein assay standard and low molecular

TABLE 2-1
Bacterial Strains and Plasmids

| Strain or Plasmid | Description | Reference or Source |
|-------------------|--|---------------------|
| <i>E. coli</i> | | |
| HB101 | <i>supE44 hsdS20(r_B-m_B-) recA13 ara-14 proA2 lacY1 galK2 rpsL20 xyl-5 mtl-1</i> | (20) |
| TG1 | <i>supE hsdΔ5 thi Δ(lac-proAB) F' [traD36 proAB⁺ lacI^q lacZΔM15]</i> | (21) |
| JM109 | <i>recA1, endA1, gyrA96, thi, hsdR17, supE44, relA1, Δ(lac-proAB), F' [traD36 proAB⁺ lacI^q lacZΔM15]</i> | (22) |
| DSS301 | TG1, <i>ΔdmsABC</i> | (16) |
| Plasmids | | |
| pTZ18R | Amp ^R <i>lacZ'</i> | Pharmacia |
| pBR322 | Tet ^R Amp ^R | Pharmacia |
| pDMS160 | pBR322 Amp ^R (<i>dmsABC</i>) ⁺ | (17) |
| pDMS223 | pTZ18R Amp ^R (<i>dmsABC</i>) ⁺ | (17) |
| pK28A | pBR322 Amp ^R (<i>dmsA</i> [Lys-28→Ala-28] <i>BC</i>) ⁺ | This study |
| pK28S | pBR322 Amp ^R (<i>dmsA</i> [Lys-28→Ser-28] <i>BC</i>) ⁺ | This study |
| pC38A | pBR322 Amp ^R (<i>dmsA</i> [Cys-38→Ala-38] <i>BC</i>) ⁺ | This study |
| pC38S | pBR322 Amp ^R (<i>dmsA</i> [Cys-38→Ser-38] <i>BC</i>) ⁺ | This study |
| pC42G | pBR322 Amp ^R (<i>dmsA</i> [Cys-42→Gly-42] <i>BC</i>) ⁺ | This study |
| pC42S | pBR322 Amp ^R (<i>dmsA</i> [Cys-42→Ser-42] <i>BC</i>) ⁺ | This study |
| pC75A | pBR322 Amp ^R (<i>dmsA</i> [Cys-75→Ala-75] <i>BC</i>) ⁺ | This study |
| pC75S | pBR322 Amp ^R (<i>dmsA</i> [Cys-75→Ser-75] <i>BC</i>) ⁺ | This study |
| pR77G | pBR322 Amp ^R (<i>dmsA</i> [Arg-77→Gly-77] <i>BC</i>) ⁺ | This study |
| pR77S | pBR322 Amp ^R (<i>dmsA</i> [Arg-77→Ser-77] <i>BC</i>) ⁺ | This study |
| Phage | | |
| M13K07 | Kan ^R | Pharmacia |

weight polyacrylamide gel electrophoresis standards were obtained from Bio-Rad. All other materials were reagent grade and were obtained from commercial sources.

C. Oligonucleotide-Directed Mutagenesis

Single stranded pDMS233 was prepared by superinfection of JM109/pDMS223 with M13K07 helper phage (23). Oligonucleotide-directed mutagenesis of *dmsA* was performed using the Amersham *in vitro* mutagenesis system and the oligonucleotides in Table 2-2. After sequencing to confirm the mutation, the mutant DNA was subcloned into the wild-type *dms* operon on a 1 kb HindIII fragment to generate the mutant *dmsA* genes. The resultant plasmids were confirmed by restriction mapping and DNA sequencing.

D. Growth of Bacteria

For phage and plasmid manipulations and for preparation of inocula, cells were grown aerobically on Luria-Bertani Broth (23) or Terrific Broth (24). *E. coli* cells were grown anaerobically at 37°C on either glycerol-DMSO media in 160 ml filled Klett flasks or in 19 liter batches on glycerol-fumarate medium (14) for 48 hours (HB101) or 24 hours (DSS301). Antibiotics were used at the following concentrations: ampicillin (100 µg ml⁻¹), kanamycin (50 µg ml⁻¹) and streptomycin (100 µg ml⁻¹).

E. Preparation of Membrane Fractions

Membrane fractions were prepared by the method of Yamato *et al.* (25) for use in expression studies and enzyme assays. This method gives a two-fold enrichment of specific activity over washed membranes. For EPR analysis membrane fractions were prepared by French Pressure lysis and differential centrifugation as described by Cammack and Weiner (18). The membranes were washed and resuspended in 100 mM MOPS, pH 7; 5 mM EDTA buffer and were stored at -70°C prior to use.

TABLE 2-2
DNA Sequence Analyses of Mutants in DmsA

| Mutant | Codon Change | Mutagenic Oligonucleotide |
|---------------|------------------------|-----------------------------------|
| K28A K28S | AAG → GCG AAG → TCG | 3'-CAGACGAAGCGGTTATC-5' T |
| C38A C38S | TGT → GCT TGT → TCT | 3'-CAGTTAACGCTGGTAGTCG-5' T |
| C42G C42S | TGC → GGC TGC → AGC | 3'-GGTAGTCGCGGGCCCGCTACGT-5' A |
| C75A C75S | TGC → GCC TGC → TCC | 3'-GTTCGCGCCGCCCTGCGTG-5' T |
| R77G R77S | CGT → GGT CGT → AGT | 3'-CCTGCCTGGGTGGGCGTTC-5' A |

F. Enzyme Assays

DmsABC activity was determined by monitoring the DMSO or TMAO dependent oxidation of BV^{•+} at 570 nm (16). The DMNH₂ and DMSO or TMAO dependent oxidation of dithionite was assayed at 317 nm (16). One unit of activity corresponds to 1 μ mole of BV^{•+} or dithionite oxidized min⁻¹.

G. Protein Determination and Polyacrylamide Gel Electrophoresis

Protein concentrations were estimated using a modified Lowry procedure (26) and a bovine serum albumin protein standard. Polyacrylamide gel electrophoresis of 12.5% polyacrylamide gels was carried out using the Bio-Rad mini-gel system and a discontinuous SDS buffer system (27). Gels were stained with Coomassie blue, destained, and the relative amount of DmsA protein was determined using a Joyce-Loebel Chromoscan 3 densitometer.

H. EPR Spectroscopy

Samples were prepared from washed membranes of *E. coli* DSS301 cells grown on glycerol-fumarate medium. Sample protein concentrations were 30 mg ml⁻¹. For reduced samples, 150 μ l of membranes were placed in a quartz EPR tube and incubated under argon for two minutes at 23°C. 5 mM dithionite was added and the sample was incubated for two minutes prior to rapid freezing in liquid nitrogen. DMSO or fumarate treated membranes were reduced with 5 mM dithionite, 25 mM DMSO or fumarate was added and the samples incubated a further two minutes before freezing. Air oxidized samples were vigorously stirred with a coiled stainless steel wire. Spectra were recorded using a Bruker ESP300 EPR spectrometer equipped with an Oxford Instruments ESR-900 flowing helium cryostat under the following conditions: temperature, 10 K; microwave power, 20 mW; microwave frequency, 9.45 GHz; modulation amplitude, 10 G_{pp}; gain, 2×10^4 (3.2×10^4 for DSS301/pBR322).

III. Results

A. Preparation of Mutants

Five conserved residues were selected for analysis. Mixed mutagenic oligonucleotides (Table 2-2) were used to replace Cys-38, Cys-42, Cys-75, Lys-28, and Arg-77 with Ser and either Ala or Gly. Ser and Ala were chosen as replacements as they are unlikely to cause structural defects (28). Gly substitutions were obtained as a result of using mixed oligonucleotides.

B. Expression and Localization of Mutant Enzymes

In membrane preparations from *E. coli* HB101 harboring a plasmid containing the *dmsABC* operon, DmsA was recognized as a major polypeptide of about 87 kDa (15). DmsB and DmsC could also be identified in the membranes but these subunits were less obvious due to co-migrating polypeptides and the diffuse staining of DmsC (29). To compare the expression/accumulation of DmsA from the mutant plasmids in HB101 we used densitometric scanning of Coomassie blue stained SDS-polyacrylamide gels (Table 2-3). The amount of DmsA accumulated varied widely. In general, the Ser substitutions accumulated DmsA to levels near the wild-type. With the exception of HB101/pK28A, the other Ala and Gly mutant plasmids accumulated lesser amounts of DmsA in the membrane. HB101/pC75A did not accumulate detectable DmsA. pC38S, pC42S, pC75S, pK28S, and pR77S were selected for detailed study as they presented the most consistent pattern of expression.

In all but one case approximately 70% of the total DMSO reductase activity was localized to the cytoplasmic membrane with the remaining 30% found in the cytoplasm. This is similar to the distribution seen with wild-type enzyme activity (30). The exception was HB101/pR77G, which accumulated about 70% of the activity in the cytoplasmic fraction. Immunoblotting (not shown) confirmed a larger amount of DmsAB in the cytoplasmic fraction of HB101/pR77G than in HB101/pDMS160 suggesting that

TABLE 2-3
Expression of DmsA in *E. coli* Cells Harboring Wild-Type and Mutant Plasmids

| Plasmid | Expression of DmsA in: | |
|---------|-------------------------|-----------------------|
| | <i>E. coli</i> HB101 | <i>E. coli</i> DSS301 |
| | Relative % ^a | |
| pBR322 | 3 | 0 |
| pDMS160 | 13 | 14 |
| pK28A | 12 | ND ^b |
| pK28S | 11 | 15 |
| pC38A | 9 | ND |
| pC38S | 11 | 5 |
| pC42G | 6 | ND |
| pC42S | 8 | 5 |
| pC75A | 0 | ND |
| pC75S | 8 | 9 |
| pR77G | 6 | ND |
| pR77S | 16 | 6 |

^a Percentage of DmsA relative to total protein was determined by densitometry scans of polyacrylamide gels. 45 µg of membrane protein was loaded per lane and the percentages shown are from a representative set of membrane preparations. The errors in the quantitation of DmsA were calculated to be 4-9% by multiple determinations of the same samples.

^b ND, not determined.

perturbation in the structure of DmsA had occurred, altering membrane localization of the catalytic dimer.

We examined the expression of the Ser substitutions in *E. coli* DSS301 which carries a total deletion of the *dms* operon (16). The levels of the DmsA proteins expressed from pC38S, pC42S and pR77S in DSS301 corresponded to only half the protein seen in HB101 membrane preparations. DSS301/pK28S accumulated DmsA to levels comparable to the wild-type enzyme. The distribution of enzyme between membrane and cytoplasm was similar in DSS301 and HB101.

C. Growth Characteristics of E. coli Expressing the Mutant Enzymes

DSS301 is unable to grow anaerobically on DMSO because DmsABC is the only enzyme able to couple DMSO reduction to energy conservation in *E. coli* (31). The deletion mutant can be complemented by the entire *dms* operon on a recombinant plasmid (16) and this provided a measure of the *in vivo* function of the mutant enzymes. DSS301 carrying the mutant plasmids were grown anaerobically on glycerol-DMSO medium producing the doubling times shown in Table 2-4. Only the wild-type, K28A, K28S and C75S enzymes were able to support growth of DSS301, although cells carrying pC75S grew much slower.

We examined growth of HB101 harboring these *dms* plasmids (Table 2-4). Although HB101 has a chromosomal copy of DMSO reductase, the mutants that did not support growth in DSS301 inhibited the growth of HB101. C75A did not inhibit growth in HB101 because this mutant did not express. The overexpressed mutant subunits compete with the chromosomally encoded wild-type DmsA for assembly into the holoenzyme resulting in this inhibition. Such effects have previously been reported in studies of DmsABC (17) and FrdABCD (32,33).

TABLE 2-4
Growth Characteristics of Cells Harboring Mutant and Wild-Type DmsABC Plasmids

| Plasmid | Doubling time ^a (hours) in: | |
|---------|--|----------------------|
| | <i>E. coli</i> DSS301 | <i>E. coli</i> HB101 |
| pBR322 | NG ^b | 6.7 ± 0.5 |
| pDMS160 | 2.0 ± 0.2 | 5.0 ± 0.9 |
| pK28A | 2.4 ± 0.2 | 5.2 ± 0.6 |
| pK28S | 2.8 ± 0.2 | 5.6 ± 0.8 |
| pC38A | NG | NG |
| pC38S | NG | 10 ± 4 |
| pC42G | NG | NG |
| pC42S | NG | 10 ± 4 |
| pC75A | NG | 6 ± 1 |
| pC75S | 7 ± 1 | 8 ± 3 |
| pR77G | NG | NG |
| pR77S | NG | 9 ± 1 |

^a Doubling times were determined from measurements of cell densities in glycerol-DMSO minimal medium using a Klett-Summerson spectrophotometer equipped with a Number 66 filter. The doubling times shown are the average of several determinations ± the standard deviation.

^b NG, no growth on glycerol-DMSO minimal medium.

D. Electron Transfer from the Artificial Electron Donor Benzyl Viologen

Membrane fractions from HB101 harboring the *dmsABC* plasmids were assayed for DMSO reductase activity using $BV^{\bullet+}$ as electron donor and DMSO or TMAO as oxidant (Table 2-5). All of the mutant enzymes displayed a specific activity higher than HB101/pBR322 membranes. C42S had the lowest specific activity (35 units mg^{-1}) which was only slightly enhanced over the specific activity of HB101/pBR322 (29 units mg^{-1}). The C42S activity may represent a combination of chromosomal *dmsABC* expression and excess C42S expression but the results suggest that this residue plays a role in $BV^{\bullet+}$ oxidase activity. When the activities were normalized to the amount of DmsA in the membrane (Table 2-5), C42S had the lowest activity again, suggesting that this mutation has decreased the efficiency of DMSO reduction.

All of the plasmids expressed DMSO: $BV^{\bullet+}$ oxidoreductase activity in DSS301. The specific activity of DSS301/pDMS160 was 79 units mg^{-1} (TMAO as oxidant) whereas DSS301/pC42S displayed the lowest specific activity (14 units mg^{-1}). This activity must come from the mutant enzyme as DSS301 had a specific activity of 0.2 units mg^{-1} with TMAO. As in HB101, the other mutant enzymes demonstrated intermediate activities.

The ratio of TMAO to DMSO activity was generally between 7 and 9, in agreement with the reported activity ratio (16). Two of the mutants had substrate activity ratios outside this range (K28S had a ratio 10.5 and C42S had a ratio of 5) but it is unlikely that these variations represent a difference in substrate utilization. Together these results suggest that of these five conserved residues only Cys-42 may play a specific role in $BV^{\bullet+}$ oxidase activity.

E. Electron Transfer from the Quinol Analog Dimethylnaphthoquinol

DMNH₂ is a quinol analog previously used to analyze electron transfer within FrdABCD (32) and DmsABC (16). It reacts only with the holoenzyme forms of these

TABLE 2-5

**Specific Activities of Membrane Preparations Containing Amplified Levels of
Mutant and Wild-Type DmsABC**

| Plasmid | Specific Activity ^a | | | | | | | Q-Pool ^b Coupling |
|---------|--------------------------------|--------|------|-------------------|-------------------|------------|------|---------------------------------|
| | Benzyl Viologen | | | | DMNH ₂ | | | |
| | TMAO | DMSO | TMAO | Normalized | TMAO | DMSO | TMAO | |
| | | | DMSO | TMAO ^c | | | DMSO | |
| pBR322 | 29 ± 3 | 5 ± 1 | 5.8 | 870 ± 10 | 0.8 ± 0.07 | 0.5 ± 0.05 | 1.9 | - |
| pDMS160 | 190 ± 18 | 21 ± 4 | 9.0 | 1400 ± 100 | 5.5 ± 1.5 | 2.1 ± 0.3 | 2.6 | + |
| pK28S | 179 ± 66 | 17 ± 5 | 10.5 | 1000 ± 100 | 8.9 ± 1.3 | 2.0 ± 0.5 | 4.5 | + |
| pC38S | 71 ± 9 | 9 ± 1 | 7.9 | 690 ± 20 | 1.0 ± 0.1 | 0.5 ± 0.2 | 2.2 | - |
| pC42S | 35 ± 9 | 7 ± 2 | 5 | 500 ± 50 | 1.3 ± 0.5 | 0.7 ± 0.4 | 1.9 | - |
| pC75S | 84 ± 14 | 12 ± 2 | 7 | 1000 ± 200 | 2.2 ± 0.5 | 1.1 ± 0.1 | 2.0 | + |
| pR77S | 138 ± 34 | 16 ± 3 | 8.6 | 700 ± 200 | 0.3 ± 0.1 | 0.1 ± 0.04 | 2.9 | - |

^a Membranes were prepared from HB101 cells grown on glycerol-fumarate medium. BV⁺:substrate and DMNH₂:substrate enzyme activities are expressed as units mg⁻¹ of protein ± the standard deviation. Assays were carried out in triplicate on three independent membrane preparations.

^b Membranes were prepared from DSS301 cells grown on glycerol-fumarate medium and the ability of DmsABC to oxidize the menaquinone pool was examined.

^c BV⁺:TMAO activities were normalized for the amount of DmsA expression as determined by densitometry and are expressed as units mg⁻¹ of DmsA ± the standard deviation. Each specific activity was normalized for the amount of DmsA present in that particular preparation and the normalized activities were then averaged and the standard deviation determined.

reductases, in contrast to benzyl viologen which will transfer electrons to either the catalytic dimer or holoenzyme. DMNH₂-dependent reduction of TMAO and DMSO by HB101 membranes is shown in Table 2-5. All mutants, except R77S, display specific activities greater or equal to the background (HB101/pBR322). C38S and C42S have low levels of activity and it is unclear if this activity results from chromosomal or plasmid expression. R77S has very low activity suggesting that this residue is essential for DMNH₂ oxidase activity.

All mutant enzymes possessed DMNH₂ activity in DSS301 where the endogenous DMNH₂:TMAO activity is only 0.025 units mg⁻¹. C38S and C42S had specific activities of 0.3 and 0.2 units mg⁻¹, respectively, suggesting that these residues are not essential for DMNH₂ oxidase activity but play a role in the efficiency of the reaction. Similarly, R77S had a very low specific activity of 0.05 units mg⁻¹ suggesting that this residue, although not essential for BV^{•+} dependent activity, has a major effect on DMNH₂ oxidase activity. Interestingly, the ratio of TMAO to DMSO activity with DMNH₂ as electron donor was near two compared to 5 to 10 for BV^{•+} suggesting that the mechanisms of the benzyl viologen and DMN reactions differ.

F. Ability of Wild-type and Mutant Enzymes to Oxidize the Menaquinone pool

The membrane menaquinone pool is in equilibrium with several terminal reductases including FrdABCD and DmsABC. Functional DmsABC is able to draw electrons from Frd/ 3CD through the menaquinone pool to reduce DMSO, and the reverse also is true. We can follow this reaction using EPR spectroscopy of the endogenous [Fe-S] clusters in these proteins (17). DSS301 membranes contain high levels of FrdABCD which can be used to determine if plasmid encoded DmsABC is able to catalyze DMSO-dependent menaquinol oxidation. We have used the Q-pool coupling assay to determine whether the DmsA mutants are able to accept electrons from the endogenous quinone pool (Table 2-5). Figure 2-3A shows the spectra obtained from

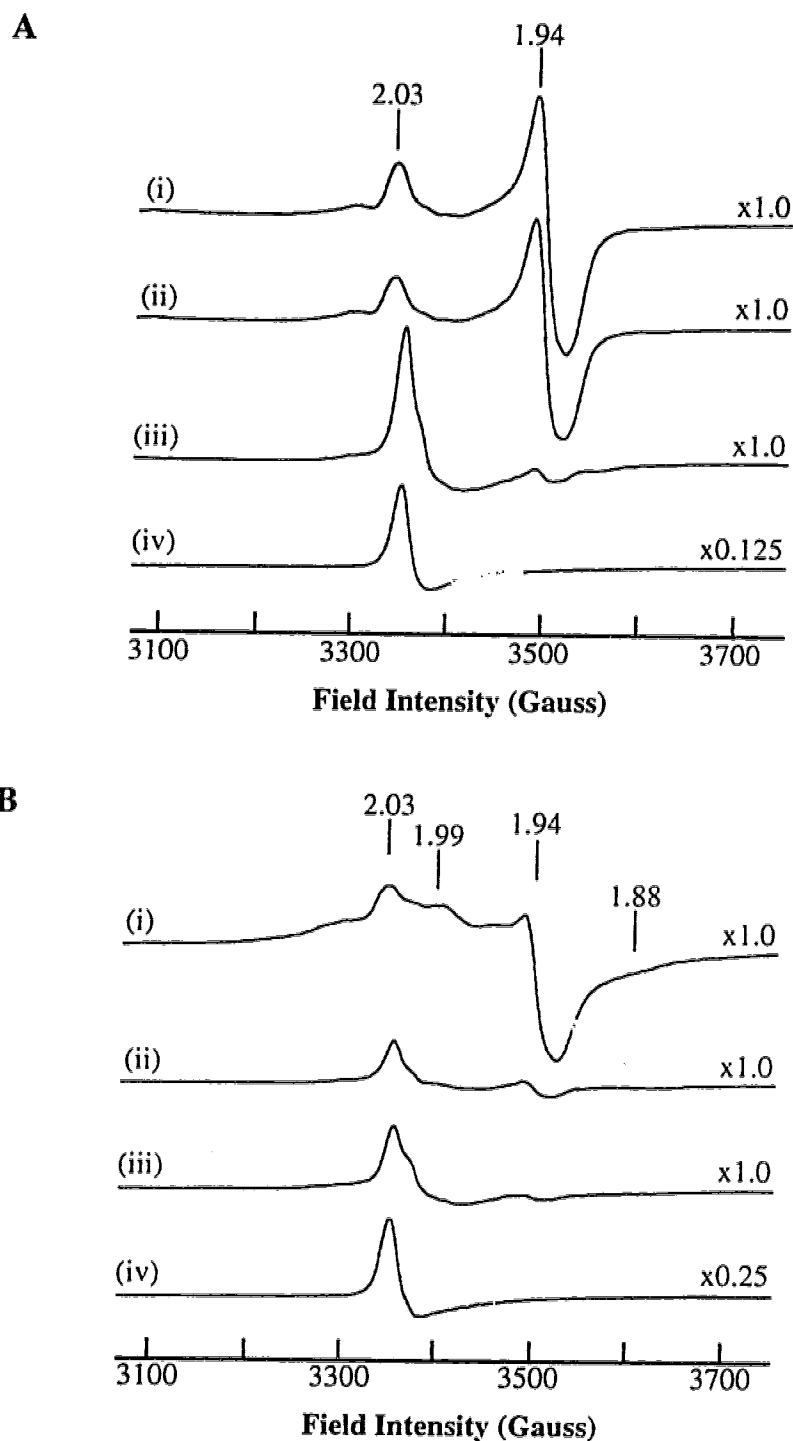


Figure 2-3 Oxidation of the Q-Pool by DmsABC

EPR spectra are of DSS301/pBR322 membranes (A) and DSS301/pDMS160 membranes (B): (i) reduced with dithionite; (ii) reduced with dithionite and treated with 25 mM DMSO; (iii) reduced with dithionite and treated with 25 mM fumarate; (iv) air oxidized. The g-values of the EPR signals are indicated at the top of the spectra.

E. coli DSS301/pBR322 membranes. When reduced with dithionite, the prominent features are a peak at $g = 2.03$ and a peak-trough at $g = 1.94$ which are characteristic of the reduced FR1 [2Fe-2S] cluster of FrdABCD (19). Addition of 25 mM DMSO or TMAO (data not shown) does not change the spectrum of these membranes but the addition of 25 mM fumarate causes the FR1 features to diminish and a sharp peak at $g = 2.02$ with a broad trough immediately upfield to appear. These new features are characteristic of the oxidized [3Fe-4S] center of FrdABCD, FR3 (19). In Figure 2-3B, the spectra of membranes from DSS301/pDMS160 are shown. In the dithionite reduced sample the FrdABCD signal is still present but a new peak at $g = 1.99$ and a trough at $g = 1.88$ are also visible. These features are part of the spectrum of reduced DmsABC (18). When 25 mM DMSO (or TMAO) is added, the dithionite reduced features of both DmsABC and FrdABCD are diminished while the oxidized FR3 signal appears. Similarly, the addition of fumarate to reduced membranes also causes both enzymes to become oxidized. This coupling demonstrates that DmsABC is able to interact with and accept electrons from the quinone pool to reduce substrate. Reverse electron flow to the quinone pool from the [Fe-S] clusters of DmsABC also occurs.

Figure 2-4A shows EPR spectra of the DSS301/pK28S mutant membranes which have been reduced with dithionite. The dithionite reduced spectrum is a composite of FrdABCD and DmsABC which can be oxidized by either fumarate or DMSO. The K28S mutant enzyme is coupled to the quinone pool as is expected from the wild-type growth properties of this enzyme. The C75S enzyme also enables DSS301 to grow on DMSO medium and it too shows coupling to the quinone pool (data not shown). The C38S, C42S and R77S mutants were unable to support growth on DMSO and all have EPR spectra similar to that of DSS301/pR77S, as shown in Figure 2-4B. There was no oxidation of the reduced spectra of either DmsABC or FrdABCD by the addition of DMSO. The C38S, C42S and R77S mutant enzymes were not able to consume electrons by reducing DMSO. Addition of fumarate caused both DmsABC or FrdABCD to be

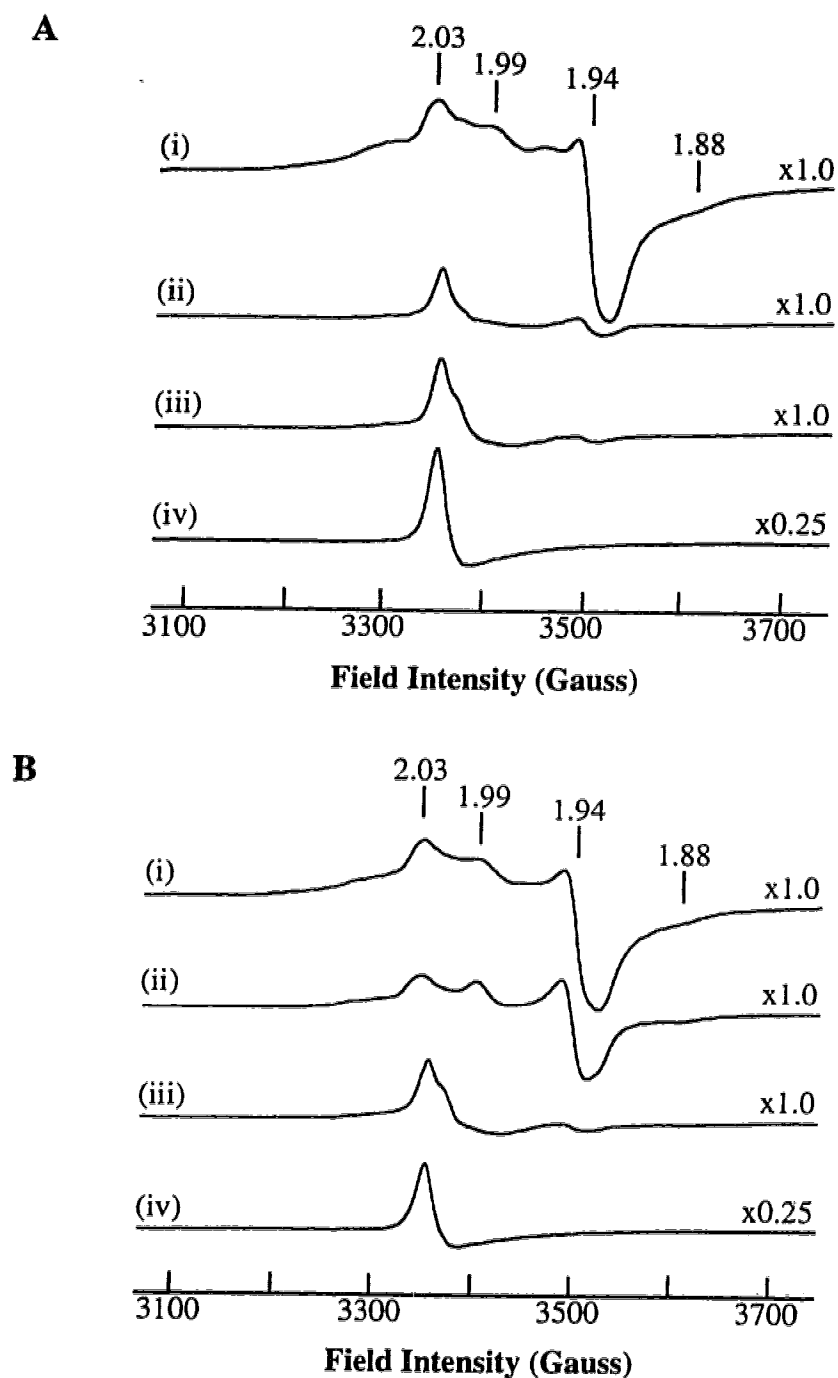


Figure 2-4 Ability of Mutant Enzymes to Oxidize the Q-pool

EPR Spectra of DSS301/pK28S (A) and DSS301/pR77S (B) membranes: (i) reduced with dithionite; (ii) reduced with dithionite and treated with 25 mM DMSO; (iii) reduced with dithionite and treated with 25 mM fumarate; (iv) air oxidized.

oxidized, thus the mutant enzymes are still able to interact with the quinone pool and transfer electrons at the level of the [Fe-S] clusters in DmsB. However, they are not capable of completing the electron transfer to DMSO in the catalytic site of DmsA and are therefore unable to grow.

IV. Discussion

E. coli DmsABC, (1) belongs to a family of membrane-bound, prokaryotic dehydrogenases and reductases that includes the *E. coli* nitrate reductases (NarGHI (2) and NarZYV (5)), *W. succinogenes* polysulfide reductase (PsrABC (7)) and the formate dehydrogenases from *E. coli* (FdnGHI (8) and FdhF/HycCD (10,11)), *M. formicicum* (FdhAB/FdhC (12,13)) and *W. succinogenes* (FdhABC (9)). Members typically contain three subunits: a large molybdopterin-containing catalytic subunit (DmsA, NarG), a Cys rich electron transfer subunit ligating [Fe-S] clusters (DmsB, NarH) and a membrane anchor subunit (DmsC, NarI). Multiple amino acid sequence alignment clearly shows the relationship of the catalytic and electron transfer subunits while the anchor subunits appear to be far less conserved. The catalytic subunits contain several regions of sequence similarity which are present in all members of the family; presumably some of these regions participate in complexing the molybdopterin cofactor. The order of these regions from amino to carboxy terminus is constant but their relative spacing varies greatly (4). Interestingly, biotin sulfoxide reductase (BisC, (6)), which receives its reducing equivalents from a small, heat-stable, thioredoxin-like protein (protein-SH), lacks the amino terminal region (Figure 2-1). The other eight enzymes require a Cys-rich electron transfer subunit and this suggested to us that Region 1 may be necessary for electron transfer to the catalytic subunit. The results presented herein confirm this hypothesis.

The eight homologous proteins contain three Cys residues equivalent to Cys-38, Cys-42 and Cys-75 of DmsA (Figure 2-1). DmsA contains an additional conserved Cys residue at position 34 but this amino acid is replaced by His in the nitrate reductases.

Changing Cys-34 of DmsA to His did not inhibit growth on glycerol-DMSO medium (Trieber and Weiner, unpublished results). These proteins also contain conserved basic residues corresponding to Lys-28, Arg-77, and Arg-90 of DmsA. Mutagenesis of Arg-90 to Ser (Rothery and Weiner, unpublished data) did not alter any measurable activity of DMSO reductase. Additional conserved residues including Gly-78 and Pro-94 were not mutated due to their potential structural role. The roles of DmsA residues Lys-28, Cys-38, Cys-42, Cys-75, and Arg-77 in DmsABC function were examined by site-directed mutagenesis.

Lys-28 – Mutation to the neutral amino acids Ser or Ala did not alter the growth, expression or catalytic activities of DmsABC, indicating that this conserved residue is not important for the activities we measured.

Cys-38 – Mutation to Ser produced an enzyme which could not support growth on DMSO although the membrane localization was wild-type and accumulation of mutant enzyme was not greatly impeded. The enzyme catalyzed BV^{•+} oxidase activity at approximately 50% of the HB101/pDMS160 level and had low DMNH₂ oxidase activity. It could not accept electrons from DmsB for reduction of DMSO.

Cys-42 – C42S could not support growth on DMSO. Again, the membrane localization was wild-type and accumulation of this enzyme was not greatly reduced. This enzyme had the poorest BV^{•+} oxidase activity and low DMNH₂ activity, suggesting that Cys-42 was necessary for optimal activity. C42S could not reduce DMSO with electrons from DmsB.

Cys-75 – Mutation to Ser produced an enzyme which supported growth on DMSO. The membrane localization was normal. It displayed relatively high BV^{•+} and DMNH₂ activity and could transfer electrons from the DmsB [Fe-S] clusters.

Arg-77 – This residue was essential for growth and for DMSO reduction coupled to DMNH₂ and menaquinol oxidation. The R77S mutant had near wild-type activity with BV^{•+} and its localization and accumulation were normal.

We have combined these results into a working model which is shown in Figure 2-5. In this model the BV^{•+} oxidase activity requires only the DmsA subunit. The observation that R77S has high BV^{•+} activity but cannot accept electrons from the DmsB [Fe-S] clusters indicates that BV^{•+} probably donates electrons directly to the DmsA subunit which can be used to reduce substrate. Of the conserved residues studied, only Cys-42 in DmsA plays a role in electron transfer from BV^{•+}.

The DMNH₂ activity has been assumed to accurately reflect the physiological function of DMSO reductase as it required all three subunits (16,31). However, the data presented here indicates that it is possible to isolate mutants with reasonable levels of DMNH₂ activity such as C38S and C42S, which are not functional and are unable to transfer electrons from the menaquinone pool. Interestingly, in HB101, these mutants had activity levels equal to or greater than that of the control strains (HB101/pBR322) which supported growth on DMSO. Thus, there is no correlation between observing DMNH₂-dependent activity and growth, although mutants with a higher level of activity (greater than 1 unit mg⁻¹) grow. This suggests that electrons from DMNH₂ follow a different path to the active site. Functional electron transfer from the menaquinone pool requires Cys-38, Cys-42 and Arg-77 but not Lys-28, Cys-75 or Arg-60. In all cases the enzyme assembled functional [4Fe-4S] clusters which could be reduced by dithionite and which could transfer their electrons back to the menaquinone pool, but in Cys-38, Cys-42, and Arg-77 the enzyme was unable to transfer these electrons on through DmsA.

V. Bibliography

1. Bilous, P. T., Cole, S. T., Anderson, W. F., and Weiner, J. H. (1988) *Mol. Microbiol.* **2**, 785-795
2. Blasco, F., Iobbi, C., Giordano, G., Chippaux, M., and Bonnefoy, V. (1989) *Mol. Gen. Genet.* **218**, 249-256

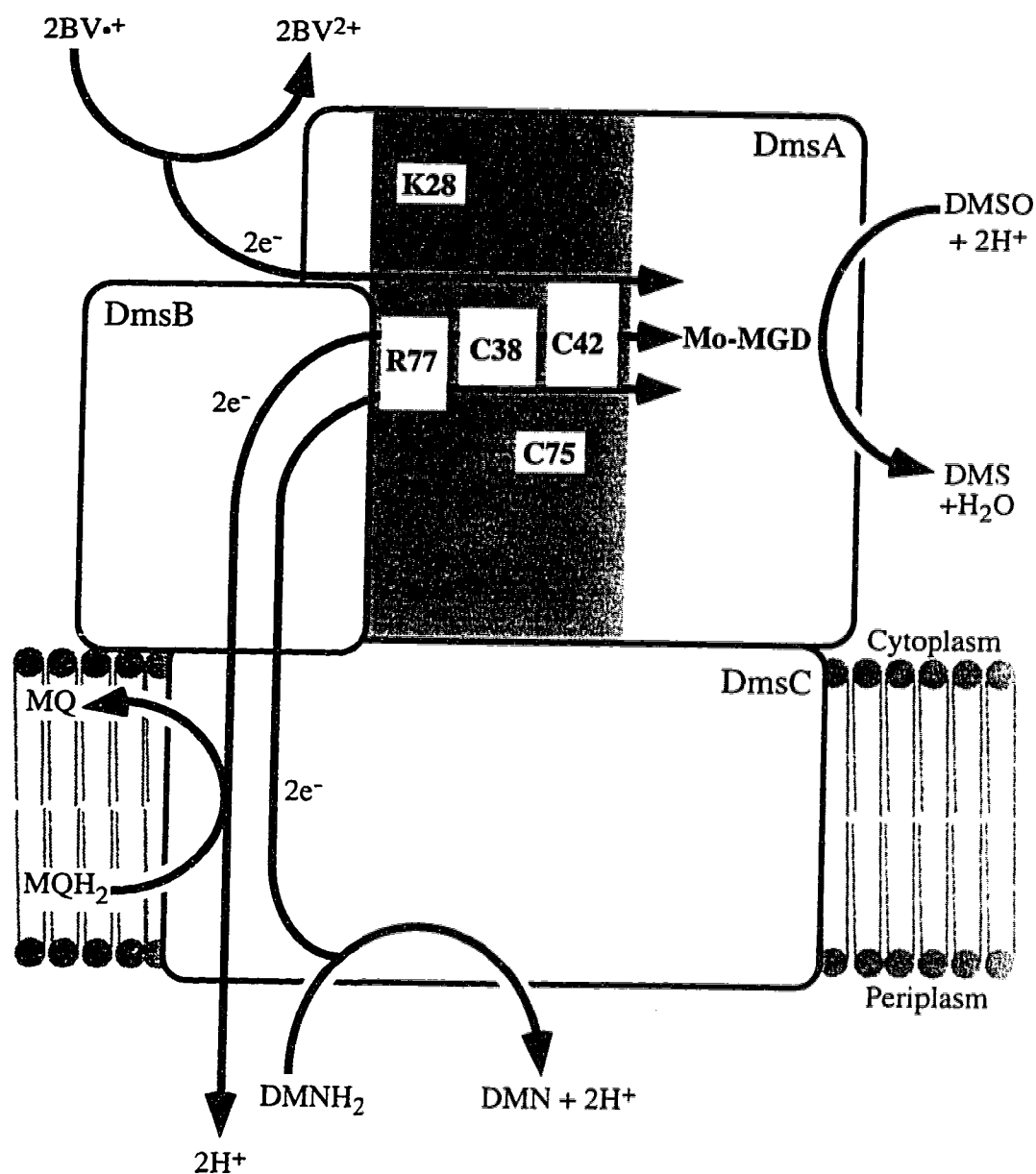


Figure 2-5 Model for Electron Transfer Through DmsABC

The amino acids shown in the shaded area are the residues examined in this study.

3. Wootton, J. C., Nicolson, R. E., Cock, J. M., Waters, D. E., Burke, J. F., Doyle, W. A., and Bray, R. C. (1991) *Biochim. Biophys. Acta* **1057**, 157-185
4. Weiner, J. H., Rothery, R. A., Sambasivarao, D., and Trieber, C. A. (1992) *Biochim. Biophys. Acta* **1102**, 1-18
5. Blasco, F., Iobbi, C., Ratouchniak, J., Bonnefoy, V., and Chippaux, M. (1990) *Mol. Gen. Genet.* **22**, 104-111
6. Pierson, D. E., and Campbell, A. (1990) *J. Bacteriol.* **172**, 2194-2198
7. Krafft, T., Bokranz, M., Klimmek, O., Schröder, I., Fahrenholz, R., Kojro, E., and Kröger, A. (1992) *Eur. J. Biochem.* **206**, 503-510
8. Berg, B. L., Li, J., Heider, J., and Stewart, V. (1991) *J. Biol. Chem.* **266**, 22380-22385
9. Bokranz, M., Guttman, M., Kortnor, C., Kojro, F., Fahrenholz, F., Lauterbach, F., and Kröger, A. (1991) *Arch. Microbiol.* **156**, 119-128
10. Sauter, M., Böhm, R., and Böck, A. (1992) *Mol. Microbiol.* **6**, 1523-1532
11. Zinoni, F., Birkmann, A., Stadtman, T. C., and Böck, A. (1986) *Proc. Natl. Acad. Sci. U.S.A.* **83**, 4650-4654
12. White, W. B., and Ferry, J. G. (1992) *J. Bacteriol.* **174**, 4997-5004
13. Shuber, A. P., Orr, E. C., Recny, M. A., Schendel, P. F., May, H. D., Schauer, N. L., and Ferry, J. G. (1986) *J. Biol. Chem.* **261**, 12942-12947
14. Bilous, P. T., and Weiner, J. H. (1985) *J. Bacteriol.* **162**, 1151-1155
15. Weiner, J. H., MacIsaac, D. P., Bishop, R. E., and Bilous, P. T. (1988) *J. Bacteriol.* **170**, 1505-1510
16. Sambasivarao, D., and Weiner, J. H. (1991) *J. Bacteriol.* **173**, 5935-5943
17. Rothery, R. A., and Weiner, J. H. (1991) *Biochemistry* **30**, 8296-8305
18. Cammack, R., and Weiner, J. H. (1990) *Biochemistry* **29**, 8410-8416
19. Johnson, M. K., Kowal, A. T., Morningstar, J. E., Oliver, M. E., Whittaker, K., Gunsalus, R. P., Ackrell, B. A. C., and Cecchini, G. (1988) *J. Biol. Chem.* **263**, 14732-14738
20. Boyer, H. W., and Roulland-Dussoix, D. (1969) *J. Mol. Biol.* **41**, 459
21. Gibson, T. J. (1984), Ph. D. Thesis, Cambridge University, England
22. Yanisch-Perron, C., Vieira, J., and Messing, J. (1985) *Gene* **33**, 103-119

23. Sambrook, J., Fritsch, E. F., and Maniatis, T. (1989) *Molecular Cloning: A Laboratory Manual*, 2nd ed. Ed., Cold Spring Harbor Laboratory, Cold Spring Harbor, NY
24. Tartof, K. D., and Hobbs, C. A. (1987) *Bethesda Res. Lab. Focus* **9**, 12
25. Yamato, I., Anraku, Y., and Hirosawa, K. (1975) *Biochemistry* **77**, 705-718
26. Markwell, M. A. D., Haas, S. M., Bieber, L. L., and Tolbert, N. E. (1978) *Anal. Biochem.* **87**, 206-210
27. Laemmli, U. K. (1970) *Nature (London)* **227**, 680-685
28. Bordo, D., and Argos, P. (1991) *J. Mol. Biol.* **217**, 721-729
29. Bilous, P. T., and Weiner, J. H. (1988) *J. Bacteriol.* **170**, 1511-1518
30. Sambasivarao, D., Scraba, D. G., Trieber, C., and Weiner, J. H. (1990) *J. Bacteriol.* **172**, 5938-5948
31. Sambasivarao, D., and Weiner, J. H. (1991) *Curr. Microbiol.* **23**, 105-110
32. Weiner, J. H., Cammack, R., Cole, S. T., Condon, C., Honoré, N., Lemire, B. D., and Shaw, G. S. (1986) *Proc. Natl. Acad. Sci. USA* **83**, 2056-2060
33. Westenberg, D. J., Gunsalus, R. P., Ackrell, B. A. C., and Cecchini, G. (1990) *J. Biol. Chem.* **265**, 19560-19567

Chapter 3

Engineering a Novel Iron-Sulfur Cluster into the Catalytic Subunit of *Escherichia coli* Dimethyl Sulfoxide Reductase*

* A version of this chapter has been published. Trieber, C. A., Rothery, R. A. and Weiner, J. H. (1996) J. Biol. Chem. 271, 4620-4626.

I. Introduction

DmsABC is a member of a family of molybdenum-containing oxidoreductases which reduce DMSO (1), TMAO (2), nitrate (3-8), biotin sulfoxide (9,10) and polysulfide (11) or oxidize formate (12-18). These enzymes share seven regions of sequence similarity located throughout the length of the polypeptides. Region 1 of DmsA has been demonstrated in Chapter 2 to be involved in electron transfer from DmsB to DMSO. This region in the periplasmic nitrate reductase, NapAB, from *T. pantotropha* has been suggested to ligate a [4Fe-4S] cluster (19). Region 1 of the subunit of *E. coli* formate hydrogenlyase that contains the formate dehydrogenase activity (FdhF) may also ligate an [Fe-S] cluster based on iron analysis (20).

Ferredoxins that contain [4Fe-4S] clusters usually ligate these clusters by Cys Groups consisting of four Cys residues spaced such that the first two Cys residues are separated by two amino acids while the spacing between the second, third and fourth Cys residues is somewhat variable. A Cys Group from the thermophilic methanogen *Methanococcus thermolithotrophicus* (21) has four amino acids separating the first two ligands but a Cys Group with three intervening residues has not been identified. The first three Cys residues and one distal Cys, often from a second Cys Group elsewhere in the protein, provide the ligands to the cluster (22,23). Alignment of the amino-terminal regions of the large subunits of the molybdoenzymes (Figure 3-1) shows four conserved Cys residues arranged in a manner reminiscent of a ferredoxin [4Fe-4S] cluster binding Cys Group. The sequences can be divided into three types. Type I enzymes contain three Cys residues spaced similarly to a bacterial ferredoxin Cys Group and one other conserved Cys which could provide the fourth ligand. The Type II enzymes also have four Cys residues but the spacing is such that three amino acids instead of two separate the first and second Cys residues. DmsABC belongs to this group as do the two membrane-bound *E. coli* nitrate reductases in which the first Cys is replaced by a His. His

Type I

| | | |
|-----------------|--|----|
| S7 NarB: | IDTAKTLCPYCGVCGGLEAVPPAQPGRATVRDREGTPIWQIRGDRQHPSSQGMVCVKG | 73 |
| Kp NasA: | MTETRRTCPYCGVCGGVIAASRAPHQVS.....VRGDEQHPANFGRLCVKG | 46 |
| Ec FdhF: | MKKVVTVCPCYCASGCKINLVVDNGKIVRA.....EAAQKTNQGTCLKG | 45 |
| Mf FdhA: | SKKVKTICTYCSVCGCGII.....AEVV.....DGVVVRQEVADHPISQGGHCCKG | 98 |
| Ws FdhA: | SKKVKTICTYCSVCGCGII.....AEVV.....DGVVVRQEVADHPISQGGHCCKG | 98 |
| Ec FdnG: | AKEIRNTCTYCSVCGCGLLMYSLGDGAKNA.....REAIYHIEGDDHPVSRGALCPKG | 98 |
| Ec FdoG: | TRETRNTCTYCSVCGCGLLMYSLGDGAKNA.....KASIFHIEGDDHPVNRGALCPKG | 98 |
| Ae NapA: | LKWSKAPCRFCGTGCGVT.....VAVK.....DNKVATQGDPOAEVNKGLNCVKG | 90 |
| Tp NapA: | ITWSKAPCRFCGTGCGVM.....VGVK.....EGRVVATHGDLLAEVNRGLNCVKG | 87 |
| Ws PsrA: | AKFVPSICEMCTSSCTIE.....ARVE.....GDKGVFIRGNPKDKSRGGKVCARG | 93 |

Type II

| | | | | | | |
|-----------------|--------|--------|--------|---------------------------------------|------------------|---------|
| | 34 | 38 | 42 | 75 | | |
| Ec DmsA: | KVIWSA | CTVNC | CGSRCP | LRMHVVDGEIKYV.....ETD·NTGDDNYDGLHQVRA | CLRG | 78 |
| Ec NarG: | KIVRST | HGVNCT | GTGCSW | KIYVKNGLVT.....WETQQT | DYPRTRPDLPNHEPRG | CPRG 99 |
| Ec NarZ: | KIVRST | HGVNCT | GTGCSW | KIYVKNGLVT.....WEIQQT | DYPRTRPDLPNHEPRG | CPRG 99 |

Type III

| | | |
|-----------------|---|----|
| Ec TorA: | TPSLLTPRRATAAQAAATDAVISKEGILTGSWGAIRATVKDGRFVAAKPFELDKYPSK· | 86 |
| Rs BisC: | MITTRVPHCSHWGAYTLLVDEGRIVGVEPFAHDPAPSEL | 39 |
| Ec BisC: | ME | 2 |

Figure 3-1 Sequence Alignment of the Cysteine Residues in Region 1

The enzymes are *Synechococcus* ssp. 7 NarB (5), *K. pneumoniae* NasA (6), *E. coli* FdhF (18), *M. formicicum* FdhA (15), *W. succinogenes* FdhA (13), *E. coli* FdnG (12), *E. coli* FdoG (14), *A. entrophus* NapA (7), *T. pantotropha* NapA (8), *W. succinogenes* PsrA (11), *E. coli* DmsA (1), *E. coli* NarG (3), *E. coli* NarZ (4), *E. coli* TorA (2), *R. sphaeroides* BisC (10), and *E. coli* BisC (9). Conserved Cys residues are shown in bold and the residues that were mutated in this study are underlined.

can be a ligand to a [4Fe-4S] cluster, as in the nickel-iron hydrogenase from *Desulfovibrio gigas*, but the first two ligands of this cluster, His and Cys, are separated by two amino acids (24). The Type III enzymes include the biotin sulfoxide reductases (BisC) and TMAO reductase (TorA) that share sequence identity with the other molybdoenzymes but do not contain the Cys region.

The [Fe-S] clusters of DmsABC have been characterized by EPR spectroscopy. The enzyme contains four [4Fe-4S] clusters with midpoint potentials, $E_{m,7} = -50, -120, -240, \text{ and } -330 \text{ mV}$ (25). These clusters are believed to be ligated by the four ferredoxin-like Cys Groups (I-IV) in DmsB (25,26), although the possibility exists that the Cys region in DmsA might be able to ligate a cluster. Site-directed mutagenesis of DmsB Cys Groups III (27) and I (Rothery and Weiner, unpublished results) has demonstrated that these Cys Groups provide ligands for two [4Fe-4S] clusters.

The DmsA Cys region has previously been examined through the use of site-directed mutagenesis (Chapter 2). Cys38, Cys42, and Cys75 were mutated to Ser and only the C75S mutant enzyme was able to support growth on DMSO. All three mutant enzymes retained some level of catalytic activity with an artificial electron donor, $BV^{+\bullet}$, and with the quinol analog, DMNH₂. The C38S and C42S mutants were unable to use electrons from the quinone pool to reduce substrate, although the [4Fe-4S] clusters responded to the redox state of the quinone pool. In this chapter we show that the DmsA Cys Group does not coordinate an EPR-visible [Fe-S] cluster but when the second Cys of this group is mutated, a [3Fe-4S] cluster assembles into the mutant enzyme.

II. Materials and Methods

A. Bacterial Strains and Plasmids

Many of the *E. coli* strains and plasmids used in this study are described in Table 2-1. *E. coli* strain F36 is a mutant of HB101 which is impaired in molybdenum cofactor insertion into DmsABC (25). *E. coli* TG1 was used for routine DNA manipulation and is

the parent strain of *E. coli* DSS301 which carries a deletion of the entire *dmsABC* operon (28). The plasmids used were the vector pBR322, pDMS160 which contains the *dmsABC* operon cloned into pBR322 (27) and pC38S and pC38A which are derivatives of pDMS160 containing point mutations in the *dmsA* gene. pTZ18R was used as a cloning vector and to sequence fragments containing mutant DNA.

B. Materials

Synthesis of oligonucleotides and DNA sequencing were carried out in the Department of Biochemistry DNA Core Facility at the University of Alberta using an Applied Biosystems model 392 DNA synthesizer and a model 373A DNA sequencer (Perkin Elmer). Restriction endonucleases and modifying enzymes were obtained from Life Technologies Inc. All other materials were reagent grade and were obtained from commercial sources.

C. Site-Directed Mutagenesis

Manipulations of strains and plasmids were carried out as described in Sambrook *et al.* (29). The double mutant of *dmsA* with substitutions in residues Asn-37 and Cys-38 was generated through PCR mutagenesis of pC38S using the following mutagenic primers: 5'GTACAGTTTGCTCTGGTAG^{3'} and 5'CGACTACCAGAGCAAAGTG^{3'} (30). The mutant product was cloned into pTZ18R and sequenced. The fragment bearing the double mutation was subcloned into the wild-type operon to construct the plasmid pC38S,N37C.

D. Growth of Bacteria

Cultures were grown anaerobically at 37°C. F36 (19 liters) and HB101 (1 liter) cultures were grown on glycerol-fumarate medium for 48 hours (31). F36 cultures for whole cell preparations (1 liter) were grown on glucose-peptone-fumarate medium for 16 hours (32). DSS301 was grown on glycerol-DMSO media in 160 ml filled Klett flasks

(31). Antibiotics were used at the following concentrations; ampicillin and streptomycin, 100 $\mu\text{g ml}^{-1}$, kanamycin, 40 $\mu\text{g ml}^{-1}$.

E. Harvesting of Cells and Preparation of Membrane Fractions

For whole cell EPR samples, cells were harvested, washed and resuspended in degassed 100 mM MOPS, pH 7.0; 5 mM EDTA buffer containing 20 mM succinate (27). Glycerol-fumarate grown cells were harvested, washed and resuspended in 50 mM, MOPS, pH 7.0; 5 mM EDTA buffer. Phenylmethanesulfonyl fluoride (0.2 mM) was added and cells were subjected to French pressure lysis and differential centrifugation to prepare crude membrane fractions (25). For EPR experiments, the membranes were washed and resuspended in 100 mM MOPS, pH 7.0, 5 mM EDTA buffer. Membranes for dithionite reduction at pH 9 were washed and resuspended in 100 mM CHES, pH 9.0; 5 mM EDTA buffer. Membranes were stored at -70°C prior to use.

F. Protein Determination and Polyacrylamide Gel Electrophoresis

Protein concentrations were estimated by a modification of the Lowry procedure (33) using a Bio-Rad bovine serum albumin protein standard. Polyacrylamide gel electrophoresis was carried out using the Bio-Rad mini-gel system and a discontinuous SDS buffer system (34). Gels (12.5% acrylamide) were stained with Coomassie Blue, destained and the relative amount of DmsA protein was determined using a Joyce-Loebel Chromoscan 3 densitometer.

G. Enzyme Assays

DmsABC activity in crude HB101 membrane preparations was determined by monitoring the TMAO-dependent oxidation of $\text{BV}^{\bullet+}$ (25). One unit of activity corresponds to one $\mu\text{mol BV}^{\bullet+}$ oxidized min^{-1} .

H. EPR Spectroscopy

Samples were prepared as described by Cammack and Weiner (25) from either whole cells or washed membranes. Dithionite reduced samples were prepared as described in Chapter 2 but the length of the incubation with dithionite was increased to ten minutes. Ferricyanide oxidized samples were prepared by incubating membrane samples with 150 μ M potassium ferricyanide for 2 minutes prior to freezing in liquid nitrogen. Redox titrations were performed at 25°C using the following mediators: quinhydrone, 2,6-dichloroindophenol, 1,2-naphthoquinone, toluyene blue, phenazine methosulfate, thionine, duroquinone, methylene blue, and resorufin. Membranes were incubated under argon and the redox potential poised with small additions of sodium dithionite (reductive titration) or potassium ferricyanide (oxidative titration). After addition of dithionite or ferricyanide, membranes were equilibrated for at least two minutes before removing a sample to a quartz EPR tube and freezing.

Spectra were recorded using a Bruker ESP300 EPR spectrometer equipped with an Oxford Instruments ESR-900 flowing helium cryostat. Instrument conditions and temperatures are described in the individual figure legends. The microwave power required for half saturation ($P_{1/2}$) of the [3Fe-4S] cluster signals was calculated using the empirical equation $S \propto \sqrt{P}/(1+P/P_{1/2})^{0.5b}$ where S is the signal height, P is the microwave power, and b is the homogeneity parameter (35). Spin quantitations were carried out by double integrations of spectra from redox titrations (microwave power, 2 mW; temperature, 12 K) (36). The presence of background signals (primarily fumarate reductase) in the membranes was partly compensated for by subtracting the baseline intensity (at approximately 0 mV) from the fully oxidized and reduced intensities.

III. Results

A. Growth Properties and Enzyme Activities of the Cys-38 mutants

The ability of the mutant enzymes to support growth on DMSO was assessed using the *dmsABC* deletion strain, DSS301 (Table 3-1). Only the wild-type enzyme was able to support growth. DSS301 was not used for further characterization of the mutant enzymes due to the large amounts of fumarate reductase produced by this strain (27). The specific activities of HB101 membrane preparations were assayed using TMAO as the electron acceptor and the artificial electron donor, BV^{•+} (Table 3-1). Both mutant enzymes showed decreased specific activities when compared with the wild-type enzyme, as shown previously. The relative amounts of enzyme present in the F36 membrane preparations used for the EPR studies were determined by densitometry (Table 3-1). The relative percentage of DmsA in the F36/pC38A membranes is lower than in the wild-type or C38S preparations.

B. EPR Characteristics of Dithionite Reduced F36 membranes Containing Overexpressed Wild-Type and Mutant DmsABC

In F36, the Mo-MGD cofactor is not inserted into DmsABC and cannot interfere with the [Fe-S] signals in the redox titrations as occurs when DmsABC is expressed in HB101 (25). Although the enzyme produced in F36 is inactive, it assembles the [Fe-S] clusters normally. Figure 3-2 shows the EPR spectra of reduced membranes at 12 K. F36/pBR322 membranes contained very little DmsABC, expressed from the chromosomal copy of the operon. The spectrum from these membranes shows a peak at $g = 2.02$ and a peak-trough at about $g = 1.94$. These features are characteristic of the reduced [2Fe-2S] cluster of fumarate reductase, FR1 (37,38). F36/pDMS160 membranes contained a high level of DmsABC and the spectrum of the dithionite reduced samples (Figure 2b) is very similar to spectra obtained from both purified and membrane bound DmsABC (25,27). The spectrum contains peaks located at $g = 2.06$, $g = 2.02$, $g = 1.99$,

TABLE 3-1
Characteristics of the DmsA Mutant Enzymes

| Plasmid | Growth on DMSO ^a | Specific Activity ^b | Expression ^c |
|------------|-----------------------------|--------------------------------|-------------------------|
| | | | Relative % DmsA |
| pBR322 | NG | 6.0 ± 0.7 | 2 |
| pDM3160 | + | 38 ± 2 | 15 |
| pC38A | NG | 15 ± 1 | 10 |
| pC38S | NG | 19 ± 1 | 13 |
| pC38S,N37C | NG | 19 ± 2 | 12 |

- ^a The ability of the mutant enzymes to support growth on glycerol-DMSO media in the *dmsABC* deletion strain, DSS301, was determined by monitoring the increase in cell turbidity with a Klett-Summerson spectrophotometer. (+) indicates growth; NG, no growth.
- ^b Specific activities of HB101 membrane preparations from 1 liter cultures are expressed as units mg⁻¹ protein ± the standard deviation.
- ^c The percentage of DmsA relative to total protein in F36 membranes was determined by densitometry. The error in the relative percentage of DmsA is estimated to be approximately 4% by multiple determinations.

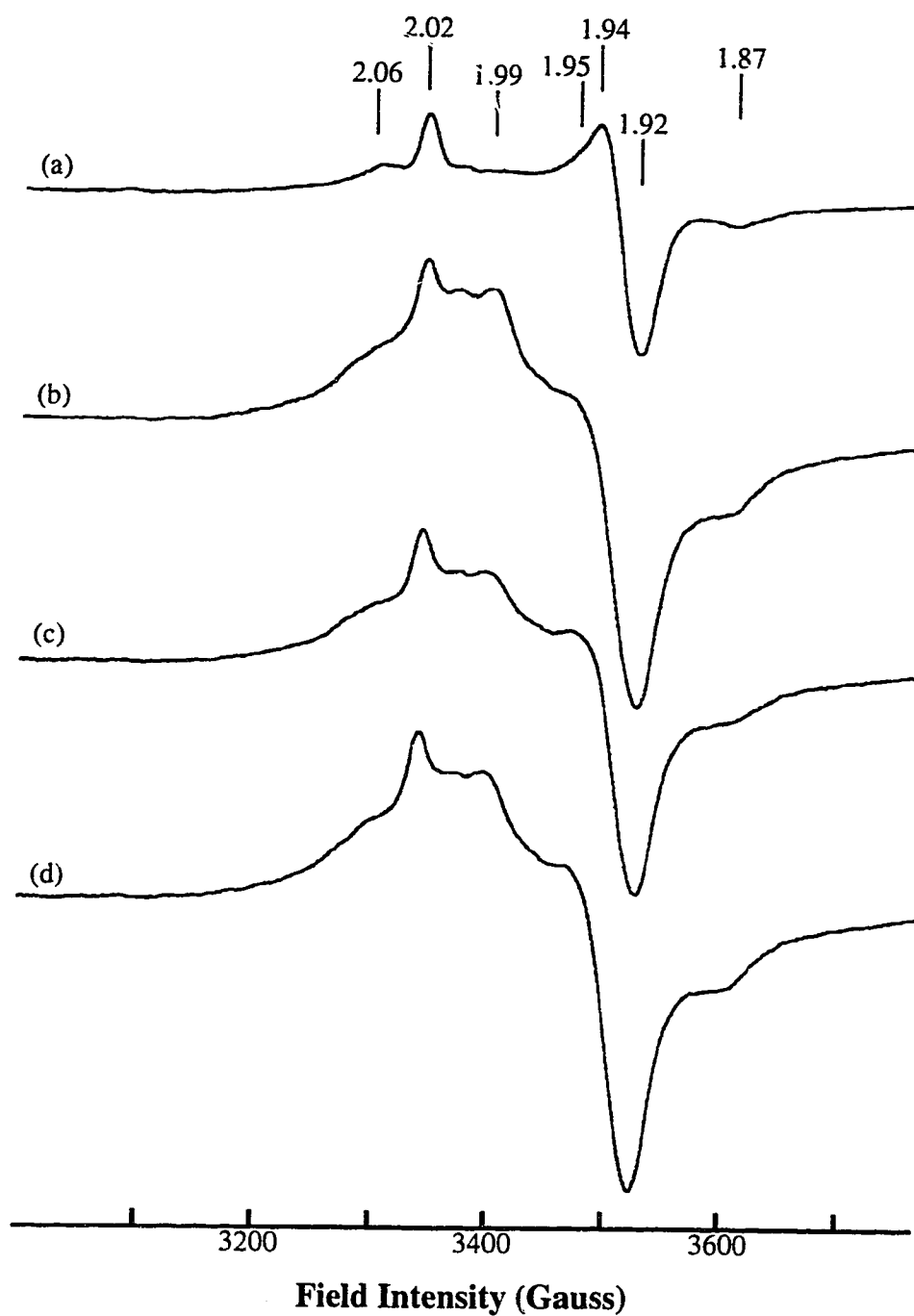


Figure 3-2 EPR Spectra of Reduced F36 Membranes

Spectra are of dithionite reduced membranes of (a) F36/pBR322, (b) F36/pDMS160, (c) F36/pC38A, and (d) F36/pC38S. Spectra were recorded under the following conditions: temperature, 12 K; microwave power, 20 mW; microwave frequency, 9.45 GHz; modulation amplitude, 10 G_{pp} at 100 KHz.

and $g = 1.95$. Two troughs are observed at $g = 1.92$ and $g = 1.87$. The peak at $g = 2.02$ is most likely due to fumarate reductase which would also contribute to the peak-trough at $g = 1.95$ to $g = 1.92$ (27). The peaks at $g = 2.06$, $g = 1.99$ and the peak-trough at $g = 1.95$ to $g = 1.92$ arise from DmsABC. Repeating the dithionite reduction at pH 9, to decrease the redox potential, did not change the spectrum observed.

Figure 3-2 (c and d) shows the spectra of dithionite reduced F36 membranes containing the C38A and C38S mutant enzymes, respectively. The features of these spectra are very similar to that of F36/pDMS160 membranes and all of the DmsABC features are present. The slight difference in the size of some of the features in the reduced EPR spectrum of the C38A mutant enzyme is due to the lower amount of enzyme present. Reduction by dithionite at pH 9 did not highlight any difference between the spectra of the wild-type and mutant enzymes (data not shown).

C. EPR Characteristics of Oxidized F36 Membranes Containing Amplified Wild-Type and Mutant DmsABC

Figure 3-3 shows EPR spectra recorded at 12 K of F36 membranes oxidized with ferricyanide. The spectrum of F36/pBR322 membranes (Figure 3-3a) has a small peak at $g = 2.02$ with a broad trough immediately upfield, characteristic of the oxidized [3Fe-4S] cluster of fumarate reductase, FR3 (37,38). The spectrum of F36/pDMS160 membranes (Figure 3b) shows similar features to that of F36/pBR322 membranes indicating that FR3 is the major EPR visible species present. Spectra from the mutant enzymes show major new features. The spectrum of F36/pC38S membranes (Figure 3-3d) is comprised of a sharp peak at $g = 2.03$ and a peak-trough centered at $g = 2.00$. The F36/pC38A spectrum (Figure 3-3c) is similar but the signal is broader than in F36/pC38S membranes. The EPR spectra of the oxidized mutant enzymes can be attributed to centers having axial symmetry with approximate g -values of $g_z = 2.03$ and $g_{xy} = 2.00$. Oxidized spectra of HB101 membranes containing the C42S and C75S mutant enzymes were similar to that of FR3,

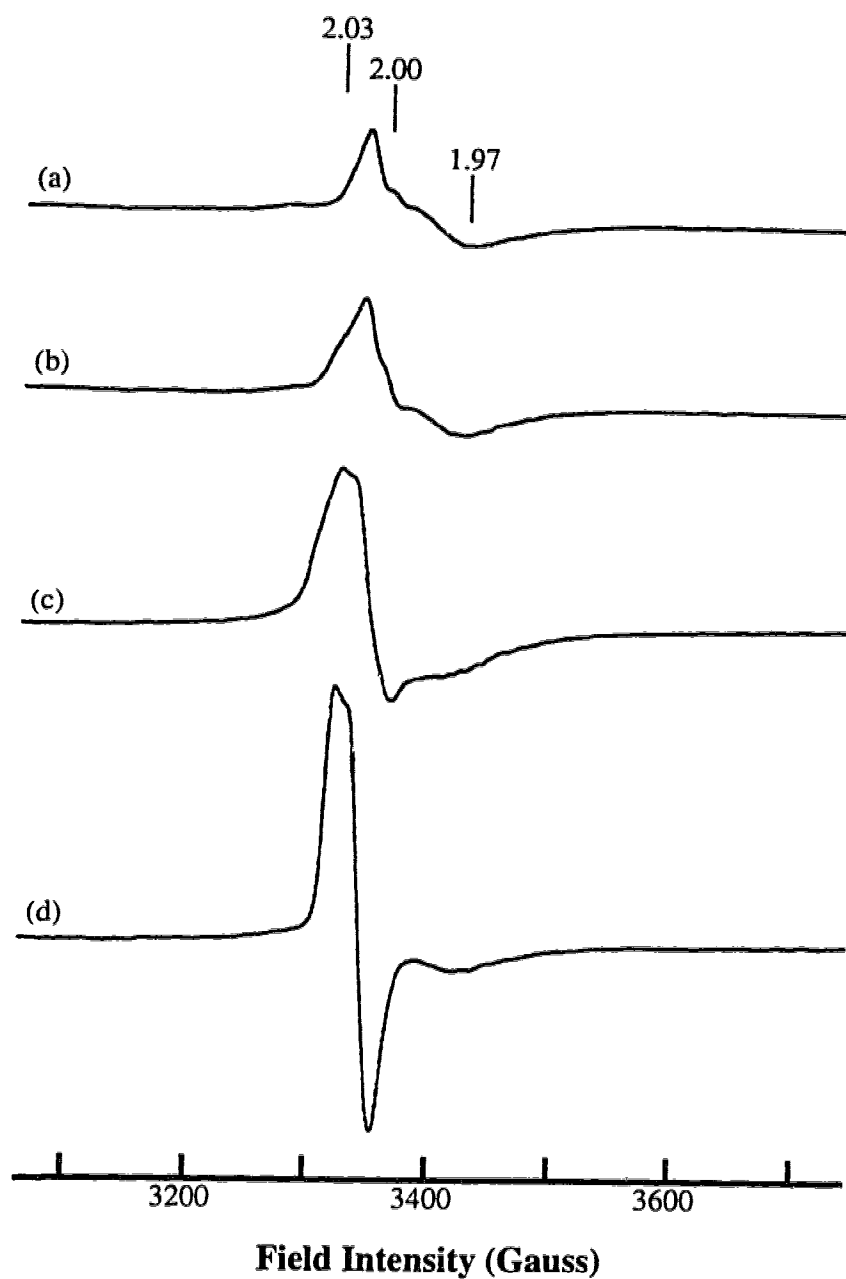


Figure 3-3 EPR Spectra of Oxidized Membranes

Spectra are of ferricyanide oxidized membranes of (a) F36/pBR322, (b) F36/pDMS160, (c) F36/pC38A, and (d) F36/pC38S. Instrument parameters were as described for Figure 3-2.

indicating that these mutants do not assemble significant amounts of a [3Fe-4S] cluster ligated in DmsA (data not shown).

To identify the nature of the paramagnetic species present in the oxidized Cys-38 mutants, we studied the microwave power saturation properties and the temperature dependences of the new signals. Figure 3-4 shows the effect of increasing microwave power on the mutant center signals at 12 K. Microwave power saturation data obtained from F36/pC38A membranes were fitted to an empirical equation to obtain the microwave power required for half saturation of the signal, the $P_{1/2}$ (35). A two component model was required to fit the data giving $P_{1/2}$ values of 1 mW (40%) and 185 mW (60%). The presence of two components suggests that the protein conformation around the cluster is not homogeneous. Microwave power saturation data from the F36/pC38S membranes were fitted to one component with a $P_{1/2}$ of 9 mW. Figure 3-5 shows the effect of temperature on the intensity of the new signals. The F36/pC38A and F36/pC38S signals reached a maximum intensity at 9 K and 11 K that decreases until, at 30 K, they were hardly visible. The microwave power saturation and temperature dependences of the new centers in the C38A and C38S mutants are typical of the behavior of [3Fe-4S] clusters (39,40). We therefore assign these signals to new [3Fe-4S] clusters ligated by the DmsA Cys Group in the mutant enzymes.

D. Redox Titrations of the C38A and C38S Mutant Enzymes

Redox titrations were carried out to determine the midpoint potentials of the [4Fe-4S] clusters and the new [3Fe-4S] clusters in the DmsA mutant enzymes (Table 3-2). In the mutant enzymes four [4Fe-4S] clusters were detected with midpoint potentials close to those of the wild-type enzyme. The amount of each cluster present was very similar in the wild-type and mutant enzymes. To determine the midpoint potential of the [3Fe-4S] cluster of C38A, F36/pC38A membranes were oxidized, reduced and reoxidized (Figure 3-6A). Upon reoxidation of the membranes, most of the [3Fe-4S] clusters were

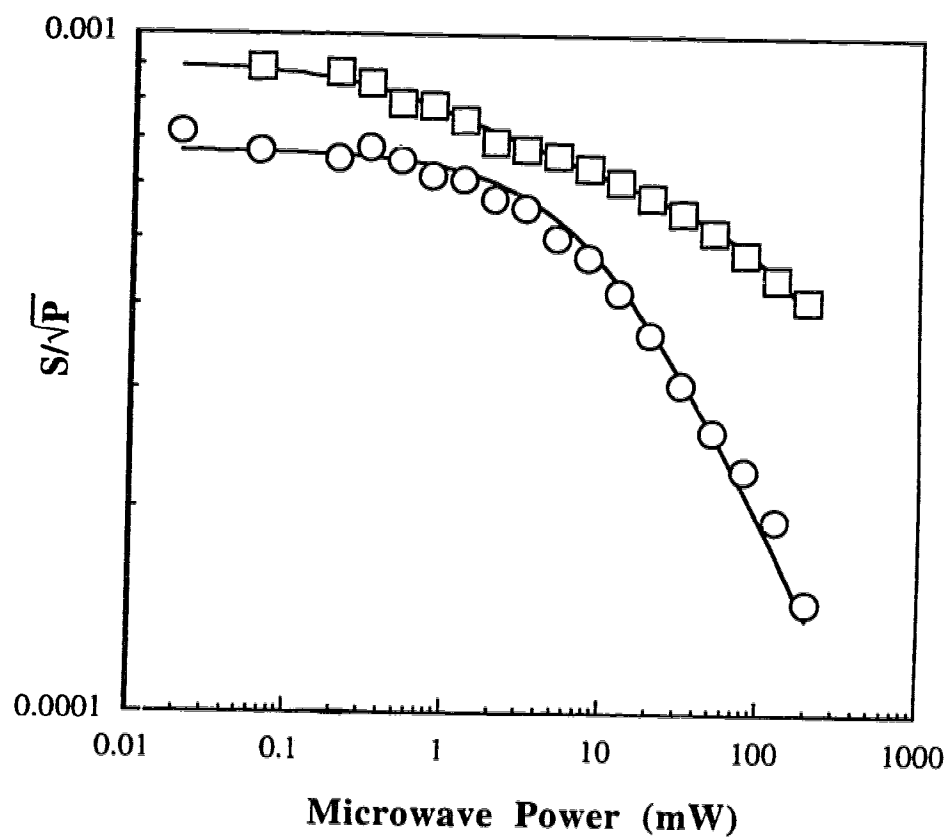


Figure 3-4 Microwave Power Dependences of the [3Fe-4S] Clusters

The saturation behavior of the $g = 2.03$ signals was plotted and fitted to an empirical equation to derive $P_{1/2}$ values. Data obtained from spectra at 12 K of membranes of F36/pC38A (□) and F36/pC38S (○) were fitted to $P_{1/2}$'s of 1 and 185 mW for C38A and 9 mW for C38S.

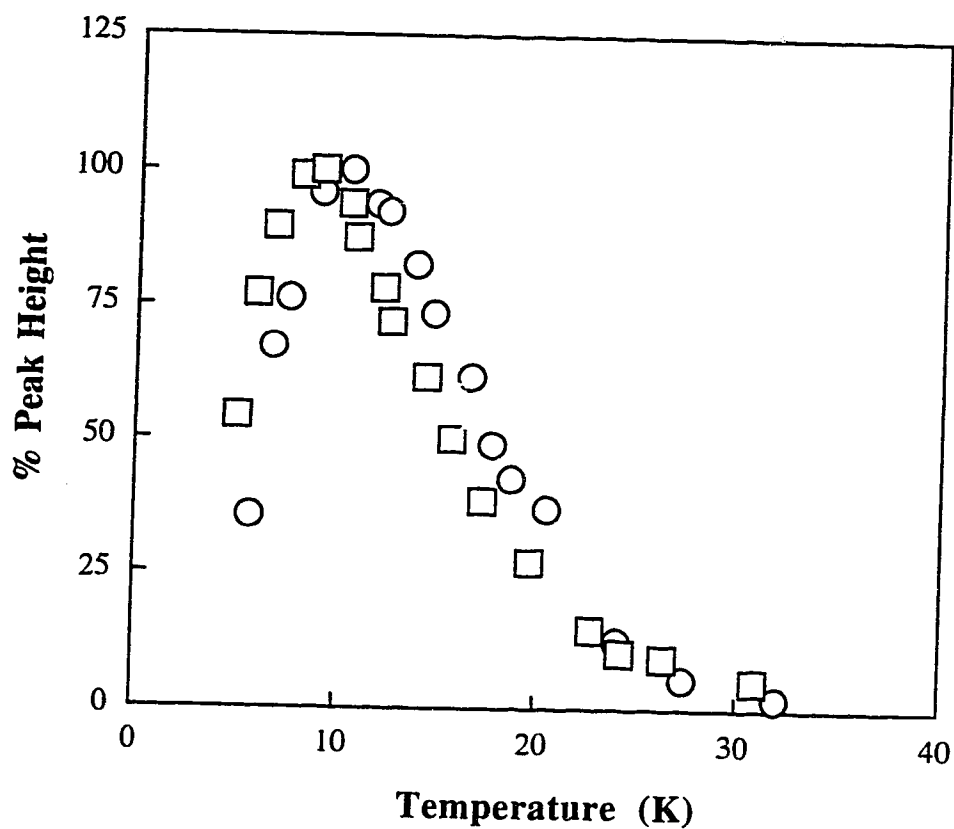


Figure 3-5 Temperature Dependences of the [3Fe-4S] clusters

The percent peak height of the $g = 2.03$ signal was measured from spectra of F36/pC38A (□) and F36/pC38S (○) ferricyanide oxidized membranes recorded at a non-saturating microwave power of 2 mW.

TABLE 3-2
Midpoint Potentials of Wild-Type and Mutant DMSO reductases

| | Midpoint Potentials (mV) | | | | | red:ox ^a |
|-----------|--------------------------|------|------|------|-----------------------|---------------------|
| | I | II | III | IV | V | |
| Enzyme | | | | | | |
| DmsABC | -50 | -120 | -240 | -340 | — | 33.6 |
| C38A | -40 | -95 | -220 | -350 | 75/140 ^b | 3.8 |
| C38S | -50 | -115 | -255 | -370 | 165, 190 ^c | 3.6 |
| C38S,N37C | -25 | -120 | -260 | -340 | 40/200 ^b | 12.9 |

^a The ratio of reduced to oxidized [Fe-S] clusters was calculated from double integration of reduced and oxidized spectra from the redox titrations.

^b Data from the redox titrations were fitted to a two component model.

^c Data from the redox titrations were fitted to two independent one-component models.

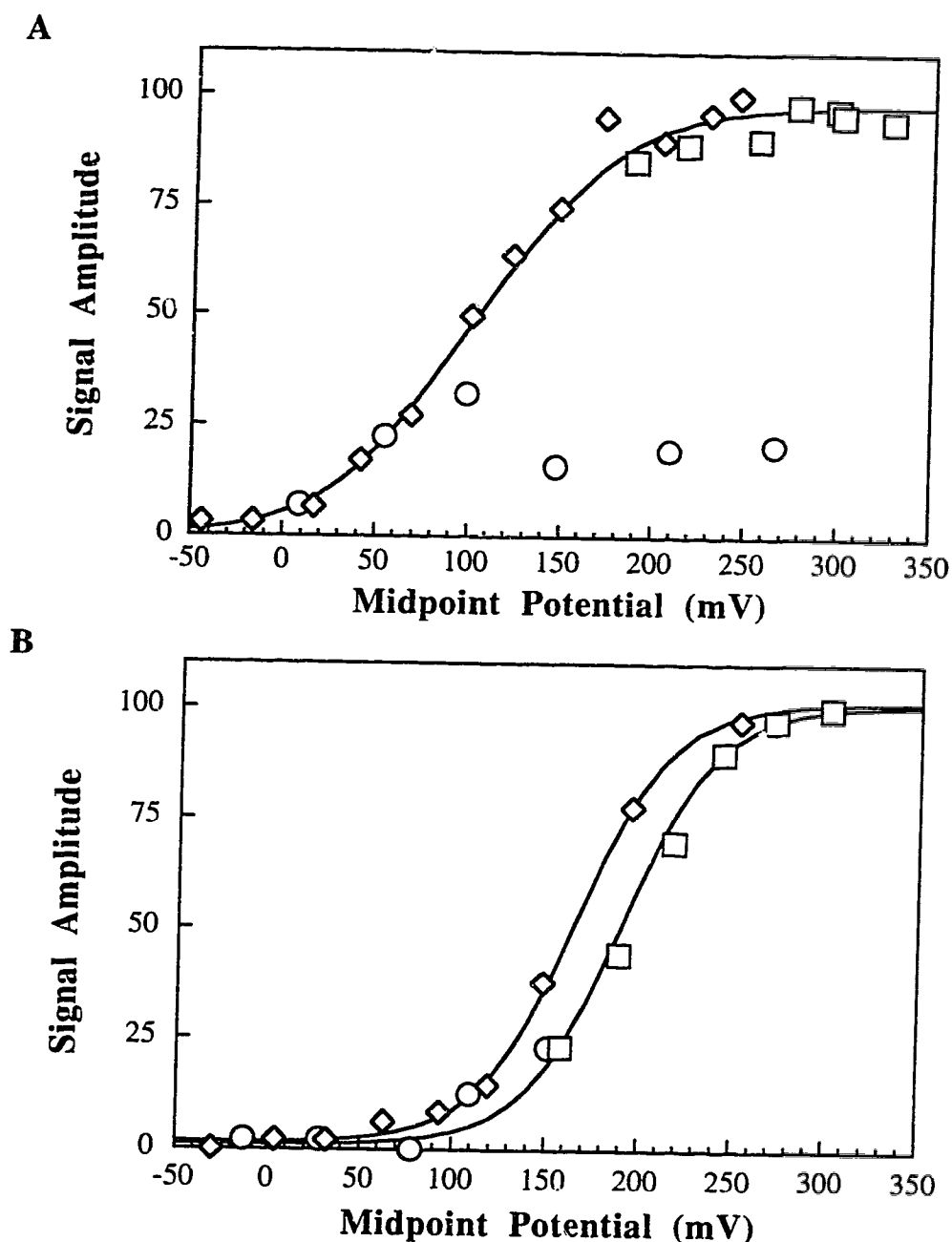


Figure 3-6 Redox Titration Curves of the New [3Fe-4S] Clusters

The amplitude of the $g = 2.03$ signal from (A) F36/pC38A and (B) F36/pC38S was measured from spectra recorded under the conditions outlined in Fig. 3-2. (\square , \circ) represent oxidative titration and (\diamond) represents reductive titration. C38A data were fitted to two components with $E_{m,7}$ values of 75 and 140 mV. C38S data were fitted in the oxidizing direction to an $E_{m,7}$ of 190 mV and in the reducing direction to an $E_{m,7}$ of 165 mV.

destroyed. Data obtained from the titration were fitted to a two-component model of the Nernst equation with $E_{m,7} = 140$ mV (69%) and 75 mV (31%). The F36/pC38S redox titration data were fitted to one component but the cluster routinely exhibited hysteresis (Figure 3-6B). The $E_{m,7}$ in the oxidizing direction was 190 mV and the $E_{m,7}$ in the reducing direction was 165 mV. The ratio of reduced [Fe-S] clusters to that of oxidized [Fe-S] clusters was determined from double integrations of reduced and oxidized samples. In the oxidized spectrum of membranes containing wild-type DmsABC there is only a small amount of [3Fe-4S] cluster visible so the ratio of reduced to oxidized [Fe-S] clusters is very large. The C38A and C38S mutants contain approximately four reduced clusters for each oxidized cluster giving a total of five clusters.

E. Mutagenesis of the DmsA Cys Group to a Consensus Ferredoxin Cys Group

Sequences known to ligate [4Fe-4S] clusters usually contain four Cys residues (22,23). The first and second Cys residues are separated by two amino acids, an exception being *M. thermolithotrophicus* ferredoxin which has four intervening residues (21). We altered the sequence of the DmsA Cys Group so that the first two Cys residues would only be separated by two amino acids. The plasmid, pC38S, was further mutated to produce pC38S,N37C which contains the sequence, CysThrValCysSerGlySerAsnCys. This spacing of Cys residues occurs in Cys Group II of DmsB and other electron transfer subunits of enzymes belonging to this family (26) and in *Azotobacter vinelandii* ferredoxin I (41,42). Expression and specific activity of the double mutant, C38S,N37C, are similar to that of C38S and this enzyme is also unable to support growth on DMSO in DSS301 (Table 3-1).

Figure 3-7 shows spectra of the ferricyanide oxidized membranes from the DmsA mutants. The double mutant ligated a [3Fe-4S] cluster but the amount of cluster was reduced to approximately 25% of the amount of cluster ligated by C38S, estimated by double integration. The line shape is similar to C38S but the signal is broader. Spectra of

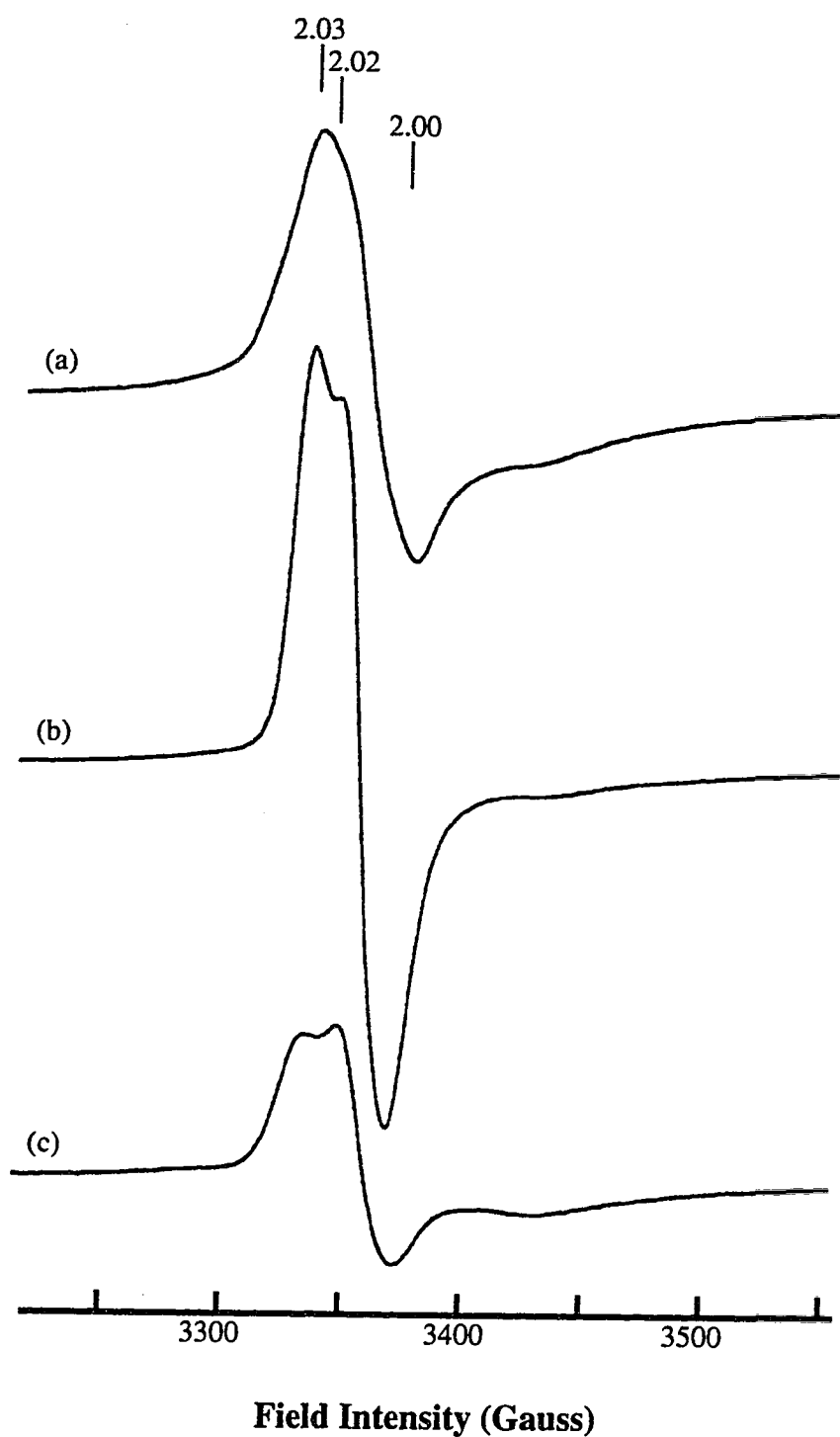


Figure 3-7 EPR Spectra of Oxidized Membranes of DmsA Mutants

Spectra are of ferricyanide oxidized membranes of (a) F36/pC38A, (b) F36/pC38S and (c) F36/pC38S,N37C. Instrument parameters were as described in Figure 3-2.

the mutants in whole cells are identical to that of the membrane preparations, indicating that the clusters in all three mutant enzymes are [3Fe-4S] clusters *in vivo* and are not [4Fe-4S] clusters altered upon oxidation during cell breakage (data not shown). The signal intensity of the double mutant appeared larger in whole cells than in the membrane samples. Redox titrations of the double mutant identify four [4Fe-4S] and one [3Fe-4S] cluster (Table 3-2) with the ratio of reduced to oxidized [Fe-S] clusters being approximately 13:1. The high ratio is likely due to the reduced amount of [3Fe-4S] cluster present in these membrane preparations.

IV. Discussion

Wild-type DmsABC has a complex EPR spectrum (Figure 3-2b) which has been interpreted as representing two pairs of interacting [4Fe-4S] clusters (25,26). Our research has been aimed at identifying which residues ligate the [Fe-S] clusters in DmsABC through the use of site-directed mutagenesis and EPR. Cys Groups III (27) and I (Rothery and Weiner, unpublished results) of DmsB each ligate a [4Fe-4S] cluster. In this report, the Cys region of DmsA was mutated so that it is unlikely to bind a [4Fe-4S] cluster. The EPR spectra of reduced membranes containing DmsA mutant enzymes was, however, found to be essentially identical to that of the wild-type enzyme (Figure 3-2). All four previously characterized [4Fe-4S] clusters are present in the mutant enzymes in the correct amounts and with mid-point potentials similar to those of the wild-type enzyme (Table 3-2). We conclude that the four EPR-visible [4Fe-4S] clusters are all ligated by the Cys Groups of DmsB.

A major new signal was observed in spectra of the oxidized DmsA mutants with a peak at $g = 2.03$ and a peak-trough at $g = 2.00$ (Figure 3-3). The line shapes of the new signals are distinct from the spectrum of fumarate reductase center FR3 (37,38). The temperature and power dependences shown in Figure 3-4 and 3-5 are similar to those of the artificial [3Fe-4S] clusters formed by site-directed mutagenesis of Cys Groups

(27,43). The multiple components, hysteresis and fragility displayed by the DmsA mutant clusters demonstrate that the cluster was unstable in this environment. It is unlikely that the [3Fe-4S] signal is due to oxidative damage of the DmsB clusters as the levels of the [4Fe-4S] clusters are the same in the wild-type and mutant enzymes and the C42S and C75S mutant enzymes do not show this new [3Fe-4S] cluster signal.

The possibility exists that the [3Fe-4S] cluster in the DmsA mutants could be generated by cluster conversion of a [4Fe-4S] cluster present in the wild-type enzyme. Conversion of [Fe-S] cluster types through site-directed mutagenesis has been demonstrated previously. In DmsB and *Synechocystis* photosystem I (clusters F_A and F_X), [4Fe-4S] clusters were converted to [3Fe-4S] clusters, although the conversion was incomplete for F_X (27,43,44). The conversion of a [3Fe-4S] to a [4Fe-4S] cluster was generated in fumarate reductase (45).

It appears that the [3Fe-4S] cluster in Cys-38 mutants is not formed via cluster conversion but that mutagenesis of Cys-38 has altered the protein environment such that a cluster can assemble. This is supported by the lack of evidence for a fifth [4Fe-4S] cluster in wild-type DmsABC. Reduction of the enzyme by dithionite results in the detection of only four [4Fe-4S] clusters and increasing the reduction potential of dithionite by increasing the pH did not reduce any additional clusters. Photoreduction with proflavin and EDTA did not reduce any additional centers (data not shown). No changes in the reduced EPR spectrum to indicate loss of a [4Fe-4S] cluster were visible in the Cys-38 mutant enzymes. Double integrations of the reduced and oxidized spectra of DmsA [3Fe-4S] containing mutants gave ratios of four to one indicating that these mutants gained an [Fe-S] cluster compared to the three to one ratio from DmsB Cys-102 mutants which altered one of the existing [Fe-S] clusters (27). Extensive EPR characterization of NarGHI (also a Type II enzyme) has identified four [Fe-S] clusters ligated by four Cys Groups in the electron transfer subunit (NarH) but no fifth cluster ligated by NarG (46-48).

The spacing of the Cys residues in DmsA was altered so the first and second Cys residues were separated by only two amino acids but the double mutant still ligated a [3Fe-4S] cluster with a line shape similar to that of the C38S cluster. The amount of this cluster was reduced and multiple components were present in the analysis. [3Fe-4S] clusters can be generated from [4Fe-4S] clusters that are damaged by oxidation but EPR analysis of whole cells expressing the double mutant demonstrated that the enzyme ligated a [3Fe-4S] cluster *in vivo*.

The role of Cys-38 in DmsA is unique. Substitution of Ser or Ala for Cys is not expected to cause much perturbation of the protein structure, indicating that the sulfhydryl of the Cys is important. In the Type I enzymes there is an abundance of conserved Gly residues in this region which are not conserved in the Type II enzymes (Figure 3-1). A cluster may be sterically hindered from assembling in this region until mutation of Cys-38 disrupts normal function and frees the Cys Group to ligate an [3Fe-4S] cluster. The natural function of the Cys Group is unknown but it could bind a metal ion. The C38S enzyme is able to interact with the quinone pool but is unable to reduce substrate demonstrating a block in the electron pathway from the [4Fe-4S] clusters to the Mo-MGD where the substrate is reduced (Chapter 2). The high $E_{m,7}$ of the [3Fe-4S] cluster in C38S relative to the potentials of the Mo(VI)/Mo(V) and Mo(V)/Mo(IV) couples (-75 and -90 mV, (25)) suggests that the [3Fe-4S] cluster may act as an "insulating cluster" (24,49) to decrease the rate of electron transfer.

We have divided the enzymes into three classes. The Type I enzymes such as NapAB, FdhF, and perhaps the other members of this type are likely to have a [4Fe-4S] cluster located in the Region 1 of the Mo cofactor binding subunit. The Type II enzymes, DmsABC and the two *E. coli* nitrate reductases, have the Region 1 Cys Group but are not likely to ligate an [Fe-S]. The Type III enzymes lack this region altogether and neither TorA or BisC have been suggested to contain [Fe-S] clusters. This region in DmsA is likely a degenerate Cys Group that has lost [Fe-S] binding capability upon evolution of

the enzyme, although in DmsA the Cys Group retains an essential role in electron transfer, perhaps interacting with the Mo-MGD.

V. Bibliography

1. Bilous, P. T., Cole, S. T., Anderson, W. F., and Weiner, J. H. (1988) *Mol. Microbiol.* **2**, 785-795
2. Méjean, V., Iobbi-Nivol, C., Lepelletier, M., Giordano, G., Chippaux, M., and Pascal, M.-C. (1994) *Mol. Microbiol.* **11**, 1169-1179
3. Blasco, F., Iobbi, C., Giordano, G., Chippaux, M., and Bonnefoy, V. (1989) *Mol. Gen. Genet.* **218**, 249-256
4. Blasco, F., Iobbi, C., Ratouchniak, J., Bonnefoy, V., and Chippaux, M. (1990) *Mol. Gen. Genet.* **22**, 104-111
5. Andriesse, X., and Bakker, H. (1993) *EMBL database*, Accession number X74597
6. Lin, J. T., Goldman, B. S., and Stewart, V. (1993) *J. Bacteriol.* **175**, 2370-2378
7. Siddiqui, R. A., Warnecke-eberz, U., Hengsberger, A., Schneider, B., Kostka, S., and Friedrich, B. (1993) *J. Bacteriol.* **175**, 5867-5876
8. Berks, B. C., Richardson, D. J., Reilly, A., Willis, A. C., and Ferguson, S. J. (1995) *Biochem. J.* **309**, 983-992
9. Pierson, D. E., and Campbell, A. (1990) *J. Bacteriol.* **172**, 2194-2198
10. Pollock, V. V., and Barber, M. J. (1995) *Arch. Biochem. Biophys.* **318**, 322-332
11. Krafft, T., Bokranz, M., Klimmek, O., Schröder, I., Fahrenholz, R., Kojro, E., and Kröger, A. (1992) *Eur. J. Biochem.* **206**, 503-510
12. Berg, B. L., Li, J., Heider, J., and Stewart, V. (1991) *J. Biol. Chem.* **266**, 22380-22385
13. Bokranz, M., Guttman, M., Kortnor, C., Kojro, F., Fahrenholz, F., Lauterbach, F., and Kröger, A. (1991) *Arch. Microbiol.* **156**, 119-128
14. Plunkett, G. I., Burland, B. D., Daniels, D. L., and Blattner, F. R. (1993) *Nucleic Acids Res.* **21**, 3391-3398

15. Shuber, A. P., Orr, E. C., Recny, M. A., Schendel, P. F., May, H. D., Schauer, N. L., and Ferry, J. G. (1986) *J. Biol. Chem* **261**, 12942-12947
16. Sauter, M., Böhm, R., and Böck, A. (1992) *Mol. Microbiol.* **6**, 1523-1532
17. White, W. B., and Ferry, J. G. (1992) *J. Bacteriol.* **174**, 4997-5004
18. Zinoni, F., Birkmann, A., Stadtman, T. C., and Böck, A. (1986) *Proc. Natl. Acad. Sci. U.S.A.* **83**, 4650-4654
19. Breton, J., Berks, B. C., Reilly, A., Thomson, A. J., Ferguson, S. J., and Richardson, D. J. (1994) *FEBS Letters* **345**, 76-80
20. Axley, M. J., Grahame, D. A., and Stadtman, T. C. (1990) *J. Biol. Chem.* **265**, 18213-18218
21. Bruschi, M., Bonicel, J., Hatachikian, E. C., Fardeau, M. L., Belaich, J. P., and Frey, M. (1991) *Biochim. Biophys. Acta* **1076**, 79-85
22. Bruschi, M., and Guerlesquin, F. (1988) *FEMS Microbiol. Rev.* **54**, 155-176
23. Matsubara, J., and Saeki, K. (1992) *Advances in Inorganic Chemistry* **38**, 223-280
24. Volbeda, A., Charon, M.-H., Piras, C., Hatchikian, E. C., Frey, M., and Fontecilla-Camps, J. C. (1995) *Nature* **373**, 580-587
25. Cammack, R., and Weiner, J. H. (1990) *Biochemistry* **29**, 8410-8416
26. Weiner, J. H., Rothery, R. A., Sambasivarao, D., and Trieber, C. A. (1992) *Biochim. Biophys. Acta* **1102**, 1-18
27. Rothery, R. A., and Weiner, J. H. (1991) *Biochemistry* **30**, 8296-8305
28. Sambasivarao, D., and Weiner, J. H. (1991) *J. Bacteriol.* **173**, 5935-5943
29. Sambrook, J., Fritsch, E. F., and Maniatis, T. (1989) *Molecular Cloning: A Laboratory Manual*, 2nd ed. Ed., Cold Spring Harbor Laboratory, Cold Spring Harbor, NY
30. Ho, S. N., Hunt, H. D., Horton, R. M., Pullen, J. K., and Pease, L. R. (1989) *Gene* **77**, 51-59
31. Bilous, P. T., and Weiner, J. H. (1985) *J. Bacteriol.* **162**, 1151-1155
32. Condon, C., and Weiner, J. H. (1988) *Mol. Microbiol.* **2**(1), 43-52
33. Markwell, M. A. D., Haas, S. M., Bieber, L. L., and Tolbert, N. E. (1978) *Anal. Biochem.* **87**, 206-210
34. Laemmli, U. K. (1970) *Nature (London)* **227**, 680-685

35. Rupp, H., Rao, K. K., Hall, D. O., and Cammack, R. (1978) *Biochim. Biophys. Acta* **537**, 255-269
36. Paulsen, K. E., Stankovich, M. T., and Orville, A. M. (1993) *Methods Enzymol.* **227**(396-411)
37. Morningstar, J. E., Johnson, M. K., Cecchini, G., Ackrell, B. A. C., and Kearney, E. B. (1985) *J. Biol. Chem.* **260**, 13631-13638
38. Johnson, M. K., Kowal, A. T., Morningstar, J. E., Oliver, M. E., Whittaker, K., Gunsalus, R. P., Ackrell, B. A. C., and Cecchini, G. (1988) *J. Biol. Chem.* **263**, 14732-14738
39. Gayda, J.-P., Bertrand, P., Theodule, F.-X., and Moura, J. J. G. (1982) *J. Chem. Phys.* **77**, 3387-3391
40. Bertrand, P., Guigliarelli, B., Meyer, J., Gayda, J.-P. (1984) *Biochimie* **66**, 77-79
41. Stout, G. H., Turley, S., Sieker, L. C., and Jensen, L. H. (1988) *Proc. Natl. Acad. Sci. U. S. A.* **85**, 1020-1022
42. Morgan, T. V., Stephens, R. J., Burgess, B. K., and Stout, C. D. (1984) *FEBS Lett.* **167**, 137-141
43. Warren, P. V., Smart, L. B., McIntosh, L., and Golbeck, J. H. (1993) *Biochemistry* **32**, 4411-4419
44. Zhao, J., Li, N., Warren, P. V., Golbeck, J. H., and Bryant, D. A. (1992) *Biochemistry* **31**, 5093-5099
45. Manodori, A., Cecchini, G., Schröder, I., Gunsalus, R. P., Werth, M. T., and Johnson, M. K. (1992) *Biochemistry* **31**, 2703-2712
46. Guigliarelli, B., Asso, M., More, C., Augier, V., Blasco, F., Pommier, J., Giordano, G., and Bertrand, P. (1992) *Eur. J. Biochem.* **207**, 61-68
47. Augier, V., Guigliarelli, B., Asso, M., Bertarand, P., Frixon, C., Giordano, G., Chippaux, M., and Blasco, F. (1993) *Biochemistry* **32**, 2013-2023
48. Augier, V., Asso, M., Guigliarelli, B., More, C., Bertrand, P., Santini, C.-L., Blasco, F., Chippaux, M., and Giordano, G. (1993) *Biochemistry* **32**, 5099-5108
49. Kowal, A. T., Werth, M. T., Manodori, A., Cecchini, G., Schröder, I., Gunsalus, R. P., and Johnson, M. J. (1995) *Biochemistry* **34**, 12284-12293

Chapter 4

Identification of a Molybdenum Ligand in *Escherichia coli* Dimethyl Sulfoxide Reductase

I. Introduction

The family of enzymes of which DmsA is a member all non-covalently bind a Mo-molybdopterin cofactor. Molybdopterin cofactors consist of a molybdenum atom (or a tungsten in some cases) associated with molybdopterin or molybdopterin dinucleotide (1). These enzymes catalyze two-electron redox reactions that result in the transfer of oxygen between substrate and water (2,3). Mo is able to react by one- or two-electron processes, cycling between the Mo(IV), Mo(V), and Mo(VI) states. Knowledge of the coordination sphere of Mo makes it possible to determine how the Mo is ligated by the cofactor and by the protein and has implications for the reaction mechanism. Biophysical studies on several eukaryotic molybdoenzymes indicate that Mo(VI) has either two oxo ligands or one oxo and one sulfido ligand (3). In the Mo(V) and Mo(IV) states a Mo=O (or the Mo=S) group is converted into a Mo-OH (Mo-SH). This redox chemistry is believed to be part of the reaction mechanism (3). The Mo is proposed to be bound to the molybdopterin by the dithiolene sulfurs (1). The structures of two forms of the molybdopterin cofactor have been determined by X-ray crystallography and confirm this coordination of the Mo as shown in Figure 1-5 (4,5). Aldehyde ferredoxin oxidoreductase (AOR) contains a tungsten dimolybdopterin cofactor in which the W is bound by the four dithiolene sulfurs of the molybdopterins and an additional two coordination sites are occupied by oxo groups, glycerol from the buffer, or both (4). No ligands of the W are from the protein. Aldehyde oxidoreductase (MOP) contains a Mo-molybdopterin cytidine dinucleotide cofactor (5). The Mo is five coordinate with two sites occupied by the dithiolene sulfurs and three oxygen ligands. Two of the oxygen ligands are presumably oxo groups while the third may come from the protein (5).

The DmsA-related enzymes that have been characterized all bind a Mo-molybdopterin guanine dinucleotide cofactor (Mo-MGD) (1,6). The sequence identity in these enzymes occurs in blocks throughout the polypeptide and it is likely that the

conserved regions are involved in cofactor ligation. Recent studies on the *E. coli* formate dehydrogenase-H (FdhF), which contains Mo and a Se-Cys residue, have shown the Se-Cys to be a ligand of the Mo (7). The Se-Cys residue of FdhF is located in a region of sequence homology and this region is shown in Figure 4-1. The residue at this position is a Se-Cys in the other two *E. coli* formate dehydrogenases (FdnG and FdoG) but is a Cys in the remainder of the formate dehydrogenases and the nitrate reductases. The S- and N-oxide reductases have a Ser in this position. Gladyshev *et al.* (7) have proposed that the Se-Cys, Cys and Ser residues at this position will ligate the Mo in the other enzymes.

To test the role of DmsA Ser-176 in Mo coordination, this residue was mutated to either Ala, which could not ligate a Mo atom, or Cys or His, both of which could potentially coordinate the Mo. All three mutant enzymes lacked both physiological and artificial DMSO reductase activity. EPR analysis of the Mo centers in the mutant enzymes indicated that significant changes occurred in the ligand field of the Mo.

II. Materials and Methods

A. Bacterial Strains and Plasmids

E. coli HB101 was used for expression of wild-type and mutant DmsABC. *E. coli* TG1 was used for routine DNA manipulation. *E. coli* DSS301 was used in growth experiments. The plasmids used were the vector pBR322, pDMS160 which contains the *dms* operon cloned into pBR322 and pDMS223 which has the *dms* operon cloned into pTZ18R.

B. Materials

Synthesis of oligonucleotides and DNA sequencing were carried out in the Department of Biochemistry DNA Core facility at the University of Alberta using an Applied Biosystems model 392 DNA synthesizer and a model 373A DNA sequencer (Perkin Elmer). Restriction endonucleases and modifying enzymes were obtained from

| | | | |
|-----------|-----|--------------------------------|---|
| Ec NarG | 211 | GTCLSFYDWY C DLPPASPQT | |
| Ec NarZ | 211 | GTCLSFYDWY C DLPPASPMT | |
| Ec FdnG | 174 | MLAVDNQARV U HGPTVASLA | |
| Ec FdoG | 174 | MLAVDNQARV U HGPTVASLA | |
| Ws FdhA | 176 | TNNLDTIARI C HAPTIVAGVS | |
| Ae NapA | 171 | SNNIDPNARH C MASAAAGFM | |
| Tp NapA | 171 | SNNLDPNARH C MASAAAYAFM | |
| Ec NapA | 150 | SNNIDPNARH C MASAVVGF | |
| Os NarB | 138 | TNNFDANSRL C MSSAVAAYI | |
| S7 NarB | 152 | TNNFDTNSRL C MSSAVSAYS | |
| Mf FdhA | 122 | THNIDHCARL C HGPTVAGLA | |
| Ec FdhF | 131 | TNNVDCCARV U HGPSVAGLH | |
| Bs NasC | 109 | TKYIDYNGRL C MSAAATAAN | |
| Kp NasA | 118 | AANIDTNSRL C MSSAVTGYK | |
| → Ec DmsA | 166 | GGYLNHYGDY S SAQIAEGLN | ← |
| Hi DmsA | 186 | GGYLNHYGDY S TAQIAVGLD | |
| Ec BisC | 99 | GGYTGHLGDY S TGAAQAIMP | |
| Ec BisZ | 165 | GGYSGHSGDY S TGAAQVIMP | |
| Hi BisC | 176 | GGFVGHKGDY S TGAAQVIMP | |
| Ec TorA | 181 | GNSVGTGGDY S TGAAQVILP | |
| Rs Dmsr | 137 | GGFVNSVGDY S TAGAQIIMP | |
| Rs BisC | 111 | GGFTGHVDY S IAAGPVILR | |
| St PhsA | 165 | .GSPNIFGHE S TCPLAYNMA | |

Figure 4-1 Sequence Alignment of the Putative Mo Binding Domain

The proteins are *E. coli* NarG (8), *E. coli* NarZ (9), *E. coli* FdnG (10), *E. coli* FdoG (11), *W. succinogenes* FdhA (12), *A. eutrophus* NapA (13), *T. pantotropha* NapA (14), *E. coli* NapA (15), *O. chalybea* NarB (16), *Synechococcus* ssp. 7 NarB (17), *M. formicicum* FdhA (18), *E. coli* FdhF (19), *B. subtilis* NasC (20), *K. pneumoniae* NasA (21), *E. coli* DmsA (22), *H. influenza* DmsA (23), *E. coli* BisC (24), *E. coli* BisZ (25), *H. influenzae* BisC (23), *E. coli* TorA (26), *R. sphaeroides* Dmsr (27), *R. sphaeroides* BisC (28), *S. typhimurium* PhsA (29), *W. succinogenes* PsrA (30). Se-Cys is denoted by a U in the *E. coli* formate dehydrogenase sequences. The residues proposed to ligate the Mo are shown in bold and the *E. coli* DmsA sequence is highlighted by arrows.

Life Technologies Inc. and the Sculptor *in vitro* mutagenesis kit was obtained from Amersham. All other materials were reagent grade and were obtained from commercial sources.

C. Site-Directed Mutagenesis

Manipulations of strains and plasmids were carried out as described in Sambrook *et al.* (31). The mutants of *dmsA* Ser-176 were generated through oligonucleotide-directed mutagenesis of single stranded pDMS223 using the Sculptor kit and mutagenic primers which substituted the Ser codon (TCC) for Ala (GCC), Cys (TGC) or His (CAC). Mutants were sequenced, subcloned into pDMS160 using EcoRI and EcoRV and sequenced again to confirm the mutation.

D. Growth of Bacteria

For growth experiments, DSS301 containing the appropriate plasmids were grown on glycerol-DMSO (32) media in 160 ml filled flasks. HB101 harboring the appropriate plasmid was grown anaerobically at 37°C in 19 liter batches on glycerol-fumarate medium supplemented with 5 μ M ammonium molybdate for 48 hours (32). Final concentrations of antibiotics used were 100 μ g ml⁻¹ of ampicillin and streptomycin, 40 μ g ml⁻¹ of kanamycin.

E. Harvesting of Cells and Preparation of Membrane Fractions

For membrane preparations, glycerol-fumarate grown cells were harvested, washed and resuspended in 50 mM MOPS, pH 7.0; 5 mM EDTA buffer. Phenylmethanesulfonyl fluoride (0.2 mM) was added to washed cells which were subjected to French pressure lysis and differential centrifugation to collect the membrane fraction (32). The membranes were washed with 100 mM MOPS, pH 7.0; 5 mM EDTA and resuspended in the same buffer. Membranes were stored at -70°C prior to use.

F. Protein Determination

Protein concentrations were estimated by a modification of the Lowry procedure (33) using a Bio-Rad bovine serum albumin protein standard.

G. Enzyme Assays

The ability of the mutant DmsABC enzymes to oxidize BV^{•+} in a DMSO or TMAO dependent manner was assayed as previously described (34). One unit of activity corresponds to 1 $\mu\text{mol BV}^{\bullet+}$ oxidized min^{-1} .

H. EPR Spectroscopy

Ferricyanide oxidized samples were incubated with 200 μM potassium ferricyanide for 10 minutes prior to freezing in liquid nitrogen. Dithionite reduced samples were prepared as described in Chapter 2 but the incubation time was increased to 10 minutes. Redox titrations of washed membranes were carried out as described in Chapter 3 using sodium dithionite and potassium ferricyanide to alter the redox potential (34). The mediators used in the redox titrations were quinhydrone, 2,6-dichloroindophenol, 1,2-naphthoquinone, toluylene blue, phenazine methosulfate, thionine, duroquinone, methylene blue, resorufin, indigotrisulfonate, indigo carmine, anthraquinone 2-sulfonic acid, benzyl viologen and methyl viologen. Spectra were recorded using a Bruker ESP300 EPR spectrometer equipped with an Oxford Instruments ESR-900 flowing helium cryostat. Instrument conditions and temperatures are described in the individual figure legends. Spin quantitations were estimated by double integration of spectra obtained under non-saturating conditions using a Cu-EDTA standard (35). For the Mo quantitations an additional correction was made to account for not integrating the hyperfine lines due to the fraction of Mo with a nuclear spin of 5/2 (36).

III. Results

A. Growth Characteristics and Enzyme Activities of the Ser-176 Mutants

E. coli DSS301 is unable to grow on glycerol-DMSO medium unless complemented with a plasmid containing the *dmsABC* operon. None of the three mutant enzymes expressed in DSS301 were able to support growth using DMSO as the terminal electron acceptor (Table 4-1). HB101 contains a wild-type chromosomal copy of the *dmsABC* operon and grows on glycerol-DMSO; this growth was completely inhibited when the Ser-176 mutant enzymes were expressed in HB101 (data not shown). Enzyme expressed from the plasmid containing the *dmsABC* operon competes for membrane assembly with the small amount of enzyme produced from the chromosome, a phenomenon that has been noted in previous studies of DmsABC mutant enzymes (37,38). The expression (Table 4-2) and membrane localization of the mutant enzymes were normal. DmsABC oxidizes BV^{•+} in a TMAO or DMSO dependent manner (Table 4-1). This ability is reduced to a level much lower than that of the background (HB101/pBR322) in the mutant enzymes. The small amount of residual activity is likely due to the chromosomal subunits present, indicating that the Ser-176 mutant enzymes are catalytically inactive. HB101 was chosen as the host for expression of DmsABC because of the large amounts of fumarate reductase in DSS301 membranes which can interfere in EPR analysis (37).

B. Mo(V) EPR Spectra in the Wild-Type and Mutant Enzymes

Figure 4-2 shows the EPR spectra at 95 K of membranes prepared from *E. coli* HB101 harboring control or mutant plasmids. The spectrum of Mo(V) in DmsABC membranes poised at -91 mV (Figure 4-2a) is identical to that previously characterized in membranes and purified DmsABC preparations (34). The line shape indicates that the Mo has rhombic symmetry with g-values of 1.982, 1.978 and 1.957 ($g_{av} = 1.972$ and $g_1 - g_3 = 0.025$). The spectrum is similar to the high pH Mo(V) signal of *E. coli* nitrate reductase

TABLE 4-1

**Enzyme Activities of Membranes Containing Amplified Levels of Wild-Type
and Mutant DmsABC**

| Plasmid | Growth ^a | Specific Activities ^b | | |
|---------|---------------------|----------------------------------|-------------|----------------------------|
| | | BV.+:TMAO | BV.+:DMSO | <u>TMAO</u> <u>DMSO</u> |
| pBR322 | NG | 16 ± 1 | 1.5 ± 0.2 | 10.7 |
| pDMS160 | + | 96 ± 10 | 10 ± 2 | 9.6 |
| pS176A | NG | 3.6 ± 0.8 | 0.4 ± 0.1 | 9 |
| pS176C | NG | 3.1 ± 0.5 | 0.36 ± 0.07 | 8.6 |
| pS176H | NG | 2.8 ± 0.8 | 0.29 ± 0.03 | 9.7 |

^a Growth of DSS301 containing one of the plasmids shown was determined from measurements of turbidity in glycerol-DMSO medium using a Klett-Summerson spectrophotometer. NG, no growth; +, growth.

^b Washed membranes were prepared from HB101 cells grown on glycerol-fumarate medium. Activities are expressed as units mg⁻¹ protein ± the standard deviation.

TABLE 4-2

**Spin Quantitation and Midpoint Potentials of the EPR Signals from HB101
Expressing Wild-Type or Mutant DmsABC**

| | Signal Intensities (nmol mg ⁻¹ protein) | | | Midpoint Potentials (mV) | |
|--------|---|--------------------|-----------------------------|-----------------------------|--------------|
| | Enzyme ^a | Mo(V) ^b | %Mo visible ^c | Mo(VI)/Mo(V) | Mo(V)/Mo(IV) |
| DmsABC | 0.36 | 0.29 | 82 | -15 | -175 |
| S176A | 0.43 | 0.39 | 90 | — | -35 |
| S176C | 0.41 | 0.16 | 40 | 27, 34 ^d | -7, -33 |
| S176H | 0.38 | ND | — | — | — |

- ^a [Fe-S] concentrations were determined from double integration of spectra of dithionite reduced membrane samples obtained at 12 K and 2 mW. The concentration of [Fe-S] was divided by 4 to estimate the concentration of enzyme.
- ^b Molybdenum concentrations were estimated from spectra obtained at 95K under the following non-saturating conditions: DmsABC, -91 mV and 20 mW; S176A, 351 mV and 2 mW; S176C, 24 mV and 2 mW. ND, not determined.
- ^c The amount of Mo(V) was divided by the enzyme concentration
- ^d S176C midpoint potentials given are for the $g = 1.992$ peak and the $g = 1.985$ peak-trough.

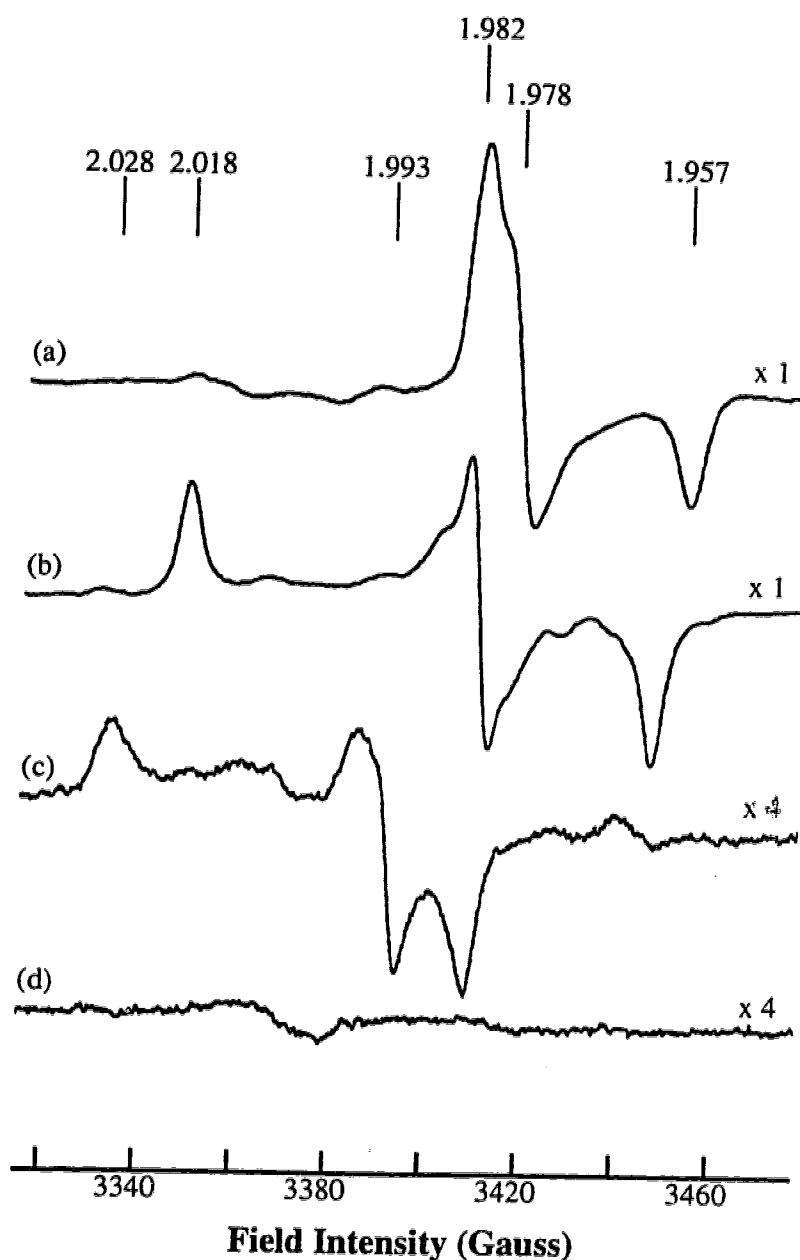


Figure 4-2 Mo(V) EPR Spectra of HB101 Membranes

Spectra: (a) HB101/pDMS160; (b) HB101/pS176A; (c) HB101/pS176C; and (d) HB101/pS176H. Sample (a) was poised at -91 mV during a redox titration. Samples (b-d) were oxidized with ferricyanide. Spectra were recorded under the following conditions: temperature, 95 K; microwave power, 20 mW; microwave frequency, 9.45 GHz; modulation amplitude, 3.02 G_{pp} at 100 KHz. Spectra were corrected for the amount of enzyme present as determined from spin quantitations (Table 4-2).

(34,39). The spectra of the mutant enzymes oxidized by ferricyanide (Figure 4-2 b and c) are dramatically different from that of DmsABC. The S176A Mo(V) signal is much more anisotropic ($g_1 - g_3 = 0.057$) with g -values at 2.018, 1.982, 1.961 ($g_{av} = 1.987$). The spectrum appears similar to the very rapid signal of xanthine oxidase (3). The S176C ferricyanide oxidized signal ($g_{1,2,3} = 2.028, 1.993, \text{ and } 1.983$) is similar to the S176A signal and has a $g_1 - g_3 = 0.045$ and a $g_{av} = 2.013$. A Mo(V) spectrum was not observed in ferricyanide oxidized S176H membranes (approximate $E_h = 430$ mV).

C. Redox Titration of the Wild-type DmsABC Mo(V) Signal

Redox titrations of DmsABC and the Ser-176 mutant enzymes were carried out to determine the midpoint potentials of the Mo(VI)/Mo(V) and Mo(V)/Mo(IV) couples. A titration of the wild-type enzyme is shown in Figure 4-3A. Of the three oxidation states through which the Mo cycles, only Mo(V) is paramagnetic so the titration curve shows the appearance and disappearance of the intermediate oxidation state. The DmsABC Mo(V) signal appeared at -250 mV, increased to a maximum at -91 mV, and then decreased until, at about 85 mV, it was no longer visible. The data from the titration were fitted to a model of the Nernst equation with two consecutive midpoint potentials ($E_{m,7}$) for the reduction of Mo(VI)/Mo(V) and Mo(V)/Mo(IV). The $E_{m,7}$ of the Mo(VI)/Mo(V) couple is -15 mV and the $E_{m,7}$ of the Mo(V)/Mo(IV) couple is -175 mV, with an average of -95 mV. The amount of Mo(V) was estimated by double integration of the spectrum of the $E_h = -91$ mV sample (Table 4-2). To calculate the percentage of Mo visible, the molybdenum concentration was divided by the amount of enzyme present in the preparation. In DmsABC approximately 80% of the total Mo was visible at -91 mV.

D. Redox Titrations of the Mo(V) Signals in the Ser-176 Mutants

In redox titrations of S176A membranes the Mo(V) signal appeared at -50 mV and increased to a maximum intensity above 125 mV. Data from the titration of the S176A membranes (Figure 4-3A) were fitted to the Nernst equation with only one midpoint

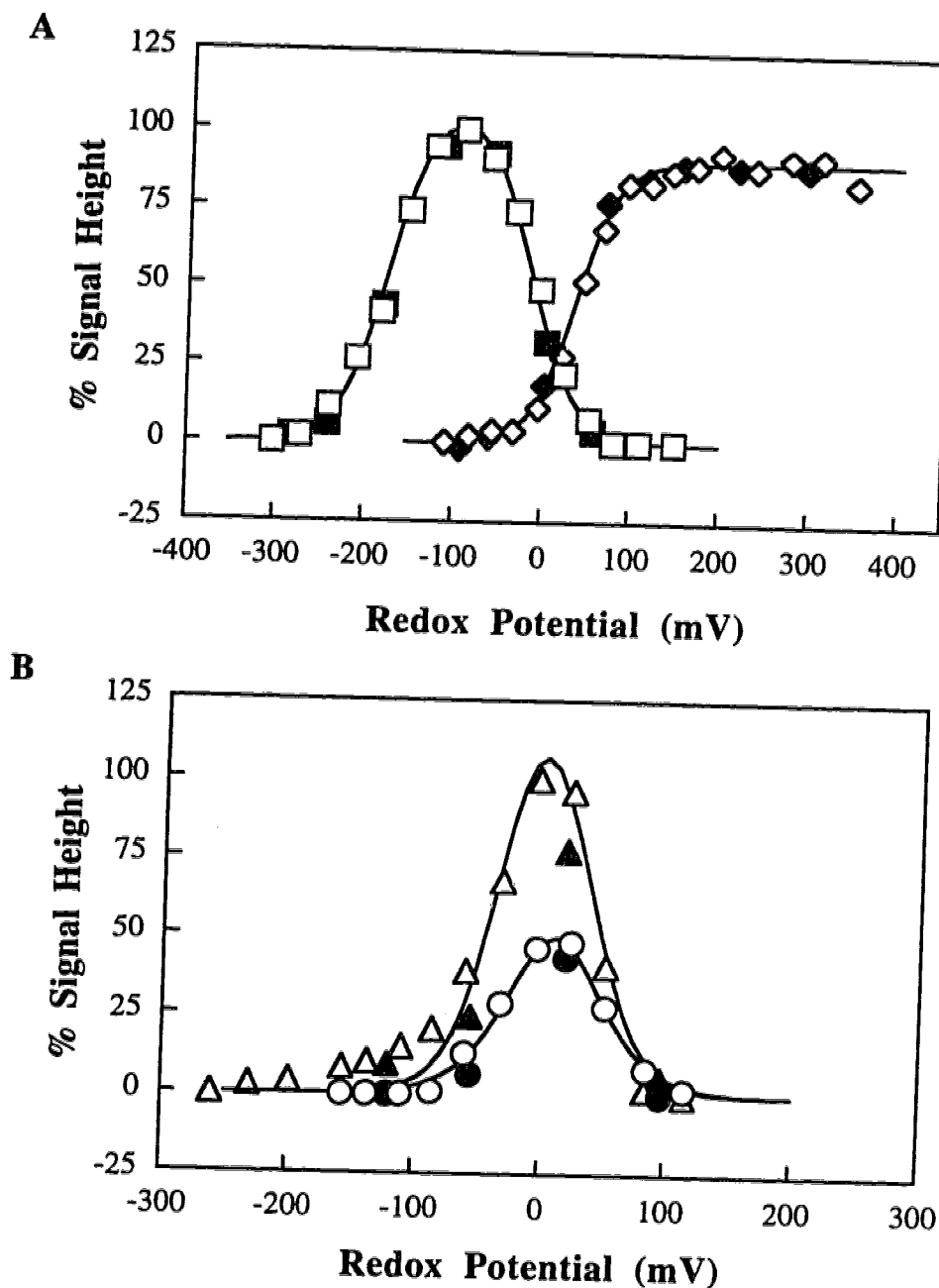


Figure 4-3 Redox Titration Curves of the Mo(V) Signals in HB101 Membranes

A) The change in signal amplitude is plotted as a function of redox potential for the $g = 1.982$ signals of HB101/pDMS160 (□, ■) and HB101/pS176A (◇, ◆) membranes. B) The change in signal amplitude of the $g = 1.992$ peak (O, ●) and the $g = 1.985$ peak-trough (Δ, ▲) of the HB101/pS176C membranes is plotted as a function of redox potential. Spectra were recorded under the conditions outlined in Figure 4-2. Open symbols represent oxidative titration and closed symbols represent reductive titration.

potential. The $E_{m,7}$ of the Mo(V)/Mo(IV) couple is 35 mV. At least 90% of the molybdenum was oxidized to Mo(V), which even at 200 μ M ferricyanide (spectrum shown in Figure 4-2b) remained in the Mo(V) state.

Spectra from a redox titration of the S176C membranes are shown in Figure 4-4. Analyses of redox titrations of the S176C mutant indicated that several Mo(V) species were present. The two largest signals, identifiable by a peak at $g = 1.992$ and a peak-trough at $g=1.985$, behaved independently showing that they arose from different species. The redox titration curves for these two features are shown in Figure 4-3B and the midpoint potentials are in Table 4-2. Integration of the $E_h = 24$ mV spectrum indicated that, at this potential, the spectrum dominated by the $g = 1.992$ species accounted for 40% of the total Mo in this enzyme. The $E_h = 346$ mV spectrum in Figure 4-4 is not equivalent to the ferricyanide oxidized spectrum (Figure 4-2c). The $E_{m,7}$ of ferricyanide is 430 mV indicating that the ferricyanide oxidized species arises at much higher potentials than the $g = 1.992$ and $g = 1.985$ species.

The S176H membranes were titrated over a range of redox potential from -435 to 350 mV but a Mo(V) signal was not detected. All of the mutant enzymes contained similar amounts of molybdopterin as analyzed by oxidation to Form A and fluorescence spectroscopy (not shown) (6).

E. EPR Spectra of Dithionite-Reduced Membranes

HB101 membrane preparations were reduced with dithionite and the spectra recorded at 12 K to examine the [4Fe-4S] clusters in the mutant enzymes (Figure 4-5). The background strain, HB101/pBR322, expressed very little DmsABC and the spectrum shows primarily the features of fumarate reductase (40). The spectrum of HB101/pDMS160 membranes is identical to that of DmsABC in membranes as previously characterized and has been interpreted as two pairs of interacting [4Fe-4S] clusters ($E_{m,7} = -50, -120, -240, \text{ and } -330$ mV) (34,37). The spectrum contains peaks at $g = 2.05$,

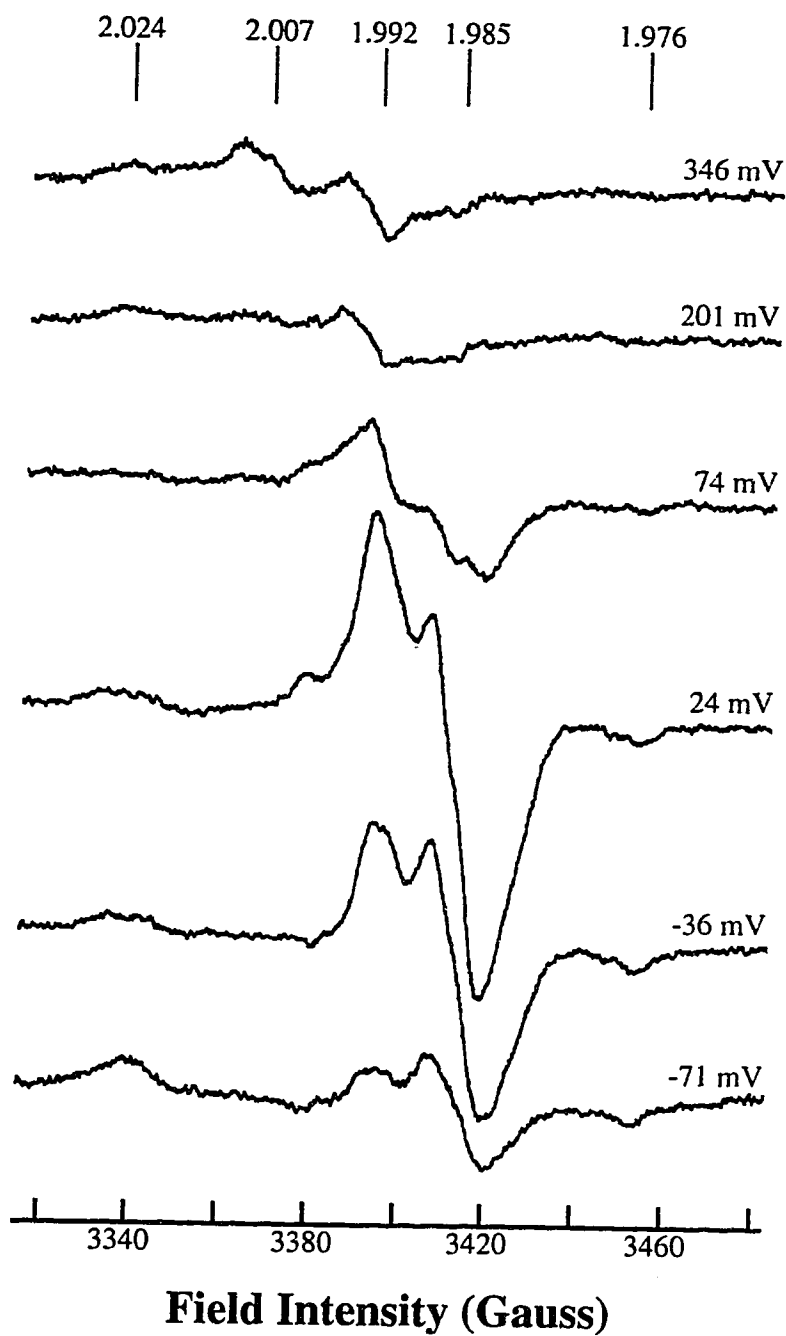


Figure 4-4 EPR Spectra of HB101/pS176C Membranes During Oxidative Titration

Spectra were recorded as described in Figure 4-2.

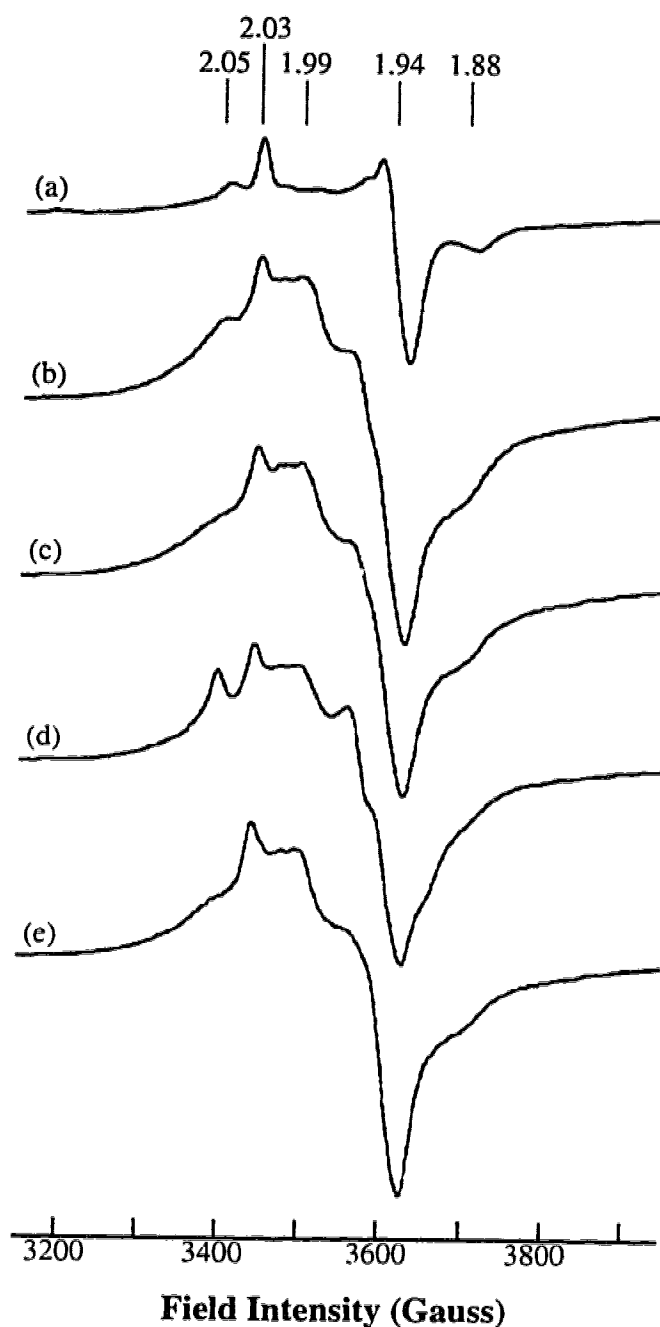


Figure 4-5 EPR Spectra of the Reduced Membranes at 12 K

Spectra: (a) HB101/pBR322; (b) HB101/pDMS160; (c) HB101/pS176A; (d) HB101/pS176C; and (e) HB101/pS176H. Samples were reduced with dithionite and frozen in liquid nitrogen. Spectra are recorded under the following conditions: temperature, 12 K; microwave power, 20 mW; microwave frequency, 9.45 GHz; modulation amplitude, 10 G_{pp} at 100 KHz. Spectra were corrected to an arbitrary protein concentration of 30 mg ml⁻¹.

2.03, 1.99, a peak-trough at $g = 1.95$ to $g = 1.92$, and a trough at $g = 1.88$. Fumarate reductase contributes to the peak at $g = 2.02$ and the peak-trough at $g = 1.95$ to $g = 1.92$. The reduced spectra of the S176A and S176H mutants are very similar to the wild-type spectrum. However, the line shape of the S176C spectrum (Figure 4-5d) is altered; the peaks at $g = 2.05$ and $g = 1.95$ are increased in size, and the $g=1.95$ shoulder is more distinct. The content of [Fe-S] clusters did not increase in this mutant and only four phases were present in analyses of the $g = 2.05$ and $g = 1.95$ features from redox titrations of S176C membranes, indicating that all four [4Fe-4S] clusters are present in the S176C mutant. The midpoint potential of the $E_{m,7} = -240$ mV [4Fe-4S] cluster appeared to be shifted to a more positive potential in this mutant (data not shown). Redox titrations of the [4Fe-4S] clusters in DmsABC are complicated by the presence of molybdenum overlapping the [Fe-S] signals making assignments of midpoint potentials difficult. Further studies are in progress to characterize the interaction between DmsA and DmsB.

IV. Discussion

DmsA is the catalytic subunit of DMSO reductase and contains a Mo-MGD cofactor. It belongs to a family of prokaryotic molybdoenzymes which share sequence homology and probably ligate the same molybdopterin cofactor, but little is known about how the cofactor is ligated by these enzymes. Although two structures of molybdopterin cofactor containing enzymes are known, neither enzyme has amino acid sequence similarity to DmsA or its family. Aided by sequence alignments, we have identified a ligand of Mo in DmsA. Mutagenesis of Ser-176 and examination of the resulting enzymes confirms that Ser-176 coordinates the Mo. The spectra of Mo(V) is sensitive to the amino acid in this position as would be expected for changes in the Mo ligation. The mutations alter the midpoint potentials of the Mo, and in the case of the S176A mutant, trap the Mo in the Mo(V) state at high potential. Substituting Cys at this position causes a

heterogeneity in the environment of the Mo and also appears to affect the line shape of at least one of the [Fe-S] clusters.

The Se-Cys residue of FdhF has been demonstrated by EPR to be a ligand of the Mo in formate dehydrogenase H (7). Enrichment of the enzyme with ^{77}Se (nuclear spin = $1/2$) caused hyperfine splitting of the Mo(V) signal indicating a direct coordination of the Mo. Mutagenesis of FdhF to replace the Se-Cys with Cys caused a major change in the shape and the g-values of the Mo(V) signal. The g_{av} decreased to approximately 2 and the anisotropy (g_1 - g_3) is greatly decreased as well. Changes in EPR parameters resulting from a change in the coordination of the Mo is also observed in the molybdenum hydroxylases when comparing the native and desulfo forms of the enzymes. The native enzymes have one oxo and one sulfhydryl ligand to Mo(V) which becomes one oxo and one hydroxyl ligand in the inactive desulfo forms (3). Comparison of Mo(V) signals indicated that replacement of the sulfhydryl ligand with a hydroxyl group decreased the g_{av} and the g_1 - g_3 (3,41). Binding of an anion to the Mo in sulfite oxidase and *E. coli* nitrate reductase also involved changes in shape, g_{av} and g_1 - g_3 (39,42-44).

Comparison of EPR spectra of wild-type DmsABC and the Ser-176 mutant enzymes (Figure 4-2) showed that major changes occurred in the Mo coordination sphere. Each different residue at this position had a unique effect on the Mo(V) signal. The increases in g_{av} values and anisotropy of the Mo(V) signals are similar to those that occurred in other molybdoenzymes upon a change in ligation of the Mo atom. These results, along with sequence comparisons with other enzymes in this family, especially FdhF, allow us to conclude that Ser-176 is a ligand of the Mo in DmsABC.

The S176A substitution caused an increase in the anisotropy of the Mo(V) signal with a shift to higher g-values. The midpoint potential of the Mo(V)/Mo(IV) couple was 35 mV, 210 mV more positive than that of the wild-type Mo(V)/Mo(IV) couple, $E_{m,7} = -175$ mV. The enzyme was trapped in the Mo(V) state at midpoint potentials increasing to

430 mV. The inability of the Mo(V) to undergo the final oxidation to Mo(VI) would prevent the reduction of DMSO to DMS ($E_{m,7} = 160$ mV), a two electron process.

Several different Mo(V) species were detected in redox titrations of the S176C mutant. The two largest signals come from species with midpoint potentials of 27 and 34 mV for the Mo(VI)/Mo(V) couples and midpoint potentials of -7 and -33 mV for the Mo(V)/Mo(IV) couples. The potentials of the individual species are closer together and shifted to a more positive potential than those of the wild-type enzyme but less than the S176A mutant. The midpoint potentials of the major S176C Mo centers indicate that the Mo cofactor should be thermodynamically capable of reducing DMSO but this mutation may affect the interactions of the Mo with the other redox centers in the enzyme. A Mo(V) signal is still present in the ferricyanide oxidized spectrum (Figure 4-2b). Under the oxidizing conditions in the redox titration, the Cys substitution may be forming disulfide bonds with another Cys residue in DmsA that may alter the Mo environment and the EPR characteristics of the Mo. The Cys substitution not only causes heterogeneity in the Mo environment but alters the line shape of the reduced [4Fe-4S] clusters as well. The Mo in DmsA is known to interact with the $E_{m,7} = -120$ mV [4Fe-4S] cluster of DmsB (34). The S176C mutation appears to affect the $E_{m,7} = -240$ mV [4Fe-4S] cluster indicating that this cluster may be near to Ser-176. It is not known how the Mo center in DmsA becomes reduced but the electrons may come sequentially from one [4Fe-4S] cluster or possibly from two [4Fe-4S] clusters (perhaps the $E_{m,7} = -120$ and -240 mV centers). The $E_{m,7} = -50$ mV center has been implicated in interactions at the quinol binding site in DmsC (45). Little information is available about the $E_{m,7} = -330$ mV center which may play a structural role or could be involved in mediating electron transfer. Further studies on the [Fe-S] clusters and the Mo will be aimed at understanding these subunit interactions and electron transfer between subunits.

No Mo(V) signal was visible in redox titrations of S176H. The mutant enzymes all had molybdopterin and previous studies of DmsABC have indicated that the

molybdopterin is not inserted into DmsABC without the Mo (6). However, the loss of a coordinating amino acid in the S176H mutant may have caused the loss of Mo from the cofactor. Alternatively, the midpoint potentials of the S176H Mo center may be shifted to a higher potential than that of ferricyanide as it is unlikely that they would be significantly less than -435 mV. The lowest midpoint potential determined for a Mo couple is -470 mV at pH 7.7 for *M. formicicum* formate dehydrogenase (46).

The midpoint potentials obtained from the titration of DmsABC in membranes are -15 mV for the Mo(VI)/Mo(V) couple and -175 mV for the Mo(V)/Mo(IV) couple, with an average of -95 mV. The midpoint potentials determined in an earlier study of DmsABC containing membranes were -75 and -90 mV, with an average of -83 mV (34). The midpoint potentials, but not the Mo(V) signal itself, were dependent upon the preparation of DmsABC and the ratio of Mo(V) to enzyme was 1/3. DmsABC loses cofactor during purification, the purified enzyme often retaining only 30% of its Mo-MGD (6,47). The amount of Mo(V) detected in membranes used for the current study accounts for over 80% of the Mo that should be present if each enzyme molecule had one Mo (Table 4-2). Care has been taken in this study to avoid repeated freeze-thaw cycles and unnecessary manipulations to prevent the loss of Mo. These membrane preparations did not exhibit a partial Mo(V) signal at potentials greater than 80 mV as did membranes in the previous study (34).

Ser-176 has been demonstrated to be a ligand of Mo in DmsA. The midpoint potentials of the Mo(VI)/Mo(V) and Mo(V)/Mo(IV) couples are dependent upon the coordination of Ser-176. In the native form of the molybdenum hydroxylases (oxo and sulfido coordination), one or both midpoint potentials are higher than the midpoint potentials of the desulfo enzymes (dioxo coordination) (41). In the DmsA family of molybdoenzymes the identity of the ligand, Se-Cys, Cys or Ser, may influence the properties of the Mo. The Mo midpoint potentials of a Se-Cys containing enzyme have not been determined but must be low, as the $E_{m,7}$ for the formate/CO₂ couple is -425 mV.

DmsABC ($E_{m,7} = -15$ and -175 mV) and DMSO reductase from *R. sphaeroides* ($E_{m,7} = 144$ and 200 mV,(48)) have intermediate midpoint potentials and Ser coordination of the Mo. *E. coli* nitrate reductase (Cys residue) has midpoint potentials of 180 and 220 mV at pH 7.1 (49). The formate dehydrogenase from *M. formicicum* which has both a Cys (Figure 4-1) and a sulfido ligand (3) has the lowest midpoint potentials of all the molybdoenzymes characterized, $E_{m,7.7} = -330$ and -470 mV (46), indicating that other elements in the Mo environment are important for determining the Mo midpoint potentials.

It is not possible to tell from our mutagenesis studies what sort of ligand may be replacing Ser-176 but there is a Ser residue adjacent to Ser-176 in DmsA that could possibly become a ligand. A water molecule is a possibility. Structural rearrangements of the mutant DmsA proteins must be slight, as conformational changes in DmsA caused by previous mutations disrupted subunit contacts and led to decreases in enzyme assembly which did not occur with these mutants. The small increase in midpoint potentials between the wild-type DmsA and the S176C mutant suggests that the two major species in the S176C titration may represent Cys ligation of the Mo. The results obtained from analysis of DmsA mutant enzymes support the hypotheses that other molybdoenzymes in this family contain an amino acid at this position in the sequence which coordinates the Mo and that the conserved sequences in DmsA are involved in cofactor binding.

V. Bibliography

1. Rajagopalan, K. V., and Johnson, J. L. (1992) *J. Biol. Chem.* **267**, 10199-10202
2. Bray, R. C. (1988) *Q. Rev. Biophys.* **21**, 299-329
3. Hille, R. (1994) *Biochim. Biophys. Acta* **1184**, 143-169
4. Chan, M. K., Mukund, S., Kletzin, A., Adams, M. W. W., and Rees, D. C. (1995) *Science* **267**, 1463-1469
5. Romao, M. J., Archer, M., Moura, I., Moura, J. J. G., LeGall, J., Engh, R., Schneider, M., Hof, P., and Huber, R. (1995) *Science* **270**, 1170-1176

6. Rothery, R. A., Simala Grant, J. L., Johnson, J. L., Rajagopalan, K. V., and Weiner, J. H. (1995) *J. Bacteriol.* **177**, 2057-2063
7. Gladyshev, V. N., Khangulov, S. V., Axley, M. J., and Stadtman, T. C. (1994) *Proc. Natl. Acad. Sci. USA* **91**, 7708-7711
8. Blasco, F., Iobbi, C., Giordano, G., Chippaux, M., and Bonnefoy, V. (1989) *Mol. Gen. Genet.* **218**, 249-256
9. Blasco, F., Iobbi, C., Ratouchniak, J., Bonnefoy, V., and Chippaux, M. (1990) *Mol. Gen. Genet.* **22**, 104-111
10. Berg, B. L., Li, J., Heider, J., and Stewart, V. (1991) *J. Biol. Chem.* **266**, 22380-22385
11. Plunkett, G. I., Burland, B.D., Daniels, D. L., Blattner, F.R. (1993) *Nucleic Acids Res.* **21**, 3391-3398
12. Bokranz, M., Guttman, M., Kortnor, C., Kojro, F., Fahrenholz, F., Lauterbach, F., and Kröger, A. (1991) *Arch. Microbiol.* **156**, 119-128
13. Siddiqui, R. A., Warnecke-eberz, U., Hengsberger, A., Schneider, B., Kostka, S., Friedrich, B. (1993) *J. Bacteriol.* **175**, 5867-5876
14. Berks, B. C., Richardson, D. J., Reilly, A., Willis, A. C., and Ferguson, S. J. (1995) *Biochem. J.* **309**, 983-992
15. Richterich, P., Lakey, N., Gryan, D., Jaehn, L., Mintz, L., Robison, K., Church, G. M. (1993) *EMBL database*, Accession number U00008
16. Unthan, M., Klipp, W., and Schmid, G. H. (1995) *EMBL database*, Accession number X89445
17. Andriesse, X., and Bakker, H. (1993) *EMBL database*, Accession number X74597
18. Shuber, A. P., Orr, E. C., Recny, M. A., Schendel, P. F., May, H. D., Schauer, N. L., and Ferry, J. G. (1986) *J. Biol. Chem* **261**, 12942-12947
19. Zinoni, F., Birkmann, A., Stadtman, T. C., and Böck, A. (1986) *Proc. Natl. Acad. Sci. U.S.A.* **83**, 4650-4654
20. Ogawa, K.-I., Akagawa, E., Yamane, K., W., S. Z., Lacelle, M., Zuber, P., and Nakano, M. M. (1995) *J. Bacteriol.* **177**, 1409-1413
21. Lin, J. T., Goldman, B.S., Stewart, V. (1993) *J. Bacteriol.* **175**, 2370-2378
22. Bilous, P. T., Cole, S. T., Anderson, W. F., and Weiner, J. H. (1988) *Mol. Microbiol.* **2**, 785-795
23. Fleischmann, R. D., Adams, M. D., White, O., Clayton, R. A., F., K. E., Kerlavage, A. R., Bult, C. J., Tomb, J.-F., Dougherty, B. A., Merrick, J. M., McKenney, K., Sutton, G., Fitzhugh, W., Fields, C. A., Gocayne, J. D., Scott,

- J. D., Shirley, R., Liu, L.-I., Glodek, A., Kelley, J. M., Weidman, J. F., Phillips, S. C. A., Spriggs, T., Hedblom, E., Cotton, M. D., Utterback, T. R., Hanna, M. C., Nguyen, D. T., Saudek, D. M., Brandon, R. C., Fine, L. D., Fritchman, J. L., Fuhrmann, J. L., Geoghagen, N. S. M., Gnehm, C. L., McDonald, L. A., Small, K. V., Fraser, C. M., Smith, H. O., and Venter, J. C. (1995) *Science* **269**, 496-512
24. Pierson, D. E., and Campbell, A. (1990) *J. Bacteriol.* **172**, 2194-2198
25. del Campillo-Campbell, A., and Campbell, A. M. (1995) *EMBL database*, Accession number U38839
26. Méjean, V., Iobbi-Nivol, C., Lepelletier, M., Giordano, G., Chippaux, M., Pascal, M.-C. (1994) *Mol. Microbiol.* **11**, 1169-1179
27. Barber, M. J., Valkenburgh, H. V., Trimboli, A. J., Pollock, V. V., Neame, P. J., and Bastian, N. R. (1995) *Arch. Biochem. Biophys.* **320**, 266-275
28. Pollock, V. V., and Barber, M. J. (1995) *Arch. Biochem. Biophys.* **318**, 322-332
29. Heinzinger, N. K., Fujimoto, S. Y., Clark, M. A., Moreno, M. S., and Barrett, E. L. (1995) *J. Bacteriol.* **177**(10), 2813-2820
30. Krafft, T., Bokranz, M., Klimmek, O., Schröder, I., Fahrenholz, R., Kojro, E., Kröger, A. (1992) *Eur. J. Biochem.* **206**, 503-510
31. Sambrook, J., Fritsch, E. F., and Maniatis, T. (1989) *Molecular Cloning: A Laboratory Manual*, 2nd ed. Ed., Cold Spring Harbor Laboratory, Cold Spring Harbor, NY
32. Bilous, P. T., and Weiner, J. H. (1985) *J. Bacteriol.* **162**, 1151-1155
33. Markwell, M. A. D., Haas, S. M., Bieber, L. L., and Tolbert, N. E. (1978) *Anal. Biochem.* **87**, 206-210
34. Cammack, R., and Weiner, J. H. (1990) *Biochemistry* **29**, 8410-8416
35. Paulsen, K. E., Stankovich, M. T., and Orville, A. M. (1993) *Methods Enzymol.* **227**(396-411)
36. Barber, M. J., Bray, R. C., Lowe, D. J., and Coughlan, M. P. (1976) *Biochem. J.* **153**, 297-307
37. Rothery, R. A., and Weiner, J. H. (1991) *Biochemistry* **30**, 8296-8305
38. Trieber, C. A., Rothery, R. A., and Weiner, J. A. (1994) *J. Biol. Chem.* **269**, 7103-7109
39. Vincent, S. P., and Bray, R. C. (1978) *Biochem. J.* **171**, 639-647

40. Johnson, M. K., Kowal, A. T., Morningstar, J. E., Oliver, M. E., Whittaker, K., Gunsalus, R. P., Ackrell, B. A. C., and Cecchini, G. (1988) *J. Biol. Chem.* **263**, 14732-14738
41. Barber, M. J., Coughlan, M. P., Rajagopalan, K. V., and Siegel, L. M. (1982) *Biochemistry* **21**, 3561-3568
42. Lamy, M. T., Gutteridge, S., and Bray, R. C. (1980) *Biochem. J.* **185**, 397-403
43. Bray, R. C., Gutteridge, S., Lamy, M. T., and Wilkinson, T. (1983) *Biochem. J.* **211**, 227-236
44. George, G. N., Bray, R. C., Morpeth, F. F., and Boxer, D. H. (1985) *Biochem. J.* **227**, 925-931
45. Rothery, R. A., and Weiner, J. H. (1996) *Biochemistry* **35**, in press
46. Barber, M. J., Siegel, L. M., Schauer, N. L., May, J. D., and Ferry, J. G. (1983) *J. Biol. Chem.* **258**, 10839-10845
47. Weiner, J. H., MacIsaac, D. P., Bishop, R. E., and Bilous, P. T. (1988) *J. Bacteriol.* **170**, 1505-1510
48. Bastian, N. R., Kay, C. J., Barber, M. J., and Rajagopalan, K. V. (1991) *J. Biol. Chem.* **266**, 45-51
49. Vincent, S. P. (1979) *Biochem. J.* **177**, 757-759

Chapter 5

Discussion and Conclusions

I. Discussion and Conclusions

The studies reported in this thesis were aimed at understanding the role of DmsA in electron transfer in DmsABC. Electron transfer in the DmsA-related family of molybdoenzymes has not been well characterized but the large degree of sequence and subunit conservation implies a common mechanism. The original multiple sequence alignment of six molybdoenzymes (DmsA, NarG, NarZ, BisC, FdhF, and *M. formicicum* FdhA) identified six regions of sequence similarity (1). Addition of several new sequences to the alignment has extended the original observations to seven regions of similarity.

A. Electron Transfer Properties of Region 1

Region 1 is conserved only in multi-subunit enzymes, suggesting a role in electron transfer between the catalytic and electron transfer subunits. The role of the conserved residues in Region 1 of DmsA was explored in Chapter 2 using site-directed mutagenesis. Of the residues examined, three were absolutely essential for growth on DMSO, Cys-38, Cys-42 and Arg-77. Lys-28 substitutions had no effect on enzyme activity and this residue is not conserved in several of the enzymes. The C75S mutant enzyme supported growth of DSS301 on DMSO and is not essential for the MQH₂:DMSO oxidoreductase activity of DmsABC. When these mutant enzymes were expressed in HB101, they inhibited the basal level of growth, indicating that the mutant DmsA subunits compete with the chromosomally encoded subunits for membrane assembly with DmsB and DmsC. Mutation of the three Cys residues caused a decrease in DmsA levels in the membrane, with Ser substitutions being assembled better than either Ala or Gly substitutions. The C75A mutant enzyme did not accumulate detectable DmsA in the membranes. The reduction in assembly of the mutant DmsABC is most likely due to a destabilization of DmsA or its contacts with the other subunits or both. A similar situation

occurs when Cys Groups I, II, and IV of DmsB are mutated. These Cys residues ligate [Fe-S] clusters and loss of an [Fe-S] cluster results in a decrease in membrane-bound enzyme for the Group I mutants and the loss of detectable enzyme for the Groups II and IV mutants (Rothery and Weiner, unpublished results). All three DmsA Cys residues examined are probably structurally as well as functionally important. The hydroxyl sidechain of Ser must partially compensate for the structural role of the Cys residues and the function of Cys-75.

The reactions catalyzed by molybdoenzymes are usually defined as two separate half reactions (2). For DmsABC, the reductive half reaction involves the oxidation of menaquinol and the reduction of the enzyme. The oxidative half-reaction occurs at the Mo which becomes oxidized during the reduction of DMSO to DMS. The two active sites are separated; one is in DmsC and one is in DmsA. Electrons from the reductive active site must be transferred through the protein to the oxidative active site, presumably through some or all of the [4Fe-4S] clusters. All of the mutant enzymes were able to reduce DMSO and TMAO so it is not likely that the oxidative active site was altered in these enzymes. The mutant enzymes assembled normal [4Fe-4S] clusters that were redox linked to the menaquinone pool. The C42S, C38S and R77S mutant enzymes were unable to be use electrons from the [4Fe-4S] clusters for the reduction of DMSO even though all of the mutant enzymes were capable of DMSO reduction with artificial reductants. Mutation of the Region 1 residues blocks electron transfer to the oxidative active site.

Benzyl viologen and DMNH₂ were also used to characterize the electron transfer capabilities of the mutant enzymes. BV^{•+} is a chromogenic dye often used as a mediator for electron transfer because it is able to donate electrons to a wide variety of proteins. Its reaction with DmsABC is artificial because it does not involve the reductive active site in DmsC but can donate electrons to the DmsAB catalytic dimer (3). The BV^{•+}:DMSO oxidoreductase activity of the R77S enzyme was relatively high but this enzyme was blocked in MQH₂ and DMNH₂ dependent activities. The reduced [Fe-S] clusters were

unable to donate electrons to reduce DMSO implying that the electrons from $BV^{•+}$ bypass the [Fe-S] clusters and may be donated directly to DmsA. A kinetic study of the catalytic dimer of *E. coli* nitrate reductase (NarGH) has indicated that the [Fe-S] clusters in that enzyme are not necessary for $BV^{•+}$ -dependent activity (4). The $BV^{•+}$:DMSO oxidoreductase activity was decreased in most of the mutant enzymes but the C42S mutant enzyme was most severely affected. The very low activity of the C42S enzyme indicates that this residue plays a major role in electron transfer from $BV^{•+}$.

The C38S, C42S and R77S enzymes which are incapable of DMSO reduction with MQH₂ are able to do so with DMNH₂ as the electron donor, implying that some of the electrons donated by DMNH₂ may also follow an alternate route. A recent report on polysulfide reductase of *W. succinogenes* (PsrABC) indicated that DMNH₂ is able to catalyze polysulfide reduction by PsrAB in the absence of the membrane anchor subunit, PsrC, indicating that alternate interaction sites for DMNH₂ may exist (5). The results obtained using the different electron donors indicate that the electrons may follow different pathways to the Mo-MGD, implying some flexibility in electron transfer in the enzyme. Region 1 of DmsA is important for functional electron transfer from the MQH₂ to DMSO.

B. The Role of Region 1 in [Fe-S] Cluster Ligation

A [4Fe-4S] cluster was found to be ligated by Region 1 of *T. pantotropha* NapA (5), raising the possibility of a [4Fe-4S] cluster being present in DmsA. DmsABC is known to contain four [4Fe-4S] clusters and the presence of a [4Fe-4S] cluster ligated by the DmsA Region 1 Cys residues would be consistent with the involvement of these residues in electron transfer. In Chapter 3, a search for an additional [Fe-S] cluster was described. EPR characterization of the wild-type enzyme and the Cys-38 mutants from the previous study was carried out. No additional [4Fe-4S] clusters were detected in EPR spectra of the wild-type DmsABC. The NapA [4Fe-4S] cluster was EPR-visible, had an $E_{m,7} = -160$ mV and was not unusual in any way. An equivalent cluster in DmsA should

be EPR-visible. If Region 1 is involved in ligating one of the previously characterized [4Fe-4S] clusters, removal of the second Cys in the group should alter or destroy that cluster. No difference in the content or EPR line shape of the [4Fe-4S] clusters of the wild-type or C38S and C38A enzymes was found. Therefore, wild-type DmsA does not ligate an EPR-visible [Fe-S] cluster and the four [4Fe-4S] clusters in the enzyme are all ligated by the DmsB Cys Groups. However, the oxidized spectrum of the Cys-38 mutants did show a fifth [Fe-S] cluster. The identity of the residue at position 38 caused a significant variation in the characteristics of the [3Fe-4S] cluster. The Cys-42 and Cys-75 mutants which were examined did not ligate a [3Fe-4S] cluster. The C38S [3Fe-4S] cluster was not detected in the Q-pool coupling assay (Chapter 2) because of the limited expression of this enzyme in DSS301 membranes and the presence of large amounts of fumarate reductase, which also has a [3Fe-4S] cluster. An attempt to convert the C38S [3Fe-4S] cluster to a [4Fe-4S] cluster was unsuccessful. Incorporation of a Cys residue at position 37 dramatically reduced the amount of [Fe-S] cluster that was formed but did not restore activity. Region 1 of DmsA does not ligate an [Fe-S] cluster and although a vestigial Cys Group is present, Cys-38 prevents assembly of an [Fe-S] cluster in this region. The Cys residues of the DmsA Cys Group may be involved in a specific function such as ligation of a metal ion or the Mo-MGD cofactor and when mutagenesis of Cys-38 disrupts this binding, the structure in this area relaxes so that a [3Fe-4S] cluster may assemble. Many of the ferredoxins which ligate a [3Fe-4S] cluster use the same arrangement of Cys residues as for a [4Fe-4S] cluster but without the second Cys. The sequence of the Cys-38 mutants is similar to that of a [3Fe-4S] binding Cys Group and allows the protein to fold appropriately for binding a [3Fe-4S] cluster. A proposed structural alteration would fit well with the observation that the levels of the mutant enzymes are decreased presumable due to small structural perturbations in this area.

C. The Function of Region 1

Region 1 contains a Cys Group which appears to be located on the electron transfer pathway between the Mo-MGD and the [4Fe-4S] clusters. A parallel situation exists in the structures of MOP and AOR (6,7). These enzymes contain [Fe-S] clusters and a Mo cofactor in the same subunit. In both structures the molybdopterin is linked by a hydrogen bond to a Cys residue which ligates an [Fe-S] cluster. The role of molybdopterin in enzyme function is unknown but the link to the [Fe-S] clusters, which are involved in electron transfer, implies that the pterin ring system may be an active participant in electron transfer. The [4Fe-4S] cluster and the molybdopterin in AOR are also linked by an Arg residue which forms hydrogen bonds to both. DmsABC is proposed to have a dimolybdopterin cofactor, as does AOR.

The Cys Group of DmsA Region 1 clearly has the ability to ligate an [4Fe-4S] cluster, as has been shown for NapA. There is, however, no evidence that this is its normal function, and an [Fe-S] cluster is only detected when Cys-38 is mutated. No additional factors, such as a metal ion, which the Cys residues could be ligating have been detected. The accumulation of the holoenzyme in the membrane is sensitive to changes in the Cys residues and Arg-77, which argues for their structural importance. The important residues of Region 1 may be conformationally linked to each other and to the molybdopterin as the Cys and Arg residues in AOR are linked to the molybdopterin. The involvement of Region 1 in electron transfer would fit with its proposed role in ligating the molybdopterin. The role of the molybdopterin has not been substantiated but it has been proposed to be involved directly in electron transfer and mediating the redox potential of the Mo (8,9). The loss of the contacts between Region 1 and the molybdopterin may be the reason for the block in electron transfer in the C38S, C42S and R77S enzymes.

A link with the Mo-MGD could explain why changes in this region affect enzyme assembly. The active site in DmsA is in close contact with DmsB, the distance between the Mo and the $E_{m,7} = -120$ mV [Fe-S] cluster has been estimated to be as close as 8 to 12 Å, based on the interaction seen in the EPR analysis (10). A small alteration in the structure, around the Mo-MGD, could disrupt DmsA and DmsB contacts and inhibit assembly.

The molybdoenzymes can be divided into three types based on the sequence of Region 1. The Type I enzymes have a near typical Cys Group and are likely to ligate a [4Fe-4S] cluster, although only the *T. pantotropha* NapA has been shown experimentally to contain a cluster. The spacing of the first three Cys residues in the Type I Cys Group (Figure 3-1) is identical to that of the AOR Cys Group. The second type which includes only DmsA and the nitrate reductases, does not have an [Fe-S] cluster. Type I and Type II enzymes may have a similar structure in this area which involves interactions between the conserved residues and the Mo cofactor. Type III, is comprised of the periplasmic TMAO and DMSO reductases and biotin sulfoxide reductases that have neither a Cys Group or an [Fe-S] cluster. These enzymes contain only one redox group, the Mo cofactor, which must be able to accept electrons from an external source via a different pathway than in the Type I and II enzymes.

D. The Ligation of the Molybdenum

The coordination of the Mo-MGD in DmsA is addressed in Chapter 4. In FdhF, the Se-Cys residue was demonstrated to be a Mo ligand. This residue occurs in a conserved region (Region 3) and suggests that Ser-176 of DmsA is involved in Mo ligation. Mutagenesis of Ser-176 produced enzymes that were unable to reduce DMSO or TMAO, demonstrating the importance of this residue for catalysis. The enzymes all assembled to normal levels in the membrane, indicating that the subunit interactions were not significantly perturbed. EPR characterization of the resultant enzymes demonstrated

that the Mo is ligated by Ser-176. The dramatic changes in EPR line-shape and midpoint potentials could only come from a major change in the coordination sphere of the Mo. The sensitivity of the Mo spectrum to the identity of the residue at position 176 further supports the role of Ser-176 in Mo ligation.

The midpoint potentials of the Mo in wild-type DmsABC were reexamined. The Mo still interacted with the $E_{m,7} = -120$ mV [4Fe-4S] cluster but there was an increase in the amount of Mo visible in the EPR spectrum of these studies compared to previous studies. The amount of Mo(V) seen is dependent on how close together the two midpoint potentials are, close potentials mean a smaller amount of Mo(V) is detectable by EPR. The increased amount of Mo visible in the present study indicates that the midpoint potential are further apart than those of the previous study but the average of the midpoint potentials is similar in both studies (-83 mV and -95 mV). The Mo midpoint potentials of the S176A and S176H mutants were substantially altered. The Mo in the S176A enzyme was unable to undergo a second electron oxidation and remained trapped in the Mo(V) state at high concentrations of ferricyanide (the approximate $E_{m,7} = 430$ mV for ferricyanide/ferrocyanide). Reduction of DMSO is a two-electron process and it is not likely that this mutant enzyme is able to donate two electrons at a physiologically relevant potential. Mo(V) was not detected in the S176H enzyme over a range of redox potentials from -435 to approximately 430 mV. This enzyme contained a significant amount of molybdopterin, presumably as the Mo-MGD cofactor. Experiments on the wild-type enzyme grown in an excess of tungstate or in a *mob* mutant strain demonstrated that molybdopterin is not inserted into the enzyme in the absence of Mo or without the addition of the guanine nucleotide (11). The midpoint potentials of the S176H mutant are probably too positive for the Mo to be oxidized by DMSO or ferricyanide or too low to be reduced by dithionite.

The S176C enzyme is different from the other two mutant enzymes. The S176C mutant enzyme was able to undergo oxidation/reduction of the Mo at reasonable redox

potentials but this enzyme was still not capable of DMSO reduction. An unexpected effect of the S176C mutation was the change in the EPR line shape of at least one of the [4Fe-4S] clusters. Redox titrations indicated that four [4Fe-4S] clusters were still present in the mutant enzyme, but that the $E_{m,7} = -240$ mV [4Fe-4S] cluster had a much higher midpoint potential. The effect of the Cys substitution implies that the $E_{m,7} = -240$ mV [4Fe-4S] cluster is in close proximity to this residue, so that a change in the structure around the Mo alters the environment of the [4Fe-4S] cluster. The S176C mutant may not function due to an alteration in the interaction between the Mo and the [Fe-S] clusters or a change in the Mo environment may interfere with DMSO binding.

The putative Mo ligand in the nitrate reductases and the non-*E. coli* formate dehydrogenases is a Cys residue. The DmsA S176C mutant displayed a number of different Mo EPR signals, indicating a heterogeneity in the Mo environment. The redox potentials of the major Mo species from S176C were higher than those of the wild-type enzyme, suggesting that Cys coordination may increase the potential of the Mo relative to Ser coordination. In the nitrate reductases (Cys coordination) the Mo redox potentials are indeed higher than those of DmsABC (Ser coordination). Of the formate dehydrogenases, which have either Se-Cys or Cys coordination, only the *M. formicicum* formate dehydrogenase (FdhABC) Mo center has been potentiometrically characterized. Its midpoint potentials are very low (-330 and -440 mV) which suits the potential of the formate/CO₂ couple ($E_{m,7} = -425$ mV) (12). This enzyme has a Cys ligand and is sensitive to cyanide inactivation, indicating that it may contain a sulfido ligand, similar to xanthine dehydrogenase. The Mo cofactor of FdhABC contains MGD but it is not known if the cofactor is a dimolybdopterin. The molybdopterin has been suggested to be a major influence on the redox potential of the Mo (8). The molybdopterin may modulated large effects on midpoint potential while coordination by the Region 3 residue may be responsible for fine-tuning the potential.

E. Structure of the Mo Cofactor in DmsABC

Recently, the Mo cofactor of *R. sphaeroides* DMSO reductase was demonstrated to contain two MGD molecules and one Mo atom for each mole of protein (13). Comparisons of the Mo cofactors from this enzyme and DmsABC have suggested that the stoichiometry of the Mo:MGD:enzyme ratio is the same in both enzymes and that the cofactor in DmsABC is likely a dimolybdopterin. The proposed structure of the cofactor (Figure 5-1) is based on the AOR tungsten cofactor structure in which the Mo is coordinated by the two dithiolene sulfurs from each molybdopterin. All of the enzymes in the related family of molybdoenzymes are proposed to bind a MGD cofactor but this does not mean that all the cofactors must have two molybdopterins. The sequence of the MOP is homologous to xanthine oxidase but MOP contains a molybdopterin cytidine dinucleotide and xanthine oxidase contains the simple molybdopterin (7).

The Mo coordination sphere is made up of four sulfur atoms and, we propose, an additional two oxygen ligands. The oxygen of Ser-176 was demonstrated to be a ligand in Chapter 4. The additional oxygen is proposed to be an oxo group. EXAFS studies of *E. coli* nitrate reductase (NarGHI) and two well characterized eukaryotic molybdoenzymes, xanthine oxidase and sulfite oxidase, have determined that all three enzymes contain oxo ligands. In the Mo(VI) state sulfite oxidase contains two oxo groups, xanthine oxidase contains one oxo and one sulfido, and nitrate reductase contains one oxo group. In the former two enzymes, reduction to Mo(IV) is accompanied by protonation of an oxo group of sulfite oxidase(14) and the sulfido group of xanthine oxidase (2). In nitrate reductase, the data is much less clear. The number of oxo groups falls from one to 0.5 indicating that half of the oxo groups have been lost but no increase in hydroxyl ligands was noted (15).

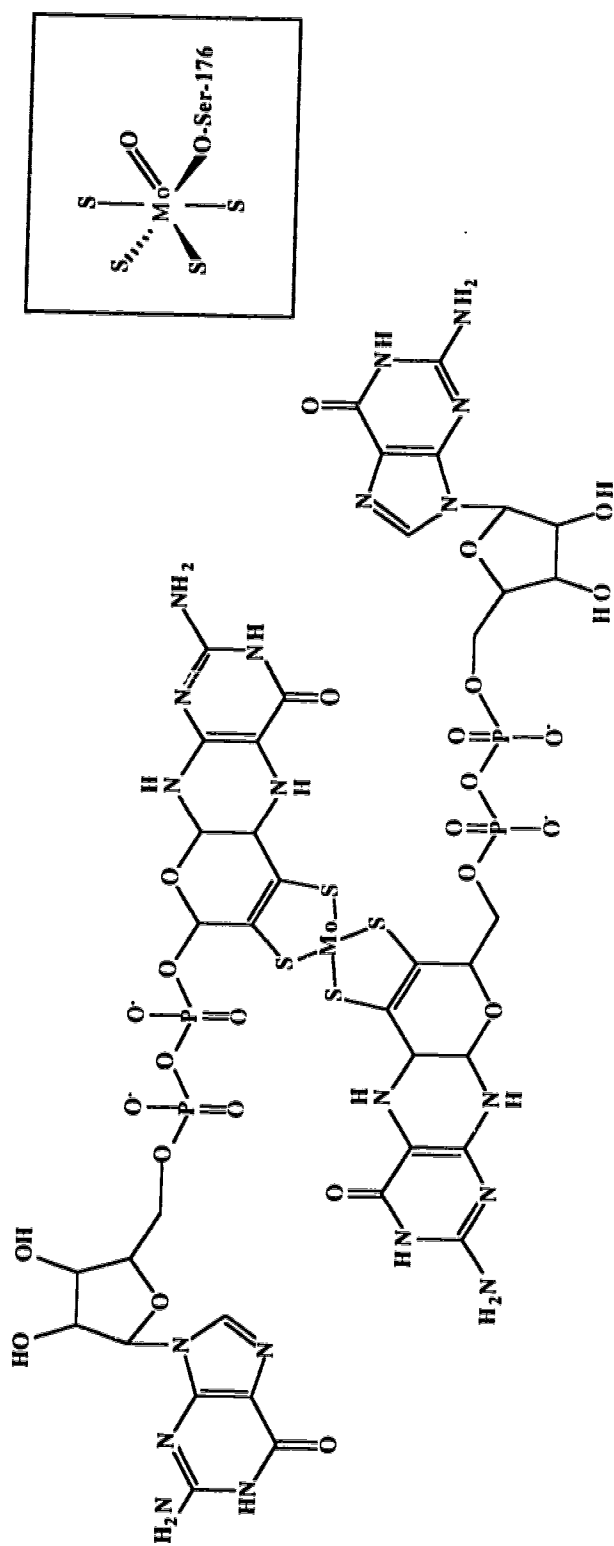


Figure 5-1 The Proposed Structure of the Mo Cofactor in *E. coli* DmsABC

The cofactor in DmsABC is likely to be Mo-dimolybdopterin guanine dinucleotide. The inset shows the proposed ligation of the Mo atom. Four ligands are from the dithiolene sulfurs of the molybdopterin. An oxo group and the oxygen of Ser-176 complete the coordination sphere.

F. The Reaction Mechanism of DmsABC

The oxygen transfer catalyzed by molybdoenzymes is believed to occur via the oxidation sphere of the Mo atom (2,16), but the mechanism is not fully understood. In the proposed reaction mechanism of xanthine oxidase, the deprotonation of xanthine (R^-) is followed by carbanion attack on the single oxo group to form a Mo-OR intermediate species. The oxo group is rapidly regenerated from water. Similarly, in the sulfite oxidase reaction scheme, the oxo ligand is the source of the oxygen transferred to sulfite and the oxo group is regenerated from water. In DMSO reductase, the mechanism would be reversed; the oxo group would become the product water produced in the reaction and the oxygen of DMSO would become a new oxo group (Figure 5-2). The proposed coordination sphere of the Mo (Figure 5-2) contains one oxo ligand. Reduction of Mo(VI) to the Mo(IV) may be accompanied by a protonation of the oxo group to form a hydroxyl group. Protons involved in the reaction may come from amino acid residues in the protein or from the solution. Mo usually forms six coordinate complexes and the coordination of DMSO to the Mo would require the displacement of the hydroxyl ligand. Model compounds have been synthesized which possess the ability to reduce DMSO to DMS (16-18). The Mo complex, $MoO(L-NS_2)(DMF)$ contains a ligand (L) which provides a nitrogen and two sulfur atoms to coordinate the Mo. An oxo group and dimethylformamide (DMF) are also ligands. The reduction of the DMSO occurs in two steps; (i) DMSO coordinates the Mo, displacing the DMF ligand, (ii) intramolecular oxygen transfer generates a $Mo=O$ unit and DMS is released. $MoO(L-NS_2)(DMF)$ can also reduce other S- and N-oxides and nitrate indicating that the mechanism proposed in Figure 5-2 is applicable to the other reductases in this family of enzymes.

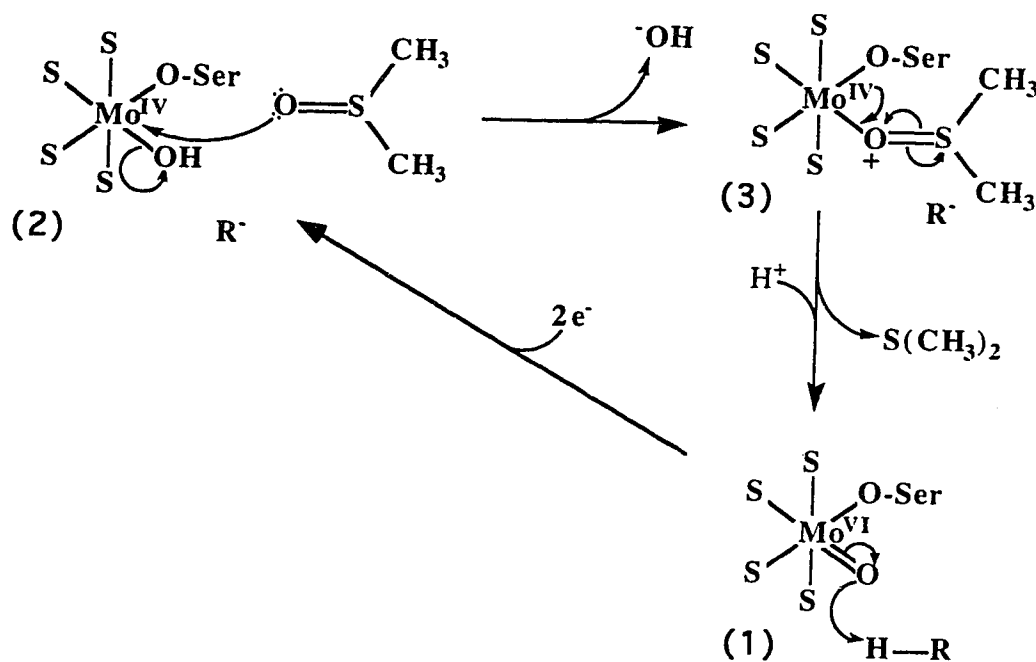


Figure 5-2 Proposed Mechanism of Oxygen Transfer in DmsABC

The mechanism of DMSO reduction is based upon the work with model Mo compounds and the proposed mechanisms of xanthine oxidase and sulfite oxidase. Central to this mechanism is the presence of an oxo ligand to Mo(VI) (1) that becomes protonated upon reduction to Mo(IV) (2). This proton may come from an amino acid sidechain as shown, or from the solvent. DMSO is able to displace the Mo(IV) hydroxyl ligand to give (3). The hydroxide ion becomes protonated to form water. Two electrons are transferred from the Mo(IV) to the oxygen atom of DMSO which rearranges to an oxo group (1) and free DMS.

G. Model for Electron Transfer

The results of the mutagenesis experiments described in this thesis have been combined with previous results obtained from other studies of wild-type and mutant DmsABC to suggest a working model for electron flow in DmsABC (Figure 5-3). This model has a quinol binding site which would encompass His-65 of DmsC. Bound quinol would undergo two one-electron oxidations (MQH_2/MQ $E_{m,7} = -74 \text{ mV}$), donating the electrons sequentially to the $E_{m,7} = -50 \text{ mV}$ [4Fe-4S] cluster ligated by Cys Group III of DmsB. The $E_{m,7} = -50 \text{ mV}$ [4Fe-4S] cluster has been demonstrated to be conformationally linked to the MQH_2 binding site in DmsC and magnetic interactions indicate that it interacts with the $E_{m,7} = -120$ [4Fe-4S] cluster (19). The $E_{m,7} = -50 \text{ mV}$ [4Fe-4S] cluster mediates electron transfer between the MQH_2 and the $E_{m,7} = -120$ [4Fe-4S] cluster. The $E_{m,7} = -120$ [4Fe-4S] cluster interacts with the Mo center (10). The electrons from the $E_{m,7} = -120 \text{ mV}$ cluster pass through the Region 1 area and reduce Mo(VI) to Mo(IV) ($E_{m,7} = -95 \text{ mV}$). The reduction of DMSO to DMS ($E_{m,7} = 160 \text{ mV}$) occurs by a two electron process, proceeding by way of the Mo coordination sphere and oxidizing the Mo(IV) back to Mo(VI). The overall reaction from MQH_2 to DMSO has a $\Delta G_0' = 45 \text{ kJ mol}^{-1}$. The flow of electrons is not always to an acceptor of higher potential but the centers are all close in redox potential and interact with each other. The midpoint potentials were determined at equilibrium and under turnover conditions these potentials may not be as important as the location of the redox groups (8).

The roles, if any, of the $E_{m,7} = -240$ and -330 mV clusters in electron transfer have yet to be determined. Substitution of Ser-176 with Cys appears to be affecting the EPR characteristics of the $E_{m,7} = -240 \text{ mV}$ cluster. The effect is probably due to a structural change in the [Fe-S] cluster environment and suggests that these two areas may be spatially linked. The $E_{m,7} = -240 \text{ mV}$ cluster may play a role in sequential electron transfer to the Mo. An alternate hypothesis is that two pathways of electron transfer may

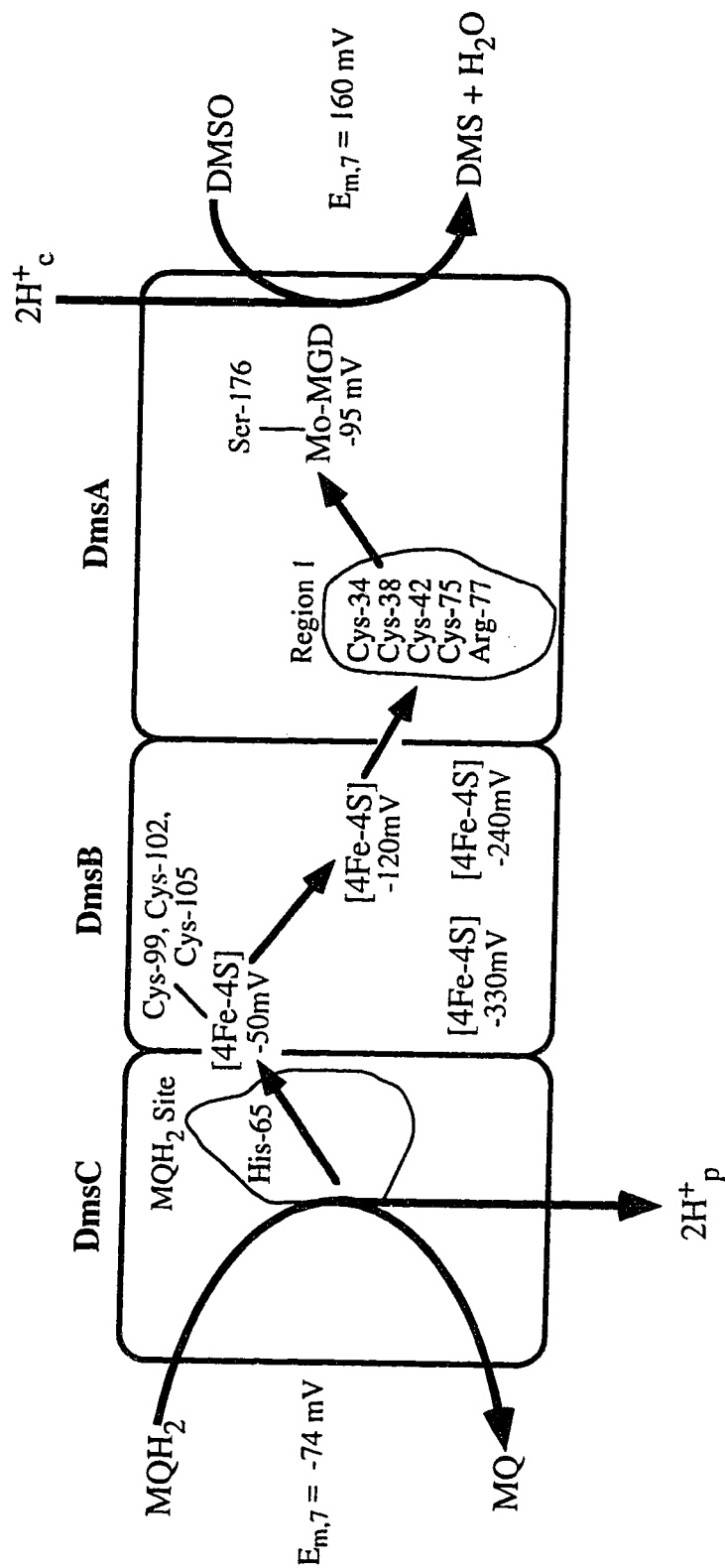


Figure 5-3 Summary of Electron Transfer Through DmsABC

The pathway of electron flow from menaquinol to DMSO is depicted. The residues involved in electron transfer and cofactor ligation are shown.

be present and the Mo may receive one electron from the $E_{m,7} = -120$ mV cluster and one from the $E_{m,7} = -240$ mV cluster. As mentioned in Chapter 1, there may also be two quinone binding sites in DmsC.

II. Future Studies

Combining sequence analysis, mutagenesis and EPR has proven to be a fruitful way of studying electron transfer. As the structures of more molybdoenzymes are solved it may be possible to begin modeling of the DmsABC structure. X-ray crystallography of membrane proteins is difficult, but many DmsA related enzymes are soluble and several contain all seven regions of sequence similarity as well as a second subunit. It may be possible to model the structure of DmsA to a similar soluble protein and DmsB to a ferredoxin.

A. The Mo-MGD Cofactor

The Mo cofactor in DmsABC is proposed to be a dimolybdopterin based on indirect comparisons with *R. sphaeroides* DMSO reductase, but this should be proven by quantitation of the amount of molybdopterin relative to the Mo. If the Mo cofactor is a dimolybdopterin, five ligands of the cofactor have been identified. EXAFS of the wild-type enzyme would determine if the proposed oxo group is present and if this group becomes protonated upon reduction of the Mo. EXAFS studies of the Ser-176 mutants would also prove interesting and may identify other residues present in the molybdenum environment. The role of the Mo in the reaction mechanism of DmsABC may be addressed using ^{17}O -labeled DMSO. The ^{17}O has a nuclear spin of 5/2 which would cause a splitting of the Mo if it became a ligand as proposed in Figure 5-2. A DmsA Cys-38/Ser-176 double mutant could determine the proximity of the [3Fe-4S] cluster (and thus Region 1) to the Mo by characterizing any possible interaction.

B. The [4Fe-4S] Clusters

Studies are in progress to assign the [4Fe-4S] clusters to the Cys Groups and characterize their interactions (Rothery and Weiner). The $E_{m,7} = -50$ mV cluster, ligated by Cys Group III, is located near the inner surface of the cytoplasmic membrane. The roles of the $E_{m,7} = -240$ and -330 mV clusters in electron transfer need to be addressed to refine the model of electron transfer in the enzyme. Previous mutagenesis attempts have altered Cys residues and in most cases the cluster was destroyed along with the protein. A more useful approach may be to mutate the residues surrounding the Cys, especially the charged residues, so that the characteristics of the cluster are changed but the cluster ligands are not. This would allow the effects of the midpoint potentials on enzyme activity to be addressed.

C. Quinone Binding

A DmsC residue involved in quinol oxidation, His-65, has been identified and it has been suggested that two quinone binding sites may be located in DmsC (19). The entire DmsC protein must be present for DmsABC to be assembled at the membrane. A number of methods have been used to identify quinone binding sites. Several residues involved in quinol oxidation in fumarate reductase have been identified and mutagenesis of similar amino acids in DmsC may identify more residues involved in quinol oxidation by DmsABC. DmsABC activity is sensitive to HOQNO and residues involved in binding may be located by isolating HOQNO resistant mutants. Other methods such as labeling the protein with a quinone analog will only work if it can be made specific for the quinol binding site of DmsC. Purified nitrate reductase was analyzed for bound quinone and the holoenzyme was found to have a stoichiometry greater than six quinones per mole of enzyme, so this approach may not be specific enough to determine the number of quinone binding sites in DmsABC (20).

D. Subunit Interactions

DmsA and DmsB are not stable without DmsC and it has not been possible to purify a catalytic dimer as in nitrate reductase or fumarate reductase. The C-terminal of DmsB appears to be necessary for the interaction of both DmsA and DmsB with DmsC (3). The whole of DmsC is necessary for interaction with DmsAB. None of the subunits may be expressed alone as DmsB and DmsA expressed individually form inclusion bodies and do not appear to bind either [Fe-S] clusters or the Mo cofactor and DmsC expressed alone is lethal to *E. coli* (Trieber, Rothery, Turner, and Weiner, unpublished results).

Combining mutants of the various subunits into one enzyme has proven useful in studying interactions between prosthetic groups and subunits. A double mutant of DmsB and DmsC was used to demonstrate interaction between an [Fe-S] cluster and a quinol analog (19). A double mutant of DmsA Cys-38S and DmsB Cys-102S has indicated that the two [3Fe-4S] clusters in these mutants are capable of interacting and studies of this interaction should be able to provide information about the location of these clusters in the enzyme (Rothery and Weiner, unpublished data). Similarly, combining the Ser-176 mutants with DmsB mutants, most notably the $E_{m,7} = -120$ and -240 mV [Fe-S] cluster mutants, could answer questions about the interaction of these centers.

E. Kinetic Studies

Kinetic studies of the oxidative half-reaction of DmsABC are currently ongoing. With $BV^{•+}$ as the electron donor, the enzyme is able to reduce a wide variety of substrates and the enzyme kinetics are being analyzed to characterize the active site (Simala Grant and Weiner). The importance of Ser-176 in ligating the Mo places Region 3 at the oxidative active site. Several residues in this region are conserved in the S- and N-oxide reductases but not in the other enzymes. The roles of some of these conserved residues in

substrate reduction are currently being addressed by site-mutagenesis (Simala Grant and Weiner). The reductive half reaction could also be characterized using MQ or its analogs.

DmsABC is related to several different groups of electron transfer enzymes. Studies of DmsABC are providing new insights into the redox properties of [Fe-S] clusters and the Mo cofactor as well as the general mechanisms of electron transfer.

III. Bibliography

1. Wootton, J. C., Nicolson, R. E., Cock, J. M., Waters, D. E., Burke, J. F., Doyle, W. A., and Bray, R. C. (1991) *Biochim. Biophys. Acta* **1057**, 157-185
2. Hille, R. (1994) *Biochim. Biophys. Acta* **1184**, 143-169
3. Sambasivarao, D., and Weiner, J. H. (1991) *J. Bacteriol.* **173**, 5935-5943
4. Buc, J., Santini, C. L., Blasco, F., Giordani, R., Cardenas, M. L., Chippaux, M., Cornish-Bowden, A., and Giordano, G. (1996) *Eur. J. Biochem.* **234**, 766-772
5. Krafft, T., Gross, R., and Kröger, A. (1995) *Eur. J. Biochem.* **230**, 601-606
6. Chan, M. K., Mukund, S., Kletzin, A., Adams, M. W. W., and Rees, D. C. (1995) *Science* **267**, 1463-1469
7. Romao, M. J., Archer, M., Moura, I., Moura, J. J. G., LeGall, J., Engh, R., Schneider, M., Hof, P., and Huber, R. (1995) *Science* **270**, 1170-1176
8. Berks, B. C., Ferguson, S. J., Moir, J. W. B., and Richardson, D. J. (1995) *Biochim. Biophys. Acta* **1232**, 97-123
9. Rajagopalan, K. V., and Johnson, J. L. (1992) *J. Biol. Chem.* **267**, 10199-10202
10. Cammack, R., and Weiner, J. H. (1990) *Biochemistry* **29**, 8410-8416
11. Rothery, R. A., Simala Grant, J. L., Johnson, J. L., Rajagopalan, K. V., and Weiner, J. H. (1995) *J. Bacteriol.* **177**, 2057-2063
12. Barber, M. J., May, H. D., and Ferry, J. G. (1986) *Biochemistry* **25**, 8150-8155

13. Hilton, J. C., and Rajagopalan, K. V. (1996) *Arch. Biochem. Biophys.* **325**, 139-143
14. George, F. N., Kipke, C. A., Prince, R. C., Sunde, R. A., Enemark, J. H., and Cramer, S. P. (1989) *Biochemistry* **28**, 5075-5080
15. George, G. N., Turner, N. A., Bray, R. C., Morpeth, F. F., Boxer, D. H., and Cramer, S. P. (1989) *Biochem. J.* **259**, 693-700
16. Enemark, J. H., and Young, C. G. (1994) *Adv. Inorg. Chem.* **40**, 1-88
17. Berg, F. M., and Holm, R. H. (1985) *J. Am. Chem. Soc.* **107**, 925-932
18. Caradonna, J. P., Reddy, P. R., and Holm, R. H. (1988) *J. Am. Chem. Soc.* **110**, 2139-2144
19. Rothery, R. A., and Weiner, J. H. (1996) *Biochemistry* **35**, 3247-3257
20. Brito, F., DeMoss, J. A., and Dubourdieu, M. (1995) *J. Bacteriol.* **177**, 3728-3735